Static structural analysis of a motorcycle's single sided swingarm

Rui Miguel Costa Dias

Master's thesis

FEUP Supervisor: Prof. Mário Vaz
Host Institution supervisor: Eng. Nuno Viriato Ramos

U.PORTO
FEUP FACULDADE DE ENGENHARIA
UNIVERSIDADE DO PORTO

Master's degree in Mechanical Engineering

2022-06-11

Abstract

There are two main types of swingarms: double and single sided swingarms. Both types of swingarm have the same function. However, there are some pros and cons to both of them, which could help in selecting one instead of the other.

The aim of this thesis is to replace a double sided swingarm of a motorcycle with a single sided swingarm. Although it is an off-road motorcycle, in this dissertation, it was assumed that the situations which this motorcycle is going to be submitted are the same as a standard road motorcycle.

Firstly, the advantages and disadvantages of each type of swingarm are described, the torsional and lateral stiffness of the initial double sided swingarm are calculated, critical points and critical situation are described and detailed. It was concluded that next to the suspension mount the structure is under the maximum stress and the critical situation is landing on the rear wheel with a normal load of 2g.

After that, a single sided swingarm is designed using Solidworks, the lateral and torsional stiffness are calculated. Following that, a sensitivity analysis was performed and later the iteration process in order to reduce the mass affecting the minimum possible stiffness was carried out.

The final design was selected and compared to the initial design. It was obtained an equivalent mass on the swingarm. However, the lateral and torsional stiffness are in the normal range of values, which did not happen in the double sided swingarm.

Finally, all the other conditions were tested in the designed single sided swingarm and the assumptions were confirmed.

Keywords: Single Sided swingarm, Double sided swingarm, Torsional Stiffness, Lateral Stiffness, finite element method, motorcycle.

Resumo

Existem dois tipos de braço oscilante: o duplo braço oscilante e o monobraço oscilante. Ambos têm a mesma funcionalidade. No entanto, há algumas vantagens e desvantagens de cada uma delas, o que pode ajudar na escolha de uma em detrimento da outra.

O objetivo desta dissertação é substituir um duplo braço oscilante de um motociclo com um monobraço oscilante. Apesar de, o motociclo escolhido ser de todo-o-terreno, neste estudo apenas se vai testar os esforços de situações a que um motociclo de estrada esteja sujeito.

Primeiramente, as vantagens e desvantagens de cada tipo de braço oscilante vão ser descritas, as rigidezes torsional e lateral do duplo braço oscilante inicial são calculadas, os pontos críticos e as situações críticas são descritas e detalhadas. Neste capítulo foi concluído que o zona crítica é a estrutura onde está apoiada a suspensão . Para além disso, concluiu-se que braço oscilante está sobre maiores esforços internos quando há uma força normal equivalente ao dobro do peso total do motociclo aplicada na roda traseira.

Seguidamente, o monobraço oscilante foi desenhado no *Solidworks* e a rigidez torsional e lateral foram calculadas. Depois, uma análise de sensibilidade foi realizada e posteriormente o processo de iteração de forma a diminuir a massa afetando o mínimo possível as rigidezes foi efetuado.

O projeto final foi selecionado e comparado com o projeto inicial. Foi obtido uma massa equivalente. No entanto, a rigidez torsional e lateral estão dentro dos valor normais, o que não acontecia no duplo braço oscilante.

Por fim, todas as outras condições foram testadas de forma a confirmar as suposições feitas.

Palavras-chave: Duplo braço oscilante, Monobraço oscilante, rigidez torsional, rigidez lateral, método dos elementos finitos, motociclo.

Agradecimentos

Começo aos meus pais e ao meu irmão apoio incondicional dado ao longo de toda a minha vida. Pelo facto de sempre terem dado valor à minha formação académica e como pessoa e por estarem sempre presentes para mim.

Em Segundo lugar, ao Prof. Mário Vaz por todo o conhecimento que foi imprescindível para a execução desta dissertação. Pela dedicação e empenho demonstrado durante a realização deste estudo.

Seguidamente, quero agradecer ao engenheiro Nuno Viriato pela sua disponibilidade.

Ao professor Luís Galamba pela ajuda indispensável, tanto pela formação que incentivou, como pela série de dúvidas que, mesmo com falta de tempo, tentou sempre solucionar.

Aos meus amigos pela grande paciência que sempre tiveram comigo, pelas imensas memórias que vou levar para o resto da minha vida, e pelo facto de me ajudarem nos momentos mais complicados.

Ao resto da minha família, em especial à minha madrinha e aos meu avós, que estão ou estiverem sempre prontos a ajudar e pela boa-disposição que funcionou como inspiração para mim.

"Never give up on your dreams. Keep sleeping"

Michael Clifford

Contents

List of Figures **xvii**

List of Tables **xxi**

1 Introduction **1**
1.1 About this project . . . 2
1.2 Method followed during the project . . . 2
1.3 Chapters . . . 3
1.4 Software . . . 3

2 Literature review **5**
2.1 Motorcycle . . . 5
2.2 The geometry of motorcycles . . . 7
2.2.1 Steering angle . . . 7
2.2.2 Roll or Lean angle . . . 7
2.2.3 Slip angle . . . 8
2.2.4 Rake or Castor angle . . . 10
2.2.5 Camber angle . . . 10
2.2.6 Wheelbase . . . 10
2.2.7 Center of Gravity (CoG) . . . 10
2.3 Degrees of freedom of a Motorcycle . . . 11
2.4 The Swingarm and its evolution . . . 11
2.5 Types of Swingarms . . . 14
2.5.1 Movement . . . 14
2.5.2 Structure . . . 15
2.5.3 Consctrution Methodology . . . 16
2.5.4 Manufacturing process . . . 17
2.6 Reinforcement elements . . . 18
2.7 Rear Suspension . . . 19
2.8 Aluminium Swingarms . . . 22
2.8.1 Aluminium DSSA . . . 22
2.8.2 Aluminium SSSA . . . 22
2.9 Carbon Fiber Swingarms . . . 25
2.9.1 Carbon Fiber DSSA . . . 25
2.9.2 Carbon Fiber SSSA . . . 26

3 Problem Description **27**
3.1 Different approaches to the problem . . . 27
3.2 Objectives of the Project . . . 28
3.3 Material . . . 31
3.4 Safety Factor . . . 34
3.5 Motorcycle Selection . . . 36
3.6 Loads . . . 37
3.6.1 Weight distribution . . . 37
3.6.2 Braking . . . 41
3.6.3 Cornering . . . 45
3.6.4 Landing on the rear wheel . . . 50
3.7 Loads in different situations . . . 52
3.8 Leyni Test . . . 52
3.9 Boundary Conditions . . . 53

4 Aluminium Double Sided Swingarm **55**
4.1 Stiffness Calculation . . . 56
4.1.1 Torsional Stiffness . . . 56
4.1.2 Lateral Stiffness . . . 59
4.2 Loads applied on the swingarm . . . 61
4.3 Load Simulation . . . 62
4.3.1 Weight distribution of the motorcycle . . . 62
4.3.2 Weight distribution of the motorcycle and rider . . . 63
4.3.3 Braking . . . 64
4.3.4 Straight line . . . 65
4.3.5 Cornering . . . 66
4.3.6 Landing on the Rear wheel . . . 67
4.3.7 Stress concentration . . . 68
4.3.8 Safety factor of each situation . . . 69
4.3.9 Conclusions . . . 69

5 Single Sided Swingarm **71**
5.1 Standard Design . . . 71
5.2 Requirements . . . 74
5.3 Stiffness Calculation . . . 74
5.3.1 Lateral Stiffness . . . 75
5.3.2 Torsional Stiffness . . . 75
5.4 Initial Design . . . 77
5.4.1 Part1 . . . 79
5.4.2 Part2 . . . 80
5.5 Second Design . . . 81
5.5.1 Part1 . . . 81
5.5.2 Part2 . . . 82
5.6 Loads calculation . . . 83
5.7 Iterations . . . 84
5.7.1 Terminology . . . 85
5.7.2 Method of Iteration . . . 85
5.7.3 Stiffness Parameter . . . 86
5.8 Part1 . . . 87
5.8.1 Hierarchy of changes . . . 87

5.8.2 Iteration . . . 92
5.8.3 Final design of Part1 . . . 92
5.9 Part2 . . . 93
5.9.1 Hierarchy of changes . . . 93
5.9.2 Iteration . . . 97
5.9.3 Final Design of Part2 . . . 97
5.10 Comparison . . . 98
5.11 Safety Factor confirmation . . . 99

6 Conclusion **101**

Bibliography **103**

A AJP PR7 **111**

B Codes **119**
B.1 Script code to calculate loads during cornering . . . 120
B.2 Script code to calculate loads on a double sided swingarm . . . 121
B.3 Script code to calculate loads on a single sided swingarm . . . 122

C Anexo em volume separado **123**

D Mesh **125**
D.1 Double Sided Swingarm . . . 125
D.2 Single Sided Swingarm . . . 126

E Final Design **129**

Notation

Symbols

Chapter 2

δ	Steering angle
ϕ	Roll / Lean angle
θ	Slip angle
ε	Rake or Caster angle
β	Camber angle
p	Wheelbase

Chapter 3

a	Distance between front wheel and the CoG
b	Distance between rear wheel and the CoG
h	Height of the CoG
m	mass
N_f	Vertical load on the front wheel
N_r	Vertical load on the rear wheel
N_{f1}	Vertical load on the front wheel considering only the motorcycle
N_{f2}	Vertical load on the front wheel considering the motorcycle+rider
N_{r1}	Vertical load on the rear wheel considering only the motorcycle
N_{r2}	Vertical load on the rear wheel considering the motorcycle+rider
a1	Distance between front wheel and the CoG considering only the motorcycle
a2	Distance between front wheel and the CoG considering the motorcycle+rider
b1	Distance between rear wheel and the CoG considering only the motorcycle
b2	Distance between rear wheel and the CoG considering the motorcycle+rider
m1	mass of the motorcycle
m2	mass of the motorcycle+rider
g	gravitational acceleration
S_f	Friction force on the front wheel
S_r	Friction force on the rear wheel
d	Deceleration
N'_f	Vertical load on the front wheel while braking
N'_r	Vertical load on the rear wheel while braking
N'_d	Dynamic Weight
W_b	Wheelbase (a+b)

μ	Coefficient of friction
a_{lf}	acceleration required to lift the front wheel
r_{lr}	deceleration required to lift the rear wheel
r_{sr}	deceleration required causing the front wheel to slide
a_{sf}	acceleration required causing the front wheel to spin
h_id	Ideal height of the CoG
F_c	Centrifugal force
V	Linear velocity
R	Radius of the curve
F_t	Lateral friction force
μ	static coefficient of friction
μ_x	effective tractive coefficient
μ_y	effective lateral coefficient of friction
R_c	radius of the rear wheel
R_r	radius of the rear sprocket
$h_{falling}$	falling vertical height
η	efficiency of the conversion of kinetic energy
δ_{static}	deflection of the component due to a static force

Chapter 4

$K_{Torsional}$	Torsional Stiffness
$K_{Lateral}$	Lateral Stiffness
F_x	Force in the x direction on the swingarm
F_y	Force in the y direction on the swingarm
F_z	Force in the z direction on the swingarm
F_k	Suspension force
M_x	Moment the center of the spacer about the x direction
M_y	Moment the center of the spacer about the y direction
M_z	Moment the center of the spacer about the z direction
R_c	radius of the rear wheel
R_r	radius of the chain sprocket
d	distance of the moment arm

Chapter 5

u	lateral distance between the mid plane of the wheel and attachment to the swingarm
e	lateral distance between the mid plane of the wheel and the chain sprocket
F_x	Force in the x direction on the swingarm
F_y	Force in the y direction on the swingarm
F_z	Force in the z direction on the swingarm
F_k	Suspension force
M_x	Moment the center of the spacer about the x direction
M_y	Moment the center of the spacer about the y direction
M_z	Moment the center of the spacer about the z direction

Acronyms

FEM	Finite Element Method
FEA	Finite Element Analysis
GP	Grand Prix
SSSA	Single Sided Swingarm
DSSA	Double Sided Swingarm
cc	cubic capacity
GT	Gran Turismo
IF	Impact Force
WD	Weight distribution
SF	Safety factor
VD	vertical displacement
WHO	World Health Organization
UN	United Nations

Units

kg	kilogram
mm	millimeter
N	Newton
kN	kilonewton
km	kilometer
h	hour
º	degree
MPa	megapascal

List of Figures

2.1 Motorcycle's degrees of freedom 6
2.2 Motorcycle assembly during a curve and representation of various angles 7
2.3 Roll Angle Representation 8
2.4 Representation of the need of the slip angle in order to make a turn 8
2.5 Representation of how a slip angle results in a lateral sliding velocity, causing a lateral force 9
2.6 Linear and angular motions of a Motorcycle 11
2.7 Motorcycle developed by Vincent Company 12
2.8 Early stages of the BMW single sided swingarm 13
2.9 BMW R80G/S with a single sided swingarm 13
2.10 Motorcycle containing a fixed arm 14
2.11 Single Sided Swingarm 15
2.12 Double Sided Swingarm 15
2.13 Boxed Swingarm 16
2.14 Tubular Single Sided Swingarm 16
2.15 Bimota DB5 motorcycle and its swingarm 17
2.16 Different swingarm reinforcement elements 18
2.17 Classical suspension design and classical suspension on Guzzi California 19
2.18 Cantilever Monoshock suspension design and Cantilever Monoshock on Aprilia RS 125 20
2.19 Schemes of rear suspension with progressive-link 21
2.20 Schemes of rear suspensions with four-bar and six-bar linkage 21
2.21 Double Sided Swingarm made of Aluminium 22
2.22 Honda RC30 and its single sided swingarm 23
2.23 Honda RC45 Swingarm 23
2.24 Ducati 916 Single Sided Swingarm 24
2.25 BMW GS1200 Single Sided Swingarm 24
2.26 Ducati's carbon fiber swingarm, Qatar 2018 25
2.27 BMW's carbon fiber swingarm which gained the innovation award 25
2.28 Ducati 1299 Superleggera single Sided Swingarm 26

3.1 Torque-angle of three swingarms used by Kawasaki Team in the 2008 Superbike Championship 29
3.2 Measurement of stiffness by *Armentani et al.*. a- Torsional stiffness without spacer and spindle. b- Lateral stiffness with spacer and spindle 30
3.3 Cost of carbon fiber and aluminium in 2010 and the expected scenario in 2030 . . 33
3.4 AJP PR7 2021 36
3.5 Simple Motorcycle model of the weight distribution 38

3.6 Simple Motorcycle model of the loads during braking 42
3.7 Influence of braking force due to deceleration on the front and rear wheel 44
3.8 Simple Motorcycle model of the loads during cornering 46
3.9 Graph the turn radius that corresponds to various road speeds for different lean angles. 47
3.10 Maximum Lean angle for different motorcycles 47
3.11 Effective roll angle 48
3.12 External loads during cornering 50
3.13 Wheelie of the front wheel 51
3.14 Wheelie of the rear wheel maneuver on a Buell SI Lightning 51

4.1 Double sided swingarm 55
4.2 *Cossalter's* aproach for measurement of torsional and lateral stiffness 56
4.3 Torsional Test according to *Cossalter* 57
4.4 Simulation of torsional test with different torques a-48.8 Nm b-122 Nm, c-244 Nm, d-1220 Nm 57
4.5 Graph representing how angular displacement and torque are related 58
4.6 Lateral stiffness test according to *Cossalter* 59
4.7 Simulation of lateral test with different loads a-500 N, b-1000 N, c-2000 N, d-5000 N 59
4.8 Graph representing how displacement and lateral load are related 60
4.9 Simulation results of the influence of the motorcycle's weight distribution on the swingarm 62
4.10 Effect of the weight distribution of the motorbike on the rear suspension mount axle 62
4.11 Simulation results of the influence of the weight distribution of the motorbike and rider on the swingarm 63
4.12 Effect of the weight distribution of the motorbike and rider on the rear suspension mount axle 63
4.13 Simulation results of the influence of braking on the swingarm 64
4.14 Effect of braking on the rear suspension mount axle 64
4.15 Simulation results of the influence of maximum tension scenario on the swingarm 65
4.16 Effect of maximum tension scenario on the rear suspension mount axle 65
4.17 Simulation results of the influence of cornering on the swingarm 66
4.18 Effect of cornering on the rear suspension mount axle 66
4.19 Simulation results of the influence of landing on the rear wheel on the swingarm . 67
4.20 Effect of landing on the rear wheel on the rear suspension mount axle 67
4.21 Stress Concentration on each situation 68

5.1 Rear wheel mount on a single sided swingarm 71
5.2 Chain sprocket location on both types of swingarms 72
5.3 Ducati Panigale V4's rear motorcycle rim 73
5.4 Rear wheel and Single sided swingarm 73
5.5 Lateral stiffness test of SSSA 75
5.6 Torsional stiffness test measurements 76
5.7 Lateral stiffness test of SSSA 77
5.8 Part1 78
5.9 Part2 78
5.10 Lateral Stiffness test Part1 79
5.11 Torsional Stiffness test Part1 80
5.12 Torsional and Lateral Stiffness test Part1 80

5.13 Hollow Structure Part1 82
5.14 Hollow Structure Part2 82
5.15 Illustration of possible modification 84
5.16 Representation of the standard range of torsional and lateral stiffness on left and on the right demonstrates that by multiplying the range interval of K_l by 2 and K_t by 1.6 both intervals become 1600-3200 in their respective units Blue-lateral stiffness, Green-torsional stiffness 86
5.17 The variation of the stiffness parameter of three points with different properties. It shows that the stiffness of parameter defined can have the same value for different torsional and lateral properties 87
5.18 Lateral stiffness decrease by changing thickness on *Part1* 88
5.19 Torsional stiffness decrease by changing thickness on *Part1* 88
5.20 Stiffness parameter change with thickness on *Part1* 89
5.21 Torsional stiffness and Lateral change with height on *Part1* 90
5.22 Stiffness Parameter variation with height on *Part1* 90
5.23 Torsional stiffness and Lateral change with width on *Part1* 90
5.24 Stiffness Parameter variation with width on *Part1* 91
5.25 Final Design Part1 *Part1* 92
5.26 Lateral stiffness decrease by changing thickness on *Part2* 93
5.27 Torsional stiffness decrease by changing thickness on *Part2* 94
5.28 Stiffness parameter change with thickness on *Part2* 94
5.29 Torsional stiffness and Lateral change with height on *Part2* 95
5.30 Stiffness Parameter variation with height on *Part2* 95
5.31 Torsional stiffness and Lateral change with width on *Part2* 96
5.32 Stiffness Parameter variation with width on *Part2* 96
5.33 Final Design *Part2* 97

B.1 Script code to calculate loads during cornering 120
B.2 Script code to calculate loads on a double sided swingarm 121
B.3 Script code to calculate loads on a single sided swingarm 122

C.1 Simulation results Part1 123
C.2 Simulation results Part2 124

D.1 Mesh Convergence double sided swingarm 125
D.2 Mesh Convergence of *Part2* single sided swingarm 126
D.3 Refined mesh on fillets with high concentration of stresses 127

List of Tables

3.1 Comparison of torsional and lateral stiffness of swingarms in the literature 31
3.2 Properties aluminium alloy Alufont-52 33
3.3 Safety factor characteristics accordingly to *Pugsley Method* 35
3.4 Ranks of Parameters given to the swingarm 35
3.5 Specifications of AJP PR7 37
3.6 Meaning of each abbreviation 39
3.7 Weight Distribution of AJP Galp 50 and AJP PR4 40
3.8 Meaning of each abbreviation 43
3.9 External loads during 2 extreme conditions 50
3.10 Loads on the motorcycle 52

4.1 Torque and calculation of angular displacement 58
4.2 Comparison of torsional Stiffness 58
4.3 Comparison of torsional and lateral stiffness of swingarms in the literature 60
4.4 Double sided Swingarm loads 61
4.5 Safety factor for each simulation 69

5.1 Properties of the second design of *Part1* 81
5.2 Properties of the second design of *Part2* 82
5.3 Single sided Swingarm loads 83
5.4 Alteration Hierarchy *Part1* 91
5.5 Iteration process of *Part1* 92
5.6 Alteration Hierarchy *Part2* 96
5.7 Iteration process of *Part2* 97
5.8 Comparison of the final designs with double sided swingarm 98
5.9 Safety factor during different conditions 99

D.1 Mesh Convergence values in double sided swingarm 126
D.2 Mesh Convergence values in *Part2* 127

Chapter 1

Introduction

Swingarm is the most important component of the rear suspension. The main purpose of a motorcycle's swingarm is to link the rear wheel to the frame and it is crucial to support the rear axle as well as pivoting vertically to allow the suspension to absorb bumps on the road [1, 2].

It is possible to find two main types of swingarms. Although, both have the same function the structure is completely different. On the one hand, there is the traditional two arms swingarm, which is component that locks the rear wheel by both sides of the axle. On the other hand, the single sided swing arm holds the rear wheel only by one side [1, 3].

As it was previously said, both types of swingarm have the same function. However, there are some pros and cons on both of them, which could help selecting one instead of the other.

The main advantage of the single sided swingarm is that it is easier to have access to the rear wheel [4], which can result in a faster maintenance in case it is needed to change the rear wheel or to simply clean the rims [5].

Usually, this type of swingarms is mainly seen in endurance races, where a single sided swingarm can save seconds with a faster change of the rear wheel [4]. This for example can be very useful, when the weather condition changes and it is needed to substitute dry to wet tires, or the opposite, and the rider prefers to use the same bike instead of switching.

Furthermore, a single sided swingarm is considered to have an aesthetically appealing design on the motorcycle, so it can be also considered a design choice [3, 6]. It also facilitates the test of different rates of chain transmission which can be helpful in competitions [2].

However, there are some drawbacks to using this type of swingarm over a traditional double sided swingarm. The most important one is the fact that there is a twisting moment acting on the swingarm as a result of the asymmetry, which is not present in a conventional symmetrical swingarm. [4, 6]. As a result, more material or a more complex design may be required, thereby increasing the unsprung mass of the motorcycle's rear end or lead to a more expensive component [6].

Other disadvantages of the single-sided swing arm include the necessity for a particular stand and the fact that, in most cases, removing the rear wheel will necessitate the use of a huge sprocket

or a special attachment.

.

1.1 About this project

This project was done with the collaboration of INEGI, *Instituto de Ciência e Inovação em Engenharia Mecânica e Engenharia Industrial*, which is a private non-profit institution, founded in 1986. The main INEGI's goal is to promote investigation of technological innovation, oriented towards industries' development [7].

The aim of the project is to characterize a component that is submitted to complex loads and to underline the importance of safety during product's conception. It is crucial to understand and identify the critical conditions that a swingarm is submitted during its lifetime. Furthermore, it is important to obtain the highest stresses during these situations and identity the critical points.

This project emphasizes the importance of simulation and numerical models as a tool to predict entire systems, test them and track the problems even before a real prototype has even been built in order to help during the conception of a new product.

1.2 Method followed during the project

1. Verify possible critical situations to the swingarm
2. Describe the loads that are applied to the motorcycle during that situation
3. Describe boundary conditions
4. Program a script in order to calculate the loads on each type of swingarm
5. Simulation tests on the double sided swingarm, in order to calculate whether or not the swingarm yields, to conclude which are the critical situation, the critical points and calculate its stiffness.
6. Design the single sided swingarm (SolidWorks), having in mind the critical points and some other characteristics found in single sided swingarms of manufacturers like Ducati.
7. Optimization of the single sided swingarm in order to reduce its mass
8. Simulation tests on the single sided swingarm to check if the swingarm yields during any situation.

1.3 Chapters

- Chapter 1: This chapter presents a brief introduction, the motivation ,and objectives of this project as well as a description of the method and report.
- Chapter 2: Description of the main parts that a motorcycle contains and the evolution of the swingarm. It will also be referred some motorcycles containing single sided swingarms, their characteristics and a possible explanation to why the company decided to have a SSSA.
- Chapter 3: The material will be selected, and it will be identified the critical situations of the swingarm, the respective loads on the motorcycle are calculated and boundary conditions are defined.
- Chapter 4: Calculation of the torsional and lateral stiffness using FEM and analysis of the critical situation.
- Chapter 5: Draw of the SSSA using Solidworks, taking into account the critical points that Chapter 4 concluded. Numerical simulation of the drawn swingarm of a single sided swingarm is used in order to optimize it.
- Chapter 6: The conclusions of the work are described and some possible future works are presented.

1.4 Software

- Solidworks
- Abaqus
- Octave
- Microssoft Office Excel
- CES Edupack

Chapter 2

Literature review

2.1 Motorcycle

The first motorcycle that has ever been built was designed was designed in Stuttgart, Germany, by the German engineers Gottlieb Daimler and Wilhelm Maybach in 1885 [8]. Ever since from early bicycles, scientist searched the way to make transport on public roads more automated and faster. With the previous goal in mind, in the last one and a half century many inventors tried to make their version of the motorcycle.

Since then, the motorcycles have been evolving becoming faster and safer.

In spite of engineers' best effort to turn the motorcycles and the others road transports as safe as possible, every year approximately 1.3 million people die as a result of road traffic accident and it is expected to increase to 2.4 million people by 2013 [9]. It is considered the leading cause of death of people aged 5-29 [9].

In the United States, the chance of a motorcyclist being killed on the road is estimated to be 30 times higher per vehicle mile traveled than that of a passenger car driver [10].

This numbers underline the importance of taking all the safety measures necessary to turn the vehicle as safe as possible. According to WHO [9], if the UN regulations vehicle safety were applied during manufacturing and production, a large number of lives could be saved. This emphasizes the significance of simulation in the development of these vehicles. Even before a prototype is produced, it is possible to test the worst outcome from the lifetime of a certain vehicle component.

These virtual tests in spite of being very helpful, cannot replace physical testing [2].

Definition of Motorcycle

Accordingly to [11] and considering the motorcycle's suspensions as a rigid body, it is possible to consider a motorcycle as composing of 4 simple rigid bodies:

- the rear assembly, which consists of the saddle, the tank, and the transmission for the motorcycle.

- the front assembly, which includes the fork, steering head, and handlebars.
- the rear wheel
- the front wheel

Due to the fact that each component of the motorbike has six degrees of freedom, the complete motorcycle has a total of 24 degrees of freedom. However, the 3 revolute joints constrain 15 degree of freedom and due to the fact that 2 wheel are in constant contact with the ground, 6 more degree of freedom are inhibited [11]. Three main movements may be connected with a motorcycle's three degrees of freedom, which results in 3 degrees of freedom, as represented in figure 2.1, which are:

- forward motion (represented by rear wheel rotation);
- roll motion along the straight line that connects the tire contact points on the road plane;
- steering rotation.

If it is considered that during certain road conditions it is possible to verify lateral and longitudinal slippage, actually, there is a total of 7 degrees of freedom [11]:

- forward motion of the motorcycle,
- roll motion;
- steering rotation, dependent of the handlebar rotation;
- front wheel's longitudinal slippage;
- rear wheel's longitudinal slippage;
- front wheel's lateral slippage;
- rear wheel's lateral slippage.

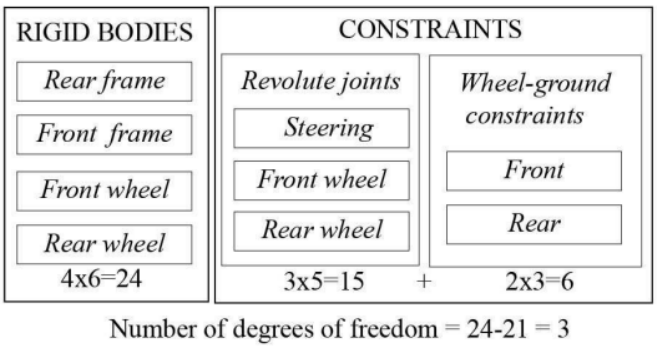


Figure 2.1: Motorcycle's degrees of freedom and its constrains Source: [11]

2.2 The geometry of motorcycles

In the beginning, it is essential to comprehend the fundamental process of a motorcycle and some terms which will be crucial to the remainder of the thesis, such as angles and distances. To comprehend this, assuming a motorcycle making a turn (figure 2.2), numerous parameters can be analyzed and described in detail.

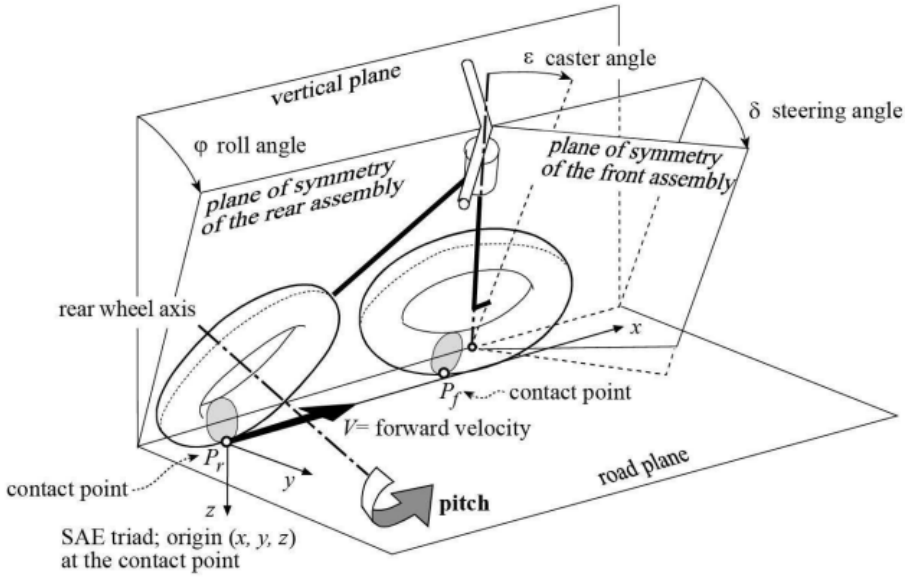


Figure 2.2: Motorcycle assembly during a curve and representation of various angles Source: [11]

2.2.1 Steering angle

The steering angle δ is the angle that the handlebar is submitted in relation to the steering axis, figure 2.2.

A positive steer angle occurs whenever the handlebars are turned to the left for a left-hand turn, while a negative angle occurs during or counter-steering, which occurs when the handlebars are pointed to the left when the turn is to the right [12].

Steering angle is reasonably simple to determine using a rotary potentiometer. These devices often have a movement range of up to 270 degrees, which is substantially more than the complete possible steering movement [11].

2.2.2 Roll or Lean angle

Roll angle or Lean angle ϕ [13] is the angle measured when a motorbike has to shift direction and the rider tends to fall over in order to make the turn. [14], as represented in figure 2.3.

In more detail, during cornering, motorcycles tend to reach a lean angle that depends on both their linear speed and the curvature of the trajectory that the motorcycle is underway, which is very similar to the road curvature [15].

Increasing the speed of the motorcycle makes necessary a bigger roll angle. Likewise, the curvature is higher for smaller curve radius, hence for tighter curves, which leads to higher roll angles. To sum up, increasing the curvature or the linear speed raises the required roll angle for a successful turn [8, 15].

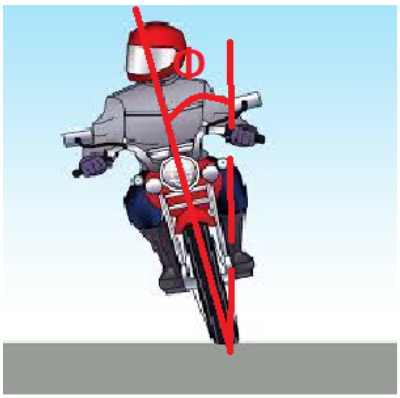


Figure 2.3: Roll Angle Representation Source: [16]

2.2.3 Slip angle

The slip angle θ is considered, the angle described between the tangent of the line of curve and the intersection between plane that contains the wheel with the plane of the road [14, 17].

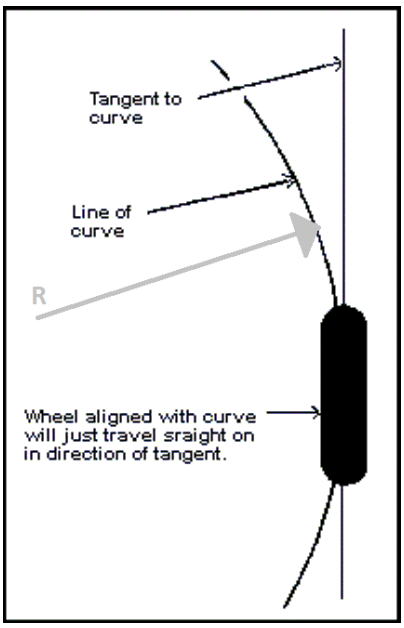


Figure 2.4: Representation of the need of the slip angle in order to make a turn Source: [12]

Considering a motorcycle that is making a turn following trajectory with radius R. As it is possible to see from figure 2.4 when a motorbike makes a curve, if the tire is aligned with the tangent direction of the curve, it is assumed that the motorcycle will not turn but will continue onward and go on a straight direction without creating any cornering force [14, 18].

Because of that, there needs to be something done in order to generate some cornering force and persuade the vehicle to make the turn [12]. It is possible to force the vehicle into turning by rotating the wheels to the inside of the curve line [14].

Although, cars work under a very large side slip angle, the same does not happen to motorcycles, which have a considerably low side slip angle and can go up to 2º [17].

According to figure 2.5, it is possible to decompose the velocity of the curve, which is tangent to the direction of the curve, into a velocity on the direction of the wheel and perpendicular to it. Because of that, it is possible to consider that the total velocity of the motorcycle is not considered just in the wheel direction but there is a sliding speed perpendicular to the wheel, in other words, the motorcycle is sliding sideways [12].

$$tan(\theta) = \frac{V_l}{V_w} \tag{2.1}$$

On the other hand, the total force generated by sliding (F_l) may likewise be divided into two components. The first one, the curve force, is characterized as being perpendicular to the direction of movement. The second, drag force (F_d), acts in the opposite direction of movement, and may be considered as a friction force [14].

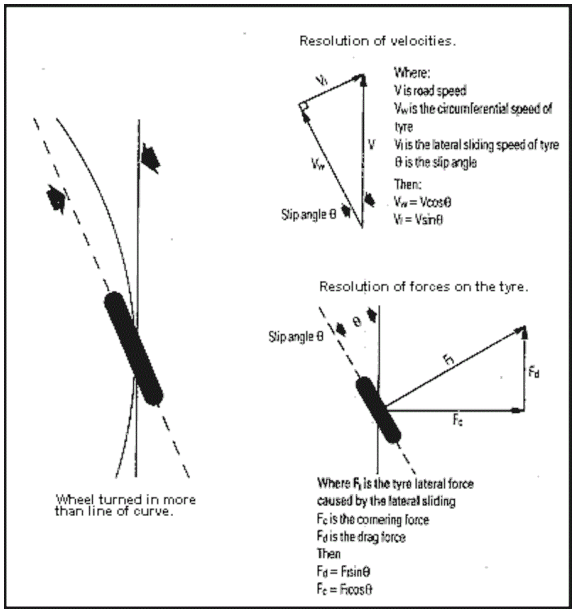


Figure 2.5: Representation of how a slip angle results in a lateral sliding velocity, causing a lateral force Source: [12]

2.2.4 Rake or Castor angle

Rake or Caster angle ε, is the angle between both the steering axis and the vertical [12]. Most of the times, in a motorcycle the castor angle varies between 22 and 30º [19].

However, competition motorcycles often have a lower castor angle, resulting in a smaller trail, which results in less stability but a considerably quicker direction compared to regular motorcycles, which have a higher castor angle and, thus, more trouble turning while having a better stability [19].

2.2.5 Camber angle

Camber angle β is defined as the inclination of the wheel. Two distinct camber angles exist, one for each wheel.

On the one hand, the camber angle of the rear wheel is always equal to the roll angle. However, on the other hand, when the steering angle is different than zero, for example during cornering, the camber angle of the front wheel is defined as a function of both the camber angle and the steering angle, hence the camber angle β is different than the roll angle ϕ [11, 12]

Comparing to cars, which operate at a very low camber angle, conventional motorbikes may have camber degrees of up to 55º while cornering [17].

2.2.6 Wheelbase

Wheelbase p is regarded to be the horizontal distance between the front and rear axles, or the distance between the motorcycle's contact points with the road.

The wheelbase depends on the motorcycle and it is designer by the manufacturer. Because of that, for each bike it is possible to find the wheelbase on the specifications of it.

However, for each type of motorbike, there is a wheelbase value that is somewhat comparable. The wheelbase of small scooters is roughly 1200mm, the one of light motorcycles (up to 125cc) is approximately 1300mm, for medium displacement motorcycles (up to 250cc) it may reach 1350mm, and in touring motorcycles the wheelbase can exceed 1600mm [11].

2.2.7 Center of Gravity (CoG)

The weight distribution is really important in the design and maintenance of the motorcycle due to the fact that a mistake can cause the center of gravity to change overloading either the front or rear wheel and causing problems of handling and changing completed the dynamics of the motorcycle. [14].

- increasing of the CoG leads to a higher weight transfer during braking and accelerating, while decreasing the lean angle at certain speed [20].
- approximating the CoG horizontally to the front wheel reduces the rear wheel's braking stability and acceleration traction. However, the probability of doing a wheelie during acceleration decreases [20].

- approximating the CoG horizontally to the rear wheel gives more stability when braking and traction while accelerating. However, doing a wheelie during acceleration becomes more likely [20].

2.3 Degrees of freedom of a Motorcycle

To understand the behaviour of a motorcycle it is important to note how it can move, in other words, what are its degrees of freedom. Most of the times people are familiar with the linear motions of the motorcycle, but this is not the case with its angular motions [12], which are illustrated in figure 2.6. All the possible angular motions and linear motions are described in this chapter.

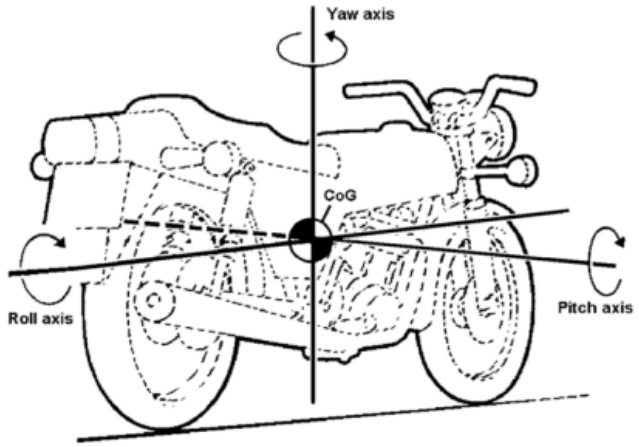


Figure 2.6: Linear and angular motions of a Motorcycle Source: [12]

- **Longitudinal/Forward Motion** - Linear motion in the direction the motorbike is traveling.
- **Lateral Motion** - Motion perpendicular to the direction of the motorbike.
- **Vertical Motion** - Linear motion in the vertical direction.
- **Pitch** - Angular motion of the motorcycle about the horizontal lateral axis.
- **Yaw** - Angular motion of the motorcycle about the vertical axis.
- **Roll** - Angular motion of the motorcycle about the longitudinal axis.

2.4 The Swingarm and its evolution

During the last two decades, due to the exponential engine power increasing that has been verified, the swingarm has required study and evolution in order to become stronger and stiffer [21]. Initially, the swingarm was nothing more than a fork with two tubes containing dampers, which was extremely weak and prone to deformation due to the arms' freedom of movement [22, 23].

As a result of the increasing stresses to which the swingarm is subjected, swingarms have become increasingly more complex, with increased thickness and diameter to support the applied loads while maintaining a low stiffness [2].

The first motorcycles didn't contain a formal suspension neither on the front wheel nor the rear wheels. However, engines were getting more and more powerful. Because of that, there was the necessity to avoid bumps [24].

Although there were already created several mechanisms of suspensions, they were not functional for a motorcycle. In 1913, an Indian created a swingarm rear suspension with four elliptic springs above. However, it was pretty flexible laterally, which caused so it to not sell. A few years later, in 1919, the British Coulson-B developed a motorcycle containing a rear suspension with short trails. It improved the comfort but it lacked rigidity so it was not really popular [24].

The swingarm took a long time to become standard because of the fact that most manufacturers preferred use rigid frames and a mechanism of springs underneath the rider's seats to minimize the impact of bumps rather than to adapt to the swingarm [25].

It was not until 1928, when the Guzzi brothers, Carlo and Giuseppe created what can be described as the first real swingarm, that was two basically to beams mounted on the rear axle that contained a rear suspension. This swingarm was introduced in Guzzi 497cc GT [25, 26]

The first swingarm being developed in Vincent company used the principle of a weight efficient strut to triangulate fork layout that was used in the production of motorcycles in 1928-1955. This approach is still being used in contemporary super bikes [12, 27, 24]. The motorcycle is represented in figure 2.7.



Figure 2.7: Motorcycle developed by Vincent Comapany Source: [25]

In 1935, Stanley Woods won a competition (The Senior Tourist at Isle of Man) using a Guzz motorcycle that contained a swingarm suspension having much better results than rigid motorcycles. This was a particularly important moment because it could not be ignored the potential of the swingarms [24].

In 1950, the famous "Norton featherbed" containing a frame with a plain swingarm showed an enormous stiffness at that time. This is probably the moment the swing just become globally recognized as the best solution [12].

Around the late 1940s, the first bikes with a single sided swingarm started to appear. However, it was not until the 1980s that this style of swingarm began to be included into commercially available versions [12, 28]. Early stages of the BMW single sided swingarm were fabricated from large diameter tubes made of steel and are represented in figure 2.8.

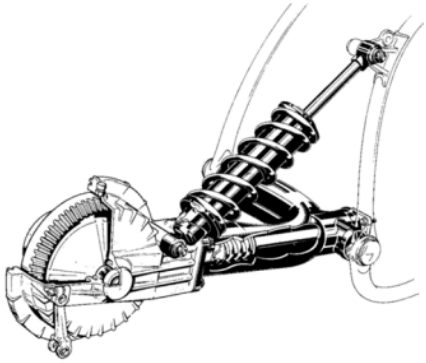


Figure 2.8: Early stages of the BMW single sided swingarm Source: [12]

In 1980, the BMW R80G/S the first motorcycle containing a singled sided swingarm was produced by BMW, shown in figure 2.9. It was called BMW Monolever and 21.864 units were sold [29, 30]. Since then, BMW has become the front runners of development of single sided swingarms and a lot of their models contain this type of technology [31].



Figure 2.9: BMW R80G/S with a single sided swingarm Source: [32]

In the 2000s, swingarms started to grow in height and lower the width in order to increase stiffness, while maintaining a low weight. This was done in order to adjust to the growing roll angles verified and the swingarm had to act as a "side way suspension" [24].

Nowadays, the significant proportion of motorcycles feature a swingarm containing reinforcement elements that increase the stiffness without changing much the weight of the component [2].

2.5 Types of Swingarms

2.5.1 Movement

There are two distinct sorts of swinging arms in terms of movement. Nowadays, every arm is termed a swingarm owing to its ability to move independently due to the suspension. However, prior to the swingarm being a standard, there were different types of techniques to avoid and minimize bumps [24].

Fixed

Fixed arms were utilized in the early days of motorbike design. It was incapable of absorbing any shock. Motorcycles equipped with this sort of arm often had springs that supported the rider's seat, therefore reducing bumps. [33].

However, there are still some motorcycles available without a swingarm, such as the one represented in figure 2.10. They are known as hardtail motorcycles and, as predicted, lack a rear suspension. The benefit of purchasing a motorbike without rear suspension is that it is much more affordable. However, comfort cannot be compared, which is why the market for this sort of motorbike is so small [34].



Figure 2.10: Motorcycle contained a fixed arm Source: [33]

Swinging

To increase the vehicle's rigidity and handling for the rider, a swinging arm was designed, which increased the vehicle's stability and strength. The swinging arm contains the suspension wheel, which enables the vehicle to move up and down independently over bumps [33]. As it was previously stated in chapter 2.4, just in 1950 this type of arms became widely used [24].

2.5.2 Structure

Single sided swingarm

The single sided swing arm, such as the one represented in figure 2.11, holds the rear wheel only by one side. As it was stated in chapter 1, the main advantage of the single sided swingarm is that it is easier to have access to the rear wheel. However, there is a twisting moment acting on the swingarm, which is not present in a conventional double sided swingarm [4].



Figure 2.11: Single Sided Swingarm Source: [35]

Double sided swingarm

The double sided swingarm is considered to be the traditional two arms swingarm, which is component that locks the rear wheel by both sides of the axle [3, 36]. Due to the fact that there is no twisting moment, it may need less material and a simpler design, which may result in a more costly component and because of that it is often the component used in the majority of motorcycles [2, 37]. A double sided swingarm is represented in figure 2.12.



Figure 2.12: Double Sided Swingarm Source: [38]

2.5.3 Consctrution Methodology

Boxed

It is a swingarm characterized by having a hollow and closed section arms. These are then fitted with feet for attaching the wheel by welding or machined inserts [39].

Boxed swingarms benefit over tubular swingarms in that they have a bigger vertical section but a smaller horizontal part, which causes the swingarm to operate as a "side way suspension" [24], resulting in much improved handling while maintaining the same performance [40]. Figure 2.13 represents a boxed swingarm.



Figure 2.13: Boxed Swingarm Source: [39]

Tubular

Due to the tubes' lower stress carrying capacity in comparison to the boxed swingarm, the stresses on this form of swingarm may be rather considerable. To boost stiffness, numerous tubes are utilized and are joined by welding. However, boxed swingarms are often preferred as opposed to tubular ones [39, 41]. Figure 2.14 shows a tubular swingarm.

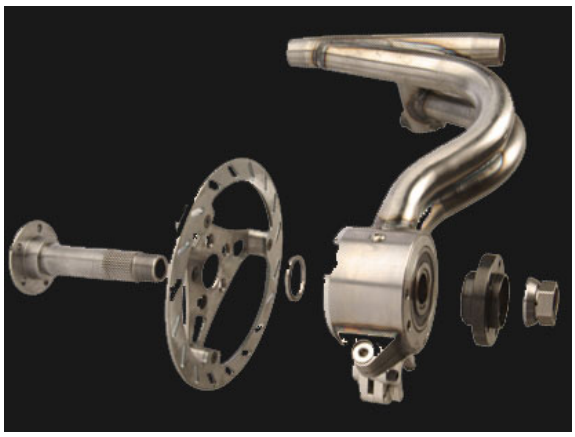


Figure 2.14: Tubular Single Sided Swingarm Source: [41]

Mixed

In this type of swingarm the tubes constitute the main part of the swingarm, there is a plate where the connection to the rear wheel is done and all the tubes are screwed there to the plate [39]. Bimota DB5 motorcycle has this kind of swingarm, represented in figure 2.15, which was designed to turn the motorcycle as aesthetically pleasing as possible [42].



Figure 2.15: Bimota DB5 motorcycle and its swingarm Source: [39]

2.5.4 Manufacturing process

Machining

Each piece is created from a raw component utilizing numerically controlled machine equipment. If the shape is very complex, it is feasible to combine many components to create a more complex structure. This technology has the benefit of allowing for variable thickness in various areas of the swingarm with great accuracy. However, since it is far more costly than the other approaches, it is only utilized in highly competitive environments where cost is not a factor [39].

Casting

A swingarm may be produced by casting it in a mold. However, various companies approach the production of swingarms with casting using different ways [39].

Yamaha [43] and AJP [30] cast the swingarm in a single piece in order to have the properties desired. In case of *Yamaha*, it is used advanced techniques for creating the core and low-pressure casting required. AJP, on the other hand, employs sand casting [30].

Additionally, it is possible to have individual swingarm components molded and then assembled using welding, as Accossato Racing does with their swingarm manufacture [44], or via screwing, as seen in the motorbike Bimota DB5 [42].

2.6 Reinforcement elements

Most cases, the swingarm characteristics is a consequence of the material chosen, the geometry and the structure of the swingarm. However, in some cases, the designer introduces a reinforcement element on the swingarm in order to increase its resistance [39].

Possible reinforcement elements applied to different swingarms are represented in figure 2.16.

- Ribs: elements that are used in casted swingarms and used to increase the structural resistance [33].
- Reinforcement truss: It may be lower or higher and permits increasing the stiffness and modifying the location of the object's cutting center without significantly affecting its weight [33].

  Cassani [45] explored the truss layout in order to increase it without adding weight. It was concluded that the truss contributes significantly to the bending and torsional stiffness of the swingarm [39].
- Internal bulkheads: elements used in boxed swingarms, which are attached to tubes that crosses the structure longitudinally [39].
- Inserts: Mainly, employed in the attachment to the frame and to the fixing of the wheel. The inserts put at certain points greatly enhance the stiffness of those positions [46].

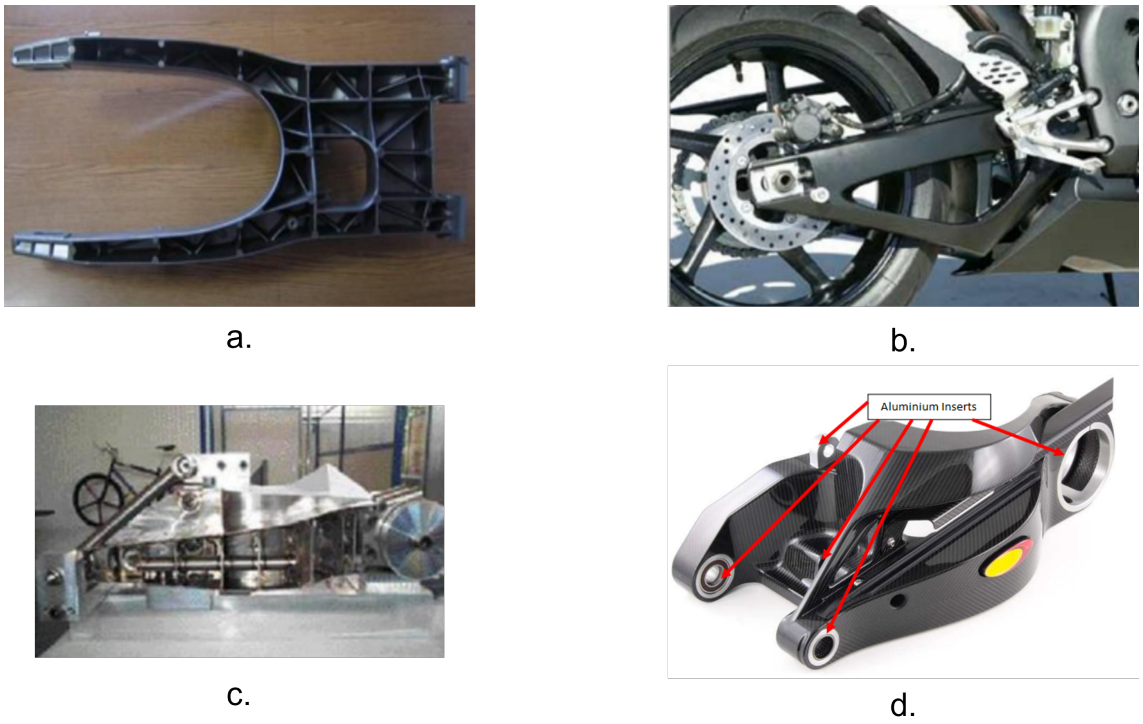


Figure 2.16: Different swingarm reinforcement elements. a. Ribs; b. Reinforcement truss; c. Internal bulkheads; d. Inserts. Source: [39, 46]

2.7 Rear Suspension

As noted before, the original motorbikes lacked a suspension system capable of absorbing road irregularities and bumps, and the initial suspension system consisted of springs beneath the seat, which was not the most effective method.

As time proceeded, however, rear suspension became widely recognized and explored in order to provide riders with the greatest potential comfort [39].

Suspension allows the wheel to move independently over bumps, supporting the chassis and rider through a spring or other elastic element without transmitting all of its movements to the chassis [24].

When suspension behavior is taken into account, the analysis of motorcycle dynamics becomes significantly more complicated. This is because imperfections on the road stimulate the suspensions, resulting in an oscillatory motion reliant on two vibration modes [45].

The classic rear suspensions were and still are one of the most common type of rear suspension verified on the rear swingarm [47]. Figure 2.17 represents the scheme of this type of rear suspension and the design on the Guzzi California motorcycle.



Figure 2.17: Classical suspension design and classical suspension on Guzzi California. Source: [47]

The advantages of this type of rear suspension were the following [11]:

- Constructional ease;
- Low reaction forces sent to the chassis;
- Efficient heat dissipation from shock absorbers.

However, there are also some drawbacks which this type of suspension [11]:

- Limitation of the vertical motion of the wheel

- Characteristic of force-displacement is not particularly progressive

To address these issues, the "Cantilever Monoshock" suspension variation of the traditional suspension was developed [47]. Monoshock designs date back to the 1930s, although substantial study and development occurred during the 1970s [22].

In 1973, Yamaha developed the idea of Vinent to create a triangular swingarm with a "Monoshock" rear suspension. This was the motorcycle that Hakan Andersson rode to win the finish round of the motorcycle world championships [24, 48]. Figure 2.18 represents the scheme of this type of rear suspension and the design on the Aprilia RS 125 motorcycle.

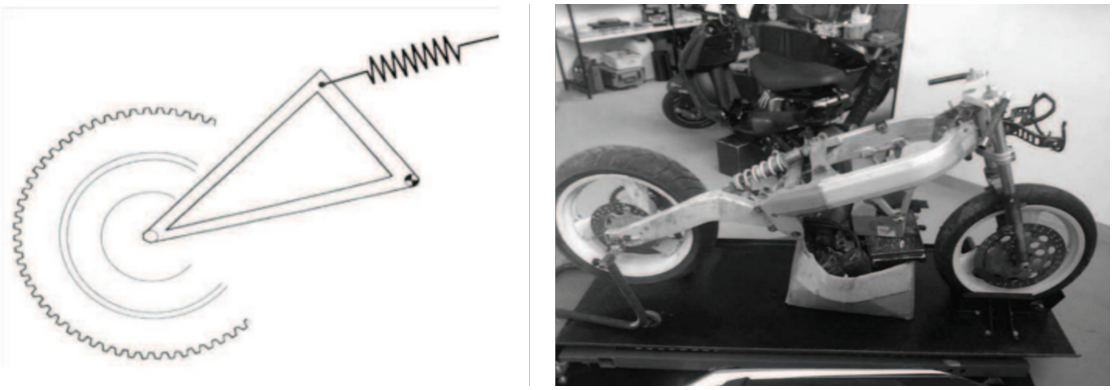


Figure 2.18: Cantilever Monoshock suspension design and Cantilever Monoshock on Aprilia RS 125 Source: [47]

This type of swingarm has the following advantages when comparing to the classical swingarm [11]:

- Ease of adjustment;
- Smaller unsprung mass;
- Higher torsional and lateral stiffness;
- Higher vertical motion of the wheel.

However, this type of rear suspension still did not have a characteristic of force-displacement particularly progressive and the fact that the spring-shock absorber unit was so close to the engine posed a difficulty [11]

To address the issue to turn the characteristic of force-displacement progressive, classic and cantilever systems came together with the introduction of a linkage in rear suspension to obtain the desired stiffness curves [11].

Modern sport and road racing motorcycles have progressive-link Monoshock suspension, which is a very modern version of the original concept [22].

Three different designs are generally based on the four-bar linkage:

- Unitrak design of Kawasaki: spring-damper situated between the rocker and the chassis (Figure 2.19.a)

- Pro-Link design of Honda: spring-damper situated between the connection rod and the chassis (Figure 2.19.b)
- Full Floater design of Suzuki: spring-damper situated between the rocker and the swingarm (Figure 2.19.c)

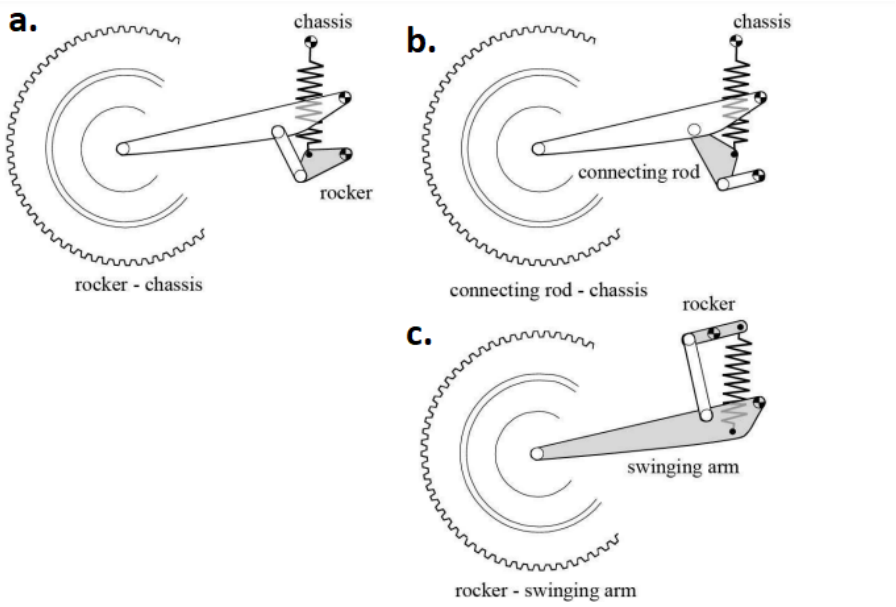


Figure 2.19: Schemes of rear suspension with progressive-link Source: [11]

Figure 2.20 represents the the four-bar linkage scheme as well as the six-bar linkage scheme.

Most of the times, the four-bar linkage is applied to motorcycles that contains a transmission using driveshaft with universal joints, for example BMW "Paralever" suspension [11].

On the other hand, although the six-bar linkage generates curves of force-displacement with unique progression of suspension stiffness, this mechanism is too complex and does not justify the gain in stiffness control [27].

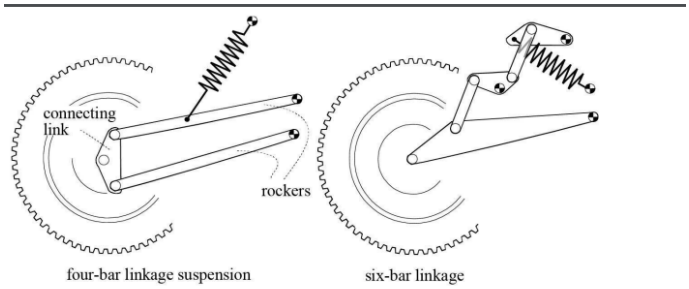


Figure 2.20: Schemes of rear suspensions with four-bar and six-bar linkage Source: [11]

2.8 Aluminium Swingarms

Aluminium is the most common material to construct swingarms. This is because it has a high stiffness-to-weight ratio in comparison to other materials and is rather affordable. Chapter 3.3 focuses on material selection and explains this material is advantageous.

2.8.1 Aluminium DSSA

Double sided swingarms made of aluminum are the most popular variety. It is often utilized by companies when projecting a swingarm, since it has a very basic design and deeply studied, making it convenient for the majority of companies to deal with. Figure 2.21 shows an aluminium double sided swingarm



Figure 2.21: Double Sided Swingarm made of Aluminium Source: [49]

2.8.2 Aluminium SSSA

Various companies produced motorcycles with single sided swingarms made of aluminium. While some companies produced it for racing, there are companies that use to regularly develop this type of swingarms in for the road, as they see more advantageous in comparison to double sided swingarms.

HondaRC30

The HondaRC30's single sided swingarm, represented in figure 2.22, is incredibly compact and lighweigh [50]. It was patented by ELF, company that worked since 1987 with Honda to produce swingarms [51].

It incorporated a special sprocket that allowed for a real faster rear wheel change and why this motorcycle was designed for endurance racing, and was responsible for the win of the back to

back World Superbike Championship in 1988 and 1989 by Fred Merkel [50, 52]. It was produced around 4700 units for 4 years that was in production and 5 of them were in Portugal [53].

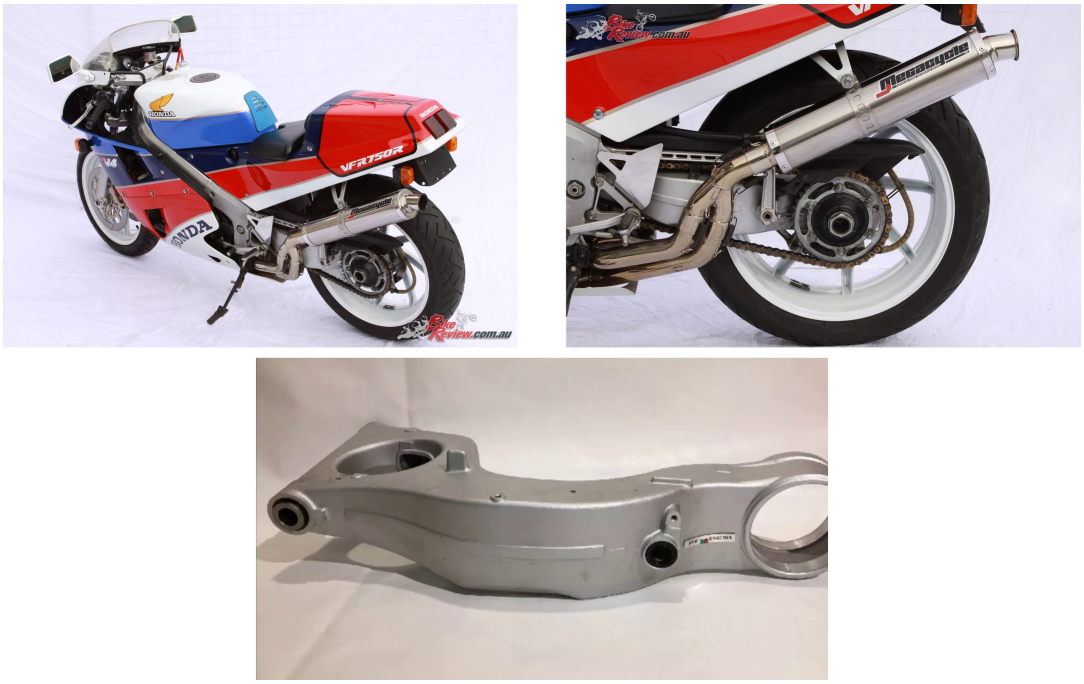


Figure 2.22: Honda RC30 and its single sided swingarm Source: [54, 55]

Honda RC45

Successor of the Honda RC30, and due to the high popularity of that later, in 1994, the Honda RC45 was also developed with a single sided swingarm, shown in figure 2.23. Initially created for road usage, it quickly made its way into competition, particularly in top-level endurance racing. Indeed, the RC45 shown here has a tremendous racing history [56].



Figure 2.23: Honda RC45 Swingarm Source: [56]

Ducati916

Ducati 916, is a motorcycle that contains an aluminium single sided swingarm, represented in figure 2.24, in order to provide faster rear wheel change during endurance racing. Ducati won 5 Superbike World Championship with Ducati 916 from 1994 to 1999 [57]. Journalist *Kevin Ash* [58] considered this motorcycle to be "one of the most influential machines of the last twenty years".



Figure 2.24: Ducati 916 Single Sided Swingarm Source: [59]

BMW GS1200

BMW has a long history of using single-sided swingarms in a lot of their models of motorcycles. They claim to be able to develop bikes with single sided swingarms that have a better torsional stiffness and are lighter than double sided swingarms [31]. This is because BMW, in some motorcycles, utilizes a transmission shaft to transmit power to the back wheel, and since the swingarm design would be more complicated, it was decided to include the transmission shaft into the swingarm [19]. The swingarm is represented in figure 2.25.

BMW GS1200, may be regarded as a large travel enduro motorcycle that lets riders to explore the world's most remote locations and must be suited for any conditions. [60]



Figure 2.25: BMW GS1200 Single Sided Swingarm Source: [61]

2.9 Carbon Fiber Swingarms

Carbon fiber swingarms are gaining popularity among the general public. It is easy to witness the benefits of carbon fiber on other components of the motorbike, including as the frame, sub-frame [62] for example of the BMW HP4 [63] , and it is only a matter of time until carbon fiber swingarms become more prevalent [64].

While carbon fiber swingarms have not yet been put into mass production motorcycles, there are some small production or specialist swingarms for racing which already using carbon fiber [62].

2.9.1 Carbon Fiber DSSA

Nowadays, carbon fiber double sided swingarms are mainly used for racing motorcycles, such as MotoGP, due to higher costs, added complexity to predict and makes disposal more challenging, as it is going to be explained more in detail in chapter 3.3.

During the MotoGP on Qatar 2018, Andrea Dovizioso's motorcycle contained a single sided swingarm made of carbon fiber represented in figure 2.26



Figure 2.26: Ducati's carbon fiber swingarm, Qatar 2018 Source: [64]

However, efforts are being done to obtain more data on this matter and how to easily implement this type of swingarm on a more regular basis. BMW Motorrad in 2018 won an award for the development of a carbon fiber swingarm, represented in figure 2.27

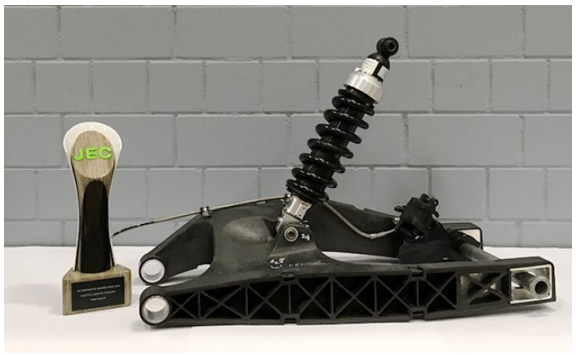


Figure 2.27: BMW's carbon fiber swingarm which gained the innovation award Source: [62]

2.9.2 Carbon Fiber SSSA

Carbon fiber swingarms with a single side are quite rare. The majority of those who have it did so as a result of a later purchase since the motorbike did not come equipped with that feature. However, in 2016, the Ducati 1299 Superleggera became the first motorbike to include a single-sided carbon fiber swingarm, [62] selling 500 units [65]. The swingarm designed by Riba Composites [65] weighs two pounds less than the aluminum model, and the carbon fiber mainframe, subframe, single-sided swingarm, and wheels are all constructed by carbon fiber [66].

Figure 2.28 shows the carbon fiber single sided swingarm of this motorcycle.



Figure 2.28: Ducati 1299 Superleggera single Sided Swingarm Source: [66]

Chapter 3

Problem Description

3.1 Different approaches to the problem

There are a lot of different approaches that was utilized in different projects of the design of a swingarm.

- *Smith* [4] applied the analysis of static load to have the minimum possible weight while maintaining the stiffness.
- *Airoldi et al.* [6] presented a swingarm made of aluminum and its redesign in carbon fiber. A genetic algorithm with 60 variables was utilized to determine the highest torsional stiffness with the least weight possible. The paper was concluded applying finite element method to the carbon fiber swingarm in order to determine if the stresses submitted to it would cause plastic deformation.
- *Sarti* [33] evaluated the torsional and lateral stiffness of SSSA and DDSA swingarms composed of both aluminum and carbon fiber in order to create an innovative carbon fiber single sided swingarm. The stiffness of the novel design was compared to that of earlier designs, and it was found that single sided carbon fiber swingarms could be used in a competitive environment.
- *Wajahath* [67] designed the best aluminum double sided swingarm feasible, taking into account the maximum loads tested during the motorcycle's life, while not considering its stiffness.
- *Chiarello* [39] converted an aluminum double sided swingarm used on a competition motorbike to a carbon fiber swingarm. It resulted in an increase in stiffness properties, such as vertical flexural stiffness by 18%, lateral flexion stiffness by 2%, and torsional stiffness by 4%, while reducing mass by 22%.
- *Spanoudakis et al.* [3] designed the front single sided swingarm of a new three-wheel electric motorcycle with the aim of keeping the overall weight to a minimum while withstanding all the loading scenarios.

- *Risitano et al* [1] goal was to relate objective data on the swingarm's stiffness and natural frequencies to the subjective comfort experienced by professional riders. For that, two riders experience three different swingarms, which were used in a competitive environment, with the main difference of them being the torsional stiffness of the swingarm. It was subsequently shown that the torsional and lateral stiffness of a motorbike might impact its handling. While a motorbike with a low stiffness value feels heavy and difficult to maneuver, a motorcycle with a high stiffness value feels easier to handle and a greater responsiveness.

- *Ramos* [27] employed an iterative strategy to increase the swingarm's lateral, vertical, and torsional stiffness while reducing its overall weight. It was demonstrated that a 66% weight reduction occurred from the first to the last iteration.

- *Cassani* [45] described the design process of the Ducati Monster S4R single sided swing arm. It was tested the rigidity of various layouts of swingarms. It was changed the truss or added a single pipe and test how it would affect to the overall behavior of the swingarm and its stiffness. In the end, it was calculated the stress field during the most dangerous loading conditions, which were considered to be the Lenyi bench test and during acceleration and added some reinforcement elements, in this case, ribs in order to support this loading conditions.

- *O'Dea* [68] utilised *Composites modeler* and fiber simulation to redesign a motorbike swingarm in carbon fiber.

3.2 Objectives of the Project

Taking into consideration the literature, it is feasible to conclude that it is ideal to have the most lateral and torsional stiffness possible in order to minimize the motorcycle's instability and improve its handling due to the faster response time, while maintaining the lowest possible weight.

Having a lightweight swingarm will reduce the unsprung mass of the rear part of the motorcycle, which improves the handling [5], enhances fuel efficiency, and reduces harmful emissions, resulting in a more environmentally friendly motorbike and increases the maximum acceleration of it.

In fact, almost all the literature takes into account mostly the effects of torsional stiffness in the motorcycle as it is possible to see from the text above and takes measures to maximise it, while having a light swingarm. However, it is also crucial that not only the swingarm is comfortable to the driver but also that it can sustain all the loading conditions that is submitted. Because of that, the aim of this project will be to design a single sided swingarm that respects the torsional and lateral stiffness that is contained in the literature and to test whether it can sustain all the loading conditions.

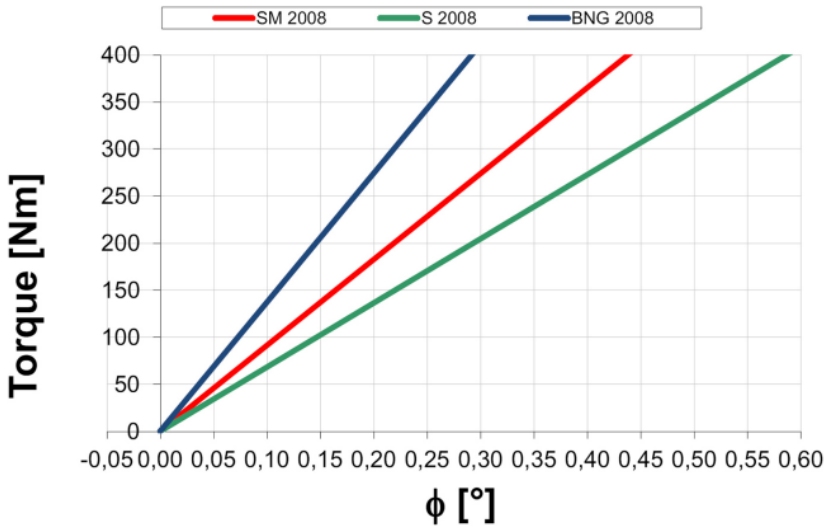


Figure 3.1: Torque-angle of three swingarms used by Kawasaki Team in the 2008 Superbike Championship. Source: [1]

General Stiffness of a Swingarm

Usually, the main concern is to obtain a good balance between torsional and lateral stiffness and have the minimum weigh possible [4]. In a single sided swingarm, such as the one that is going to be designed in this thesis, the torsional stiffness has two different values according whether it is considered clockwise or counterclockwise [1].

A data collection about the general lateral and torsional stiffness was made according to the literature. Regarding vertical stiffness, there are no reported common values in the literature [46].

- Accordingly to *Cossalter* [11], the general values of the swingarm stiffness are.
  - 800 kN/m to 1600 kN/m for lateral stiffness
  - 1000 Nm/deg to 2000 Nm/deg for torsional stiffness.

- *A*s previously stated, Risitano et al. [1] tested three distinct swingarms used by Kawasaki Team in the 2008 Superbike Championship, the primary distinction being the swingarm's torsional rigidity. These bikes were utilized in a real-world competitive situation, and measuring the stiffness of their swingarms can provide insight into the overall stiffness of motorcycles. The torsional rigidity of each of the three swingarms was determined, and because the swingarms were double-sided and almost symmetrical, the torsional stiffness values measured clockwise and counterclockwise were very similar.

  To measure the stiffness an experimental graph torque by angle was created and represented on figure 3.1 and using it and the slope of each line symbolizes the torsional stiffness of the swingarm.

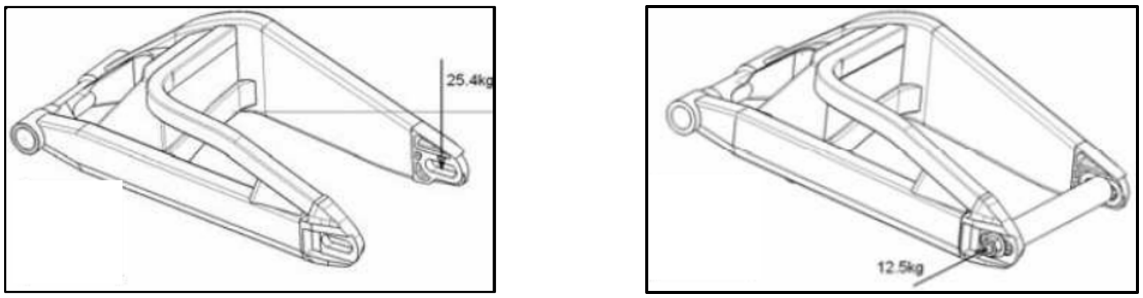


Figure 3.2: Measurement of stiffness by *Armentani et al.*. a- Torsional stiffness without spacer and spindle. b- Lateral stiffness with spacer and spindle. Source: [46]

  - S2008, made of aluminum alloy swingarm, with a mass of 5,265 kg had a torsional stiffness of 670 Nm/deg
  - SM 2008, made of aluminum alloy swingarm, with a mass of 6.850 kg had a torsional stiffness of 890 Nm/deg
  - BNG 2008, made of aluminum alloy swingarm, with a mass of 5,650 kg had a torsional stiffness of 1330 Nm/deg

- *Limebeer* [69] *and Sharp* [69, 70] stated that that it is required a torsional stiffness of 12.000 Nm/rad, which is 209.4 Nm/deg, for a high-performance motocycle in order to the frame be considered rigid.

- Research by *Armentani et al.* [71], testing the swingarms of Kawasaki ZX10R, Suzuki GSX R1000 and Honda CBR1000R both experementally and using FEA reached the values of:

  - Kawasaki ZX10R's swingarm with a torsional stiffness of 102.9 Nm/deg and a lateral stiffness of 603 kN/m.
  - Suzuki GSX R1000's swingarm with a torsional stiffness of 140.8 Nm/deg and a lateral stiffness of 804 kN/m.
  - Honda CBR1000R's swingarm with a torsional stiffness of 140.8 Nm/deg and a lateral stiffness of 965 kN/m.

  These values appear to be contradictory when comparing to the values that were stated previously. *Smith* [46] theorised that the torsional values were completely different from all other typical values due to the fact *Armentani et al.* [71] did not use spacer and spindle to measure the torsional stiffness and , because of that, higher displacements were measured by applying the load to only one arm when omitting the spacer comparing if they have used the spacer and spindle to simulate real life conditions. However, in case of lateral stiffness was determined using these elements, as it is demonstrated by figure 3.2 and the values are regarded to be trustworthy.

It is possible to create table 3.1 that summarizes the values of lateral and torsional stiffness accordingly to the literature. It is possible to have the same conclusion as *Lake* [72] about this

matter which is the fact that the values of standard value of stiffness are not coherent from one author to another. Additionally, as previously noted, no typical values of vertical stiffness have been reported in the literature.

Table 3.1: Comparison of torsional and lateral stiffness of swingarms in the literature

Swingarm Designation	Torsional Stiffness (Nm/deg)
Kawasaki ZX10R's swingarm, [71]	102.9
Suzuki GSX R1000's swingarm, [71]	140.8
Honda CBR1000R's swingarm, [71]	140.8
Limebeer [69] and *Sharp* [70][69]	209.4
S2008 Swingarm, [1]	670
SM 2008 Swingarm, [1]	890
BNG 2008 Swingarm, [1]	1330
Cossalter [11]	1000–2000
Swingarm Designation	Lateral Stiffness (kN/m)
Kawasaki ZX10R's swingarm, [71]	603
Suzuki GSX R1000's swingarm, [71]	804
Honda CBR1000R's swingarm, [71]	965
Cossalter [11]	800–1600

3.3 Material

The selection of materials is a critical part of any engineering process. The wrong material might render a project incapable of meeting its requirements [73].

It is vital to make this choice as weighted as feasible, taking into consideration the largest number of variables conceivable. There are an estimated 40000–80000 material combinations available for engineering components and making the correct choice is critical from a project standpoint [74].

This section will analyze three materials, describe each one's advantages and disadvantages, and eventually, a choice will be reached on the material that will be utilized in the project, taking everything discussed in this section into account.

Steel is regarded to be really inexpensive, typically four to six times cheaper than aluminum, and considerably more so when compared to carbon fiber [5]. It is usually chosen for swingarms due to its high durability [36]. However, recently due to the fact that steel has a really poor stiffness to weight and strength to weight ratio comparing to the other two materials there has been a shift in the industry away from the carbon steel [75].

Swathikrishnan et al. [5] designed and analysed three different swingarms with different shapes and materials. During the project, it was compared a steel to an aluminium swingarm and it was concluded that the aluminium swingarm had a similar torsional stiffness but it was 33% lighter when compared to the steel swingarm.

There are several approaches to improving vehicle economy and reducing hazardous emissions into the atmosphere. One of the most successful strategies for resolving this issue is to reduce the weight of the component being designed [74].

Transportation accounts for 27% of total aluminum demand and is the industry that requires the most aluminum [76]. Aluminium is particularly popular for applications that requires a high specific strength, low density and high stiffness to weight ratio [74]. This can be explained by the fact that a in addition to having these properties it is considered to be easy to work, weld and machine [77] and to have a particularly high corrosion resistance [74].

Furthermore, aluminium can be presented in a wide range of semi-finished shapes with high durability [78] and during impact ,opposing to steel, when the component is able to distribute the load, which reduces the deformation [79, 67] .

Composite materials, on the other hand, have emerged as the material of choice for lowering weight while maintaining high performance in recent years [80]. It enables the opportunity to reduce the component's weight and stress concentration areas while enhancing its stiffness. [2].

Bruderick et al. [81] was the first time a vehicle's structural body has been redesigned using carbon fiber. It was achieved a significant mass reduction and a higher stiffness in some automotive components, such as in the fender support system, door inner panels and windshield surround structure.

The main difference between metals and carbon fiber is the dependence on the direction of their mechanical properties. While metals such as aluminum and steel are isotropic, carbon fiber is considered to be anisotropic or orthotropic. In other words, whereas metals retain their properties in all directions, carbon fibers show a directional variation of mechanical properties [82].

Because of that, the designer is able to change the arrangement of fibers in order to alter the properties of the component and the structural stiffness of the material and obtain a higher stiffness to weight ration compared to aluminium [4].

However, utilizing carbon fibers brings higher costs, adds complexity to prediction and makes handling and disposal more challenging.

Motosports, such as Moto GP, is a sport in which costs, recycling, and life cycle are not a main concern [6]. As a result, an increasing number of carbon fiber swingarms are being used in this context. Nevertheless, some teams prefer to go with classic aluminum swingarms due to its widespread use and study, as well as their ease of detection of cracks [83].

Although, nowadays, carbon fibers are extremely more expensive comparing to aluminium [83], the industrialisation of carbon fiber may result in a price reduction of up to 70 percent, making the material considerably more attractive. In an aggressive scenario, characterized by maximum industrialization and research of carbon fiber, the delta between it and aluminum might decrease from around 80 percent now to approximately 30 percent in 2030, as represented in figure 3.3. This could lead to more and more enterprises using this material in place of standard aluminum swingarms.

The purpose of this thesis is to design and optimize a swingarm for a conventional motorcycle. As a result, production costs are a primary consideration, and aluminum will be employed due to

its high stiffness to weight ratio, low density and quick production time.

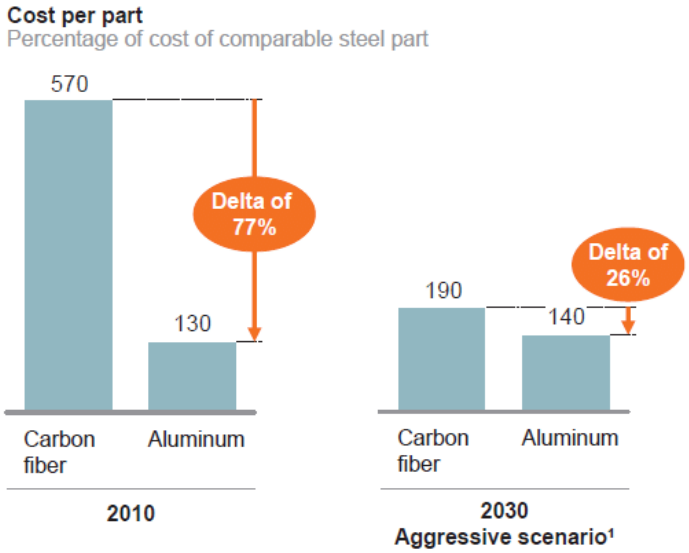


Figure 3.3: Cost of carbon fiber and aluminium in 2010 and the expected scenario in 2030 Source: [84]

Properties of Aluminium

Aluminium alloy Alufont-52 was chosen due to the excellent balance of great mechanical properties that it provides to the design and its high yield tensile strength, which is important for a component that is submitted to high loads, such as a single sided swingarm. Furthermore, this material is used in the car industry and it has really good properties under sand casting [85, 86], which is important because it is the manufacturing process desired for this project.

The mechanical properties of Aluminium that is going to be used in the design of the swingarm and it is demonstrated in table 3.2 [86, 87]. It is going to be assumed as the worst case scenario, in which the yield tensile strength is 280 MPa and the ultimate Tensile Strength 350MPa.

Table 3.2: Properties aluminium alloy Alufont-52

Property		Values
Chemical Composition	-	AlCu4Ti
Elastic Modulus	GPa	71
Poisson's Ratio		0.33
Shear Modulus	GPa	27
Mass Density	kg/m3	2750
Yield Tensile Strength	MPa	300 - 420 (280)
Ultimate Tensile Strength	MPa	400 - 475 (350)

3.4 Safety Factor

Most of the times, the selection of a safety factor is determined by the designer's experience or by code. Engineers assess whether a safety factor is adequate based on the historical performance of previously manufactured components in real life situations and whether the safety factor chosen at that time was appropriate [88].

Ultimately, the function of the swingarm and on the overall system of the motorcycle is easily understandable. However, the conditions that the motorcycle and the swingarm is submitted are too complex to be precisely understood and calculated [27].

In this chapter, to calculate the safety factor, *Pugsley* Method [89] is going to be used, in order to correctly calculate a safety coefficient that takes into account the material quality, manufacturing process and the precision of the model.

This method calculates the safety factor using equation 3.1:

$$n_{proj} = n_{sx}\, n_{sy} \tag{3.1}$$

where n_{sx} and n_{sy} are values that can be obtained by table 3.3. A, B, C, D, E are factors that the designer has to subjectively evaluate.

- **A** - quality of materials, maintenance, and inspection
- **B** - control of load applied to a component.
- **C** - Reliability of stress analysis, experimental studies, or experience with similar components.
- **D** - threat to people
- **E** - financial impact

On the one hand, quality of materials, control of load applied and reliability of stress analysis are used to obtain n_{sx} based the following grades: very good, good, satisfactory, or poor.

On the other hand, threat to people and financial impact are evaluated as very severe, severe, or not severe in order to get n_{sy}

The following ranks were attributed to the factors:

- weight loss is a priority so a material with good quality control is required. The motorcycle also to go through periodic vehicle inspections made by qualified operators: A=vg
- As it was previously stated, the loads applied to the swingarm are too complex to be determined precisely. However, some assumptions were made in order to calculate the loads applied using some reasonable approximations during the critical situations. Because of that, B is graded as good: B=g

Table 3.3: Safety factor characteristics accordingly to *Pugsley Method*
→ **vg** – very good; **g** – good; **f** – satisfactory; **p** – poor
→ **vs** – very severe; **s** – severe; **ns** – not severe

		B			
A	**C**	vg	g	f	p
vg	vg	1.1	1.3	1.5	1.7
	g	1.2	1.45	1.7	1.95
	f	1.3	1.6	1.9	2.2
	p	1.4	1.75	2.1	2.45
g	vg	1.3	1.55	1.8	2.05
	g	1.45	1.75	2.05	2.35
	f	1.6	1.95	2.3	2.65
	p	1.75	2.15	2.55	2.95
f	vg	1.5	1.8	2.1	2.4
	g	1.7	2.05	2.4	2.75
	f	1.9	2.3	2.7	3.1
	p	2.1	2.55	3.0	3.45
p	vg	1.7	2.15	2.4	2.75
	g	1.95	2.35	2.75	3.15
	f	2.2	2.65	3.1	3.55
	p	2.45	2.95	3.45	3.95

	D		
E	ns	s	vs
ns	1.0	1.2	1.4
s	1.0	1.3	1.5
vs	1.2	1.4	1.6

- This project is going to be studied based on the finite element method. Because of that, and since this method is really popular for giving great results, C is graded as very good: C=vg

- According to the World Health Organization, road accidents are one of the most common causes of death and the leading cause of death for those aged 5 to 29. [9]. Therefore, the design of the swingarm must take into consideration the potential danger a failure poses to humans, hence D is graded as very severe: D=vs

- The swingarm is aimed at a company that pretends to make profit. Furthermore, in case of a fatality or an injured the company could be in possible lawsuits. So E is going to be considered as very severe: E=vs

Table 3.4: Ranks of Parameters given to the swingarm

A	B	C	D	E
vg	g	vg	vs	vs

The evaluation of the parameters is summed up in table 3.4, which results in a $n_{sx} = 1.3$ and $n_{sy} = 1.6$, which means that the safety factor is:

$$SF = n_{sx}\, n_{sy} = 1.3 * 1.6 = 2.08$$

3.5 Motorcycle Selection

As previously stated, this project will modify a motorcycle's double sided swingarm in order to convert it to a single side swingarm. To do this, a specific motorbike will be analyzed in order to determine the loads encountered while riding it. AJP PR7 was chosen as the motorbike and represented in figure 3.4. Although it is an enduro motorcycle and required to drive off-road, in this dissertation, it was assumed that the situations which this motorcycle is going to be submitted are the same as a standard road motorcycle. In other words, it is going to be assumed that, the motorcycle designed will be aimed at road driving.

AJP Motos is a company founded in 1987, by the partners Antonio Pinto and Jorge Pinto [14, 90, 30]. The first motorbike model, ARIANA 125cc, with a 125cc two-stroke engine [14, 90]. Since then, AJP became a worldwide known brand selling products and several different motorcycles. In 2016, AJP produced a new prototype of a large trail motorbike, which was upgraded to become the AJP PR7 motorbike. The bike has been updated in recent years, but the primary characteristics remain intact [90].



Figure 3.4: AJP PR7 2021 Source: [91]

AJP PR7

As it was previously said, there are several versions of AJP PR7 that were developed over the years. Appendix A [91, 92, 93, 94] shows 4 different models of this motorcycle found in the literature.

The most recent model found in Appendix A is the one that is currently being sold by the company. However, the specifications found on their website [91], does not include the weight.

AJP PR7 660 Adventure and AJP PR7 Adventure 650, which specifications can be found in Appendix A, while having different engine capacity have the same dry weight of 155kg.

Dry weight commonly refers to the weight of the motorcycle without counting the fluids needed to drive, such as fuel and oil. On the other hand, wet weight takes into account all of the motorcycle's weight that is essential to operate it [95]. As a result, it is preferable to calculate the loads using the wet weight in order to obtain a more accurate estimate of the conditions.

Because of that, in the calculations made in this thesis it is going to be considered the weight of the 2016 model of the AJP PR7 motorbike with 600cc, which is the same value as AJP PR7 2021. Its specifications are represented in Appendix A. It has a wet weight of 165kg and some other important characteristics that is symbolized in table 3.5

Table 3.5: Specifications of AJP PR7

Wet Weight	165kg
Engine capacity	600.3
Rear Suspension	AJP progressive linkage system
Rear wheel Travel	279.4mm
Front Brakes	Single 300mm disc, 2 piston caliper
Rear Brakes	Single 240mm disc , single piston caliper
Front tyre	90/90-21
Rear Tyre	140/80-18
Seat Height	919 mm
Final Drive	Chain
Wheelbase	1532mm

3.6 Loads

As it was previously said before in section 3, most of the literature focus on increasing the torsional stiffness while reducing its weight. However, it is crucial to make sure that the swingarm can handle sufficient stresses to prevent it from yielding.

The aim of this section is to identify the conditions that could be a potential problem because of the high stresses that causes to the swingarm

This section will explore a variety of different scenarios in order to compute the loads associated with various moves. To begin, each maneuver will be explained along with the motorcycle's response, followed by an explanation and justification of the maneuver's assumptions in order to simplify the problem without impairing the results significantly, and finally, the loads will be calculated using the literature and other numerical calculation software, such as Octave.

3.6.1 Weight distribution

Assuming a basic motorbike in a flat road, the loads imposed on it by its own weight distribution may be represented figure 3.5.

As can be seen, the motorcycle's gravitational force is absorbed by the sum of the rear and front vertical loads. However, because gravity is not distributed evenly across the wheels, the normal load measured in the front wheel is not the same as the load observed in the back wheel.

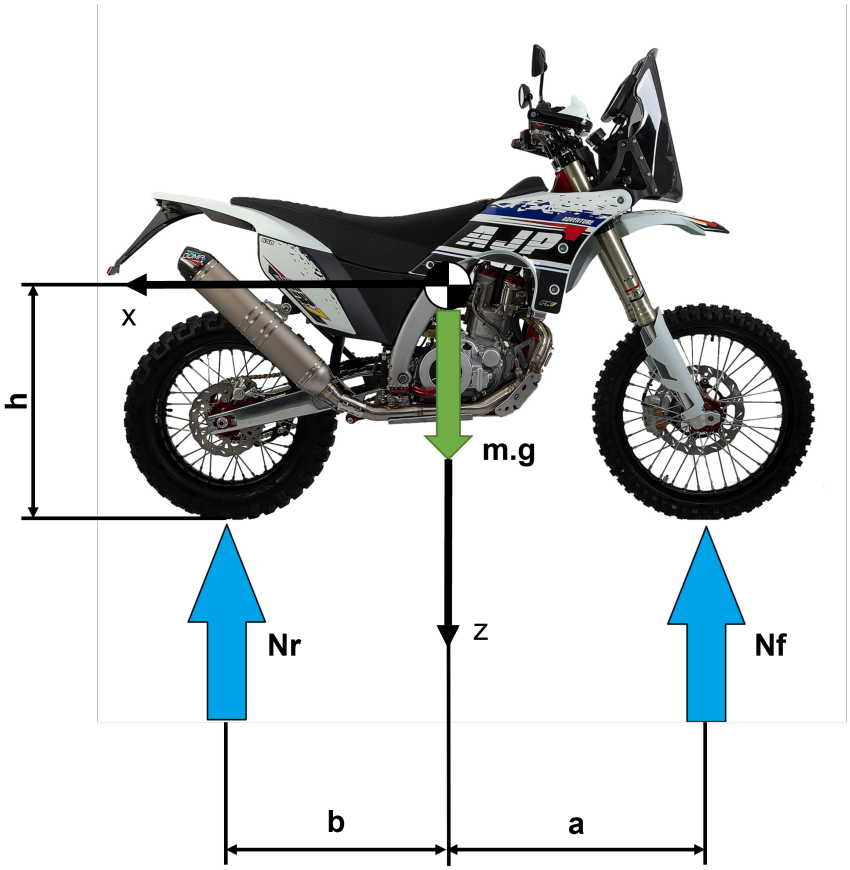


Figure 3.5: Simple Motorcycle model of the weight distribution Source: [91]

In table 3.6, the variables represented on figure 3.5 are described and the meaning is presented. If we apply a sum of forces on the z axis it is possible to conclude that:

$$N_f + N_r = mg \tag{3.2}$$

Likewise, if a sum of moments is applied to the CoG. Gravitational force cannot generate momentum since its momentum arm is zero and the vertical reactions N_r and N_f have opposite signs. The following equation can be obtained:

$$N_r\, b - N_f\, a = 0 \tag{3.3}$$

Using equation 3.2 and 3.3 it is possible to conclude that:

$$N_f = m\, g\, \frac{b}{a+b} \tag{3.4}$$

$$N_r = m\, g\, \frac{a}{a+b} \tag{3.5}$$

Table 3.6: Meaning of each abbreviation

a	Distance between front wheel and the CoG
b	Distance between rear wheel and the CoG
h	Height of the CoG
m	mass
N_f	Vertical load on the front wheel
N_r	Vertical load on the rear wheel
a_1	Distance between front wheel and the CoG considering only the motorcycle
a_2	Distance between front wheel and the CoG considering the motorcycle+rider
b_1	Distance between rear wheel and the CoG considering only the motorcycle
b_2	Distance between rear wheel and the CoG considering the motorcycle+rider
m_1	mass of the motorcycle
m_2	mass of the motorcycle+rider

Due to the fact that different motorcycles have unique behaviours of weight distribution, the values of a and b differ from one motorcycle to another.

Accordingly to *Bradley* [96], calculating the weight distribution of a motorcycle is important in order to calculate the critical acceleration for four different situations.

- Front wheel lifting while accelerating
- Rear wheel lifting while braking
- Front wheel slide while braking
- Rear wheel spin while accelerating

While a and b may be estimated using published numbers and applying certain assumptions in order to maximize swingarm stress, h_g should be regarded an interval of values when calculating these four components. This is because, while a designer can compute the ideal CoG height, it will always be dependent on the rider's choice and driving style [27].

Accordingly to *Ramos* [27], the following equations define the critical acceleration or deceleration required for the occurrence of the preceding situations.

- acceleration required to lift the front wheel

$$a_{lf} = \frac{g\ b}{h} \tag{3.6}$$

- deceleration required to lift the rear wheel

$$r_{lr} = \frac{g\ a}{h} \tag{3.7}$$

- deceleration required causing the front wheel to slide

$$r_{sr} = \frac{\mu\ g\ b}{W_b - \mu\ h} \tag{3.8}$$

- acceleration required causing the front wheel to spin

$$a_{sf} = \frac{\mu\ g\ a}{W_b - \mu\ h} \tag{3.9}$$

Weight distribution considering only the motorcycle

It was not possible to find in the literature the values of the weight distribution verified on the AJP PR7 motorcycle. However, two other AJP's motorcycles, AJP PR4 and AJP Galp 50, were analysed by *Oliveira* [30] and the values of weight distribution are displayed in table 3.7.

Table 3.7: Weight Distribution of AJP Galp 50 and AJP PR4 [30]

Axle	Galp 50 Front Wheel	Galp 50 Rear Wheel	AJP PR4 Front Wheel	AJP PR4 Rear Wheel
Empty Deposit	49.4%	50.6%	48.8%	51.2%
Full Deposit	50%	50%	48%	52%

Table 3.7 only considers the normal loads verified on the rear and front wheel caused by the self-weight of the motorcycle [30].

Considering the worst-case scenario for the swingarm of such table, namely when the AJP PR4 is regarded fully deposited, and apply it to the AJP PR7. In other words, a weight distribution of 48%,52% for the front wheel and the rear wheel will be considered, respectively in order to calculate a and b, without driver. This is a reasonable assumption, as AJP PR4 is the predecessor to AJP PR7, and thus the weight distributions may be quite similar.

Using equation 3.4 and 3.5, as well as considering N_f to be 48% and N_r to be 52% of weight distribution on the rear wheel

$$0.52\ m_1\ g = m_1\ g\ \frac{a_1}{a_1+b_1}$$
$$0.48\ m_1\ g = m_1\ g\ \frac{b_1}{a_1+b_1}$$

Accordingly to table 3.5, $a+b = 1532mm$ which means that:

$$a_1 = 0.52 * 1532 = 796.64\ mm$$
$$b_1 = 0.48 * 1532 = 735.36\ mm$$

Using equations 3.4 and 3.5, the vertical loads are:

$$N_{f1} = 165 * 9.81\ \frac{735.36}{1532} = 776.952N$$
$$N_{r1} = 165 * 9.81\ \frac{796.64}{1532} = 841.698N$$

Weight distribution considering the motorcycle+rider

However, it is frequently desirable to be informed of the distances between the axle of the wheel and the center of gravity when driving. In other words, the driver's mass must be considered.

Accordingly to Ramos [27], on modern competitive motorcycles the normal reaction usually is higher on the front wheel than on the rear wheel. However, on classic motorcycles the value of weight distribution is usually 55% on the rear wheel and 45% on the front wheel,

On the other hand, *Chakraborty* [97] considers 60% on the rear wheel and 40% on front wheel to be a more suitable approach in terms of safety.

Considering both the motorcycle and the driver as a single rigid body with a mass equal to the sum of their individual masses and assuming that the driver has a weight of 80kg. The weight distribution considered is 40% for the front wheel and 60% for the rear wheel, respectively, due to the increased load on the rear wheel and so taking into consideration the worst-case scenario for the swingarm.

The values calculated are an approximation due to the fact that, as previously said, different motorbikes have varying weight distribution characteristics and as previously stated in section, the center of mass might shift during various maneuvers, as it was referred in chapter 2.2.7.

Using equation 3.4 and 3.5 as well as considering N_f to be 40% of weight distribution on the front wheel and N_r to be 60% on the rear wheel, it is possible to calculate the normal loads on each of them.

$$0.6\ m_2\ g = m_2\ g\ \frac{a_2}{a_2+b_2}$$
$$0.4\ m_2\ g = m_2\ g\ \frac{b_2}{a_2+b_2}$$

Once again, considering from table 3.5, $a+b = 1532mm$

$$a_2 = 0.6 * 1532 = 919.2\ mm$$
$$b_2 = 0.4 * 1532 = 612.8\ mm$$

Using equations 3.4 and 3.5, the vertical loads are:

$$N_{f2} = (165+80) * 9.81\ \frac{612.8}{1532} = 961.38N$$
$$N_{r2} = (165+80) * 9.81\ \frac{919.2}{1532} = 1442.07N$$

3.6.2 Braking

Braking is considered by many authors as one of the potential critical situation for the swingarm [3]. *Spanoudakis el al.* [3], *Sonawane* [79], *Wajahath* [67] and *Pazani* [98] all considered crucial the influence of braking on the design of the swingarm. However, accordingly to *Cassani* [45], braking is less dangerous than accelerating, because he considers the load transfer as a mean of reducing stresses on the swingarm.

Load transfer

Whenever the motorcycle verifies a situation of acceleration or retardation, a condition of load transfer can be verified

On the one hand, in case the motorbike is braking, its inertia will tend to go forward and the friction between the road and the motorcycle is what causes the vehicle to slow down. While

friction is applied on the road surface, where the contact is verified between the road and the motorbike, inertia is applied to the center of gravity of the aggregate between the motorcycle and the rider. As a consequence, torque is generated, causing the motorbike to lean forward, and compressing the front suspension while extending the rear suspension [12, 99]. As the motorcycle leans forward, the weight tends to shift to the front, increasing the vertical load on the front wheel while decreasing it on the rear wheel.

In the event of acceleration, on the other hand, inertia works against the acceleration and the force generated between the road and the motorbike, which forces the motorcycle to accelerate. As a result, torque is generated, causing the motorbike to lean back and the front suspension to lengthen, while the rear suspension tends to compress causing more load on the rear wheel [12, 27].

Generally, the load transfer on a motorcycle is more noticeable to the rider than it is on other vehicles, due to the motorbike's high center of gravity (CoG) in relation to its wheelbase [27, 98].

To reduce load transfer, solutions include lengthening the wheelbase and lowering the motorcycle's center of mass [12].

Loads during braking

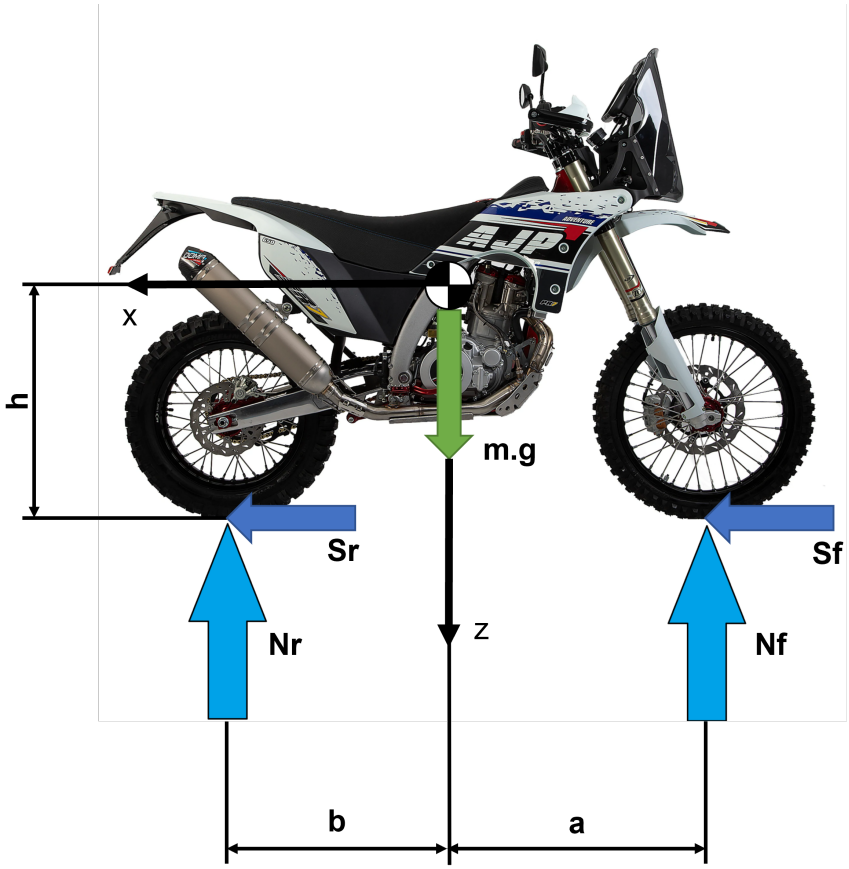


Figure 3.6: Simple Motorcycle model of the loads during braking. Source: [91]

Taking into account figure 3.6 and table 3.8, applying second's newton law to the x and z axis results in the following equations:

$$\sum F_x = m\ d_x = S_f + S_r \tag{3.10}$$

$$\sum F_z = 0 \ \rightarrow\ m\ g = N'_f + N'_r \tag{3.11}$$

Table 3.8: Meaning of each abbreviation

a	Distance between front wheel and the CoG
b	Distance between rear wheel and the CoG
h	Height of the CoG
m	mass
N'_f	Vertical load on the front wheel while braking
N'_r	Vertical load on the rear wheel while braking
S_f	Friction force on the front wheel
S_r	Friction force on the rear wheel
d	Deceleration

Similarly, if a sum of moments is calculated in CoG, gravitational force is unable to of generating momentum because its momentum arm is zero and the vertical reactions N_r and N_f have opposite signs. It is possible to obtain the following equation:

$$\sum M_{CG} = 0 \ \rightarrow\ h\ (S_f + S_r) + N'_r\ b - N'_f\ a = 0 \tag{3.12}$$

Using equation 3.10 and 3.12

$$h\ m\ d_x + N'_r\ b - N'_f\ a = 0 \tag{3.13}$$

It is possible to compute these equations and put in order to N'_r and N'_f

$$N'_f = \frac{m\ g\ b}{W_b} + \frac{m\ d_x\ h}{W_b} \tag{3.14}$$

$$N'_r = \frac{m\ g\ a}{W_b} - \frac{m\ d_x\ h}{W_b} \tag{3.15}$$

In the last chapter 3.6.1, it was possible to conclude that the distribution weight represents a vertical load on the front and rear wheel respectively of $N_f = \frac{m\ g\ b}{a+b}$ and $N_r = \frac{m\ g\ a}{a+b}$

Considering the dynamic weight, $N_d = \frac{m\ d_x\ h}{a+b}$:

$$N'_r = N_r - N_d \tag{3.16}$$

$$N'_f = N_f + N_d \tag{3.17}$$

Equations 3.14 and 3.15 illustrate how deceleration affects load transfer. It is possible to conclude that the sum of normal loads between the front and rear wheels are constant, which is predictable given that they must support the motorcycle's and rider's mass. Additionally, the same equations and as illustrated in Figure 3.7, the normal force on the rear and front wheels varies linearly with deceleration.

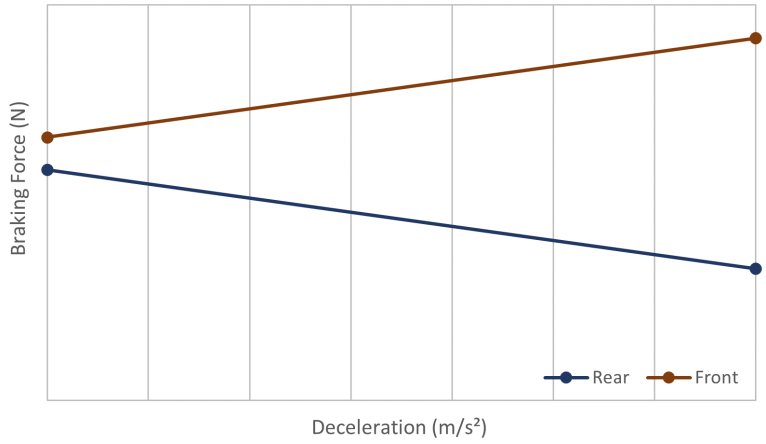


Figure 3.7: Influence of braking force due to deceleration on the front and rear wheel. Source: [97]

As stated in chapter 3.6.1, the height of the CoG should be considered an interval of values due to the fact that riders exhibit a variety of behaviors during maneuvers that affect the CoG in a number of ways.

However, in order to calculate the loads verified during braking, the height of the CoG will be considered to be the maximum height of the CoG that avoids both the lift of the rear wheel and the sliding of the front wheel.

For deceleration limit, it is commonly assumed that a motorcycle must be able to handle 1g (9.81 m/s^2) of deceleration when both brakes are used simultaneously [96]. *Huertas* [100] got the same result, having an expert driver doing 25 trials of an emergency braking resulting in a mean deceleration peak of 9.82 m/s^2.

Most of the times, tires can reach coefficients of friction μ up to 1.1 [101].

Considering equations 3.7 and 3.8, with $a = 919.2\ mm$, $b = 612.8\ mm$, $m = 245\ kg$ and $\mu = 1.1$:

$r_{lr} = \frac{g\ a}{h} \rightarrow h = a = 919.2\ mm$

$r_{sr} = \frac{\mu\ g\ b}{W_b - \mu\ h} \rightarrow$ **h=779.23mm**

Considering an ideal height of CoG of 779.23 mm, the critical deceleration for both situations are $r_{sr} = 9,81\ m/s^2$ and $r_{lr} = 12.45\ m/s^2$. Thus, the motorcycle is deemed safe if it can withstand braking deceleration of at least 9.81 m/s^2, so this value of $h_{id} = 779.23$ is going to be considered for the rest of the work.

The vehicle's design and manufacture should ensure that the vehicle can withstand emergency braking [102]. In order to maximize swingarm stresses, it is critical to consider only the rear brake, as only the rear wheel friction affects the swingarm, while front wheel friction does not increase the stresses on the swingarm.

The motorcycle emergency breaking behaviour depends heavily on the vehicles braking performance, for example whether it is a drum or disk brake, as well as the driver's response and foot action against the pedal [103]. Usually, a more experienced person has a better emergency braking responsiveness resulting in higher deceleration [96].

Accordingly to *Ariffin* [104], a disk rear brake, such as the one on AJP PR7, table 3.5, can have an emergency braking of 4.22 m/s^2, in other words the maximum deceleration can go up to 4.22 m/s^2 utilizing exclusively the rear brake.

After having calculated how high the center of mass is, it is possible to calculate the vertical loads verified on the rear and front wheel using equations 3.14 and 3.15.

$$N'_f = \frac{m\ g\ b}{W_b} + \frac{m\ d_x\ h}{W_b} = 961.38 + 530.24 = 1491.62\ N$$

$$N'_r = \frac{m\ g\ a}{W_b} - \frac{m\ d_x\ h}{W_b} = 1442.07 - 530.24 = 911.83\ N$$

To sum up, it is possible to say that in this case there was a weight transfer of 54 kg from the rear wheel to the front wheel.

3.6.3 Cornering

During power-cornering, the motorbike is subject to enormous loads due to the shift in lateral direction, and it is crucial that every component be meticulously analyzed under these extreme loads [79]. It is also important that the torsional and lateral stiffness are high enough to reduce instability and not cause handling problems during the maneuver [4].

Cornering can be analysed in a straightforward manner taking into account the stability and the equilibrium of the system of the motorcycle together with the rider [105].

During a curve, the single sided swingarm is submitted to a bigger deformation [27].

Cornering motion is one of the most difficult circumstances for a designer to evaluate. In order to adjust the center of gravity, various riders prefer to move differently in similar situations. Respecting his own "riding style," each rider moves his body back and forth and side to side in a different way [20].

Several models were created in order to study cornering motion of motorcycles in a more precise way that takes into account factors such as the variation of stiffness of tires, the aerodynamic forces and some other that would turn the problem a lot more complex [70, 105, 106, 107].

Because of that, it is really hard to make a prediction taking into account all this factors. However, there is going to be made several assumptions in order to result in an approximation:

- constant curve radius
- constant curve speed

- suspension and tires acting as a rigid body
- negligible rolling friction
- no aerodynamic forces
- the rider and motorcycle have the same roll angle

Roll angle

Motorcyclists tend to fall over during turns in order to counterbalance the moment caused by the centrifugal force generated in order to make a curve and to prevent from falling [4, 67].

The tighter the curve the more the rider has to lean [108]. It is feasible to anticipate the expected roll angle for a certain curve at a particular speed or whether a particular motorcycle can safely navigate a certain curve at a particular speed without falling.

That is because, as it was previously stated, the goal of leaning is to counterbalance the torque generated by the centrifugal force. The centrifugal force depends on the velocity and the curvature and can be described by the following equation:

$$F_c = \frac{m\,V^2}{R} \tag{3.18}$$

where V is the linear velocity of the motorcycle and R is the radius of the curve.

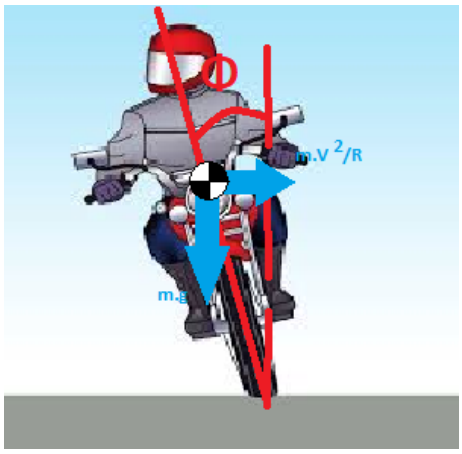


Figure 3.8: Simple Motorcycle model of the loads during cornering Source: [16]

If a sum of moments is calculated using figure 3.8 in the tire, normal force is unable to of generating torque and centrifugal force and the gravitational force have opposite signs. It is possible to obtain the following equation:

$$\sum M_t = 0 \;\rightarrow\; F_c\, cos\phi = m\, g\, sen\phi \tag{3.19}$$

Using equation 3.18 and 3.19

$$\frac{V^2}{R\,g} = tan\ \phi \tag{3.20}$$

The last equation translates the maximum curvature that a motorcycle can turn for different speeds at a certain roll angle and is represented in figure 3.9 found in the literature.

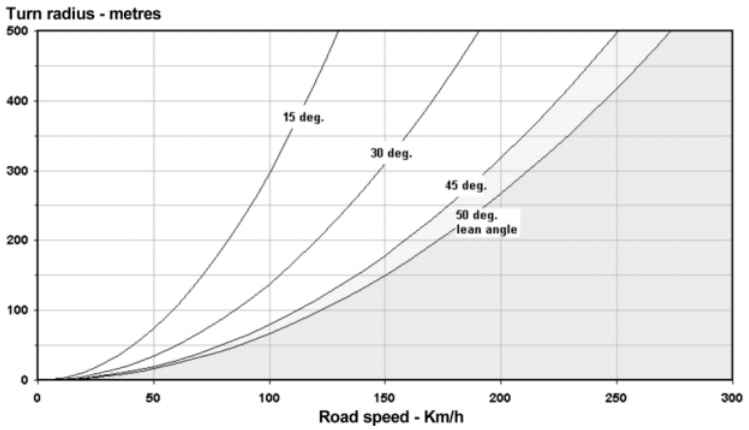


Figure 3.9: Graph the turn radius that corresponds to various road speeds for different lean angles. Source: [12]

It is essential to conclude from equation 3.20 that as cornering velocity tends to increase, so does the angle required to counterbalance the centrifugal force torque. As a result, the lean angles of competition motorcycles, where the goal is to drive as fast as possible are substantially greater than in everyday driving and can go up to 64º as it is possible to see from figure 3.10.



Figure 3.10: Maximum Lean angle for different motorcycles. Source: [109]

Effective Roll Angle

Until now, the thickness of the tire was considered to be approximately zero. However, during a turn the motorcycle while falling over tends to move the contact point from the middle plane of the tire to the periphery [45], as it is possible to see from figure 3.11.

Due to that, the angle necessary for the equilibrium of the moments is higher than the ideal, which was previously calculated [110]. Because of that, the effective roll angle is:

$$\phi = \phi_i + \Delta\,\phi = arctg(\frac{V^2}{R\,g}) + arcsin(\frac{t\ sin(\frac{V^2}{R\,g})}{h-t}) \tag{3.21}$$

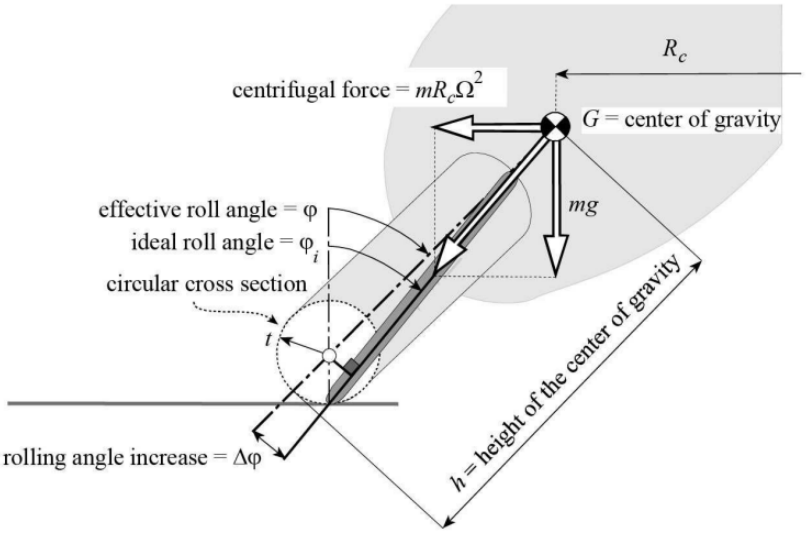


Figure 3.11: Effective roll angle. Source: [11]

Friction force

Due to the lateral contact of the tire with the ground, while cornering a lateral friction force, F_t is created [11]. This friction that acts on contact point and is also responsible to balance the moment created by the normal load [46].

The sum of lateral friction force of the rear and the front wheel must be equal to the centrifugal force in order to balance it out and for the motorcycle to be in equilibrium.

If it is supposed, once again a weight distribution of 40%-60% on the front and rear wheel respectively, it is possible to conclude that:

$$F_{t\ rear} = 0.6\,F_c \tag{3.22}$$

According to *Bergman* [111] lateral tire force and traction can be treated as the lateral and longitudinal friction force.

It is possible to incorporate a lateral and longitudinal coefficient of friction that relates the friction force in that direction to the vertical force. These coefficients are known as the effective tractive coefficient, μ_x and effective lateral coefficient of friction, μ_y, respectively and can be expressed as a function of the static coefficient of friction, μ, using the expression [111]:

$$\mu = \sqrt{\mu_x^2 + \mu_y^2} \tag{3.23}$$

The coefficient of friction is assumed to be 1.1 [6, 101]. Considering the calculation of lateral friction force using equation 3.22, μ_y can be calculated dividing the lateral tire friction force by the normal load of the rear wheel. Following that, it possible to calculate the effective tractive coefficient, μ_x:

$$\mu_x = \sqrt{\mu^2 - \mu_y^2} \tag{3.24}$$

After calculating the effective tractive coefficient, it is possible to calculate the traction force on the rear wheel, S_r:

$$S_r = \mu_x \, Nr \tag{3.25}$$

Chain tension

The torque of the chain force is balanced by the torque generated by the driving force of the rear tire [11]. Due to the fact that the radius of the tire is considered to be several times higher than the radius of the rear sprocket, it is possible to conclude that the chain pull is much higher comparing to the driving force [45].

Although the torque of this forces cancel each other, both of this forces are responsible for a compression load on the swingarm [45].

Considering R_r to be the radius of the rear wheel and R_c to be the radius of the chain sprocket, the driving force, if considered to be constant, can be related to the chain tension by the following equation [11]

$$T = \frac{R_r \, S}{R_c} \tag{3.26}$$

Loads during cornering

During cornering with a constant radius and roll angle and some other assumptions explained in this chapter a set of equations was demonstrated.

Using equations 3.20, 3.22, 3.24, 3.25 and 3.26 and considering the representation of figure 3.12, an Octave script is demonstrated on Appendix B.1 that was used to calculate the loads during cornering for a certain linear velocity of the motorcycle and a certain turn radius.

Although it was a relatively simple system of equations it was decided to implement it on a numerical calculation software in order to test under various circumstances and to calculate the maximum loads during a motorcycle turn by varying the speed and curve radius.

After some conditions analysed, 2 different load conditions were regarded to be the most interesting.

On the one hand, the first condition is a turn at high speed, when the lateral friction force is really high and the roll angle is almost the maximum for this type of motorcycles. For this condition, a motorcycle speed of 150km/h and a curve radius of 250m was considered and resulted in a roll angle of 35.632º.

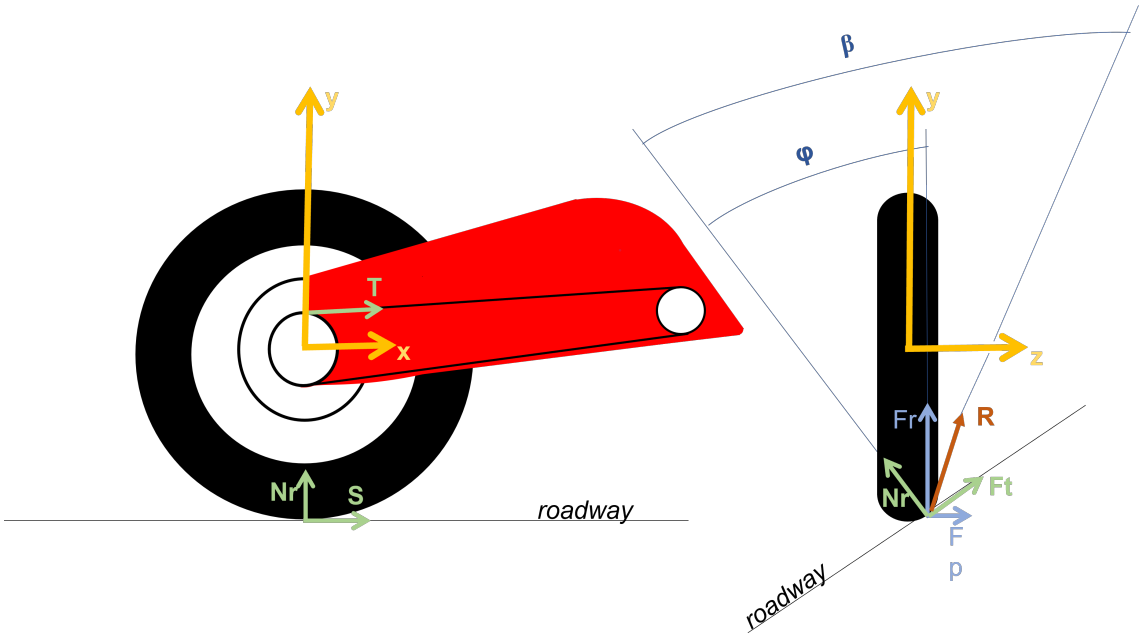


Figure 3.12: External loads during cornering

On the other hand, the second condition is regarded to be when the curve radius is infinite and so it happens when the motorcycle is in a straight line. While lateral friction is null, the maximum traction force is verified as well as the maximum chain tension. As expected the roll angle in this case is 0º.

The loads applied during both conditions are summed up in table 3.9

Table 3.9: External loads during 2 extreme conditions

Parameter		Curve	Straight line
V	km/h	150	200
R	m	250	inf
ϕ	deg	35.632	0
N_r	N	1442.1	1442.1
F_t	N	1020.8	0
μ_y	-	0.7079	0
μ_x	-	0.8420	1.1
S_r	N	1214.2	1586.3
T	N	3642.5	5287.6

3.6.4 Landing on the rear wheel

Firstly, as noted in chapter 3.6.1, excessive acceleration or deceleration might result in the front or rear wheel lifting. This maneuver is called a wheelie and demands a great deal of experience on the part of the rider, since he must position himself to avoid falling [112].

During acceleration, the front wheel may lift in case the acceleration is really excessive, as represented by equation 3.6. Figure 3.13 represents a wheelie of the front wheel.



Figure 3.13: Wheelie of the front wheel. Source: [113]

During braking, if the deceleration is excessively high, the rear wheel may lift, according to the equation 3.7. However, when the wheel strikes the ground again with a given velocity, it causes a vertical impact force on the rear wheel that, depending on the vertical speed of the motorcycle, can be extremely significant. This maneuver and is represented in figure 3.14.

Accordingly to *Schaller* [112], in these cases, high loads are submitted to the motorcycle, hence the swingarm is under high demand which implies its importance to the design of the rear suspension.



Figure 3.14: Wheelie of the rear wheel maneuver on a Buell SI Lightning. Source: [112]

Secondly, there are situations in which the entire weight of the motorbike is carried by the rear wheel when the motorcycle lands on its rear wheel. In this scenario, there will be no contact between the rear wheel and the road. Hence, there will be no friction force and normal load on

the front wheel. The motorbike can land on the rear wheel after a jump or a simple bump, with the entire weight of the motorcycle and rider supported by the rear wheel. The swingarm must be able to withstand these stresses.

Considering the equation, a falling vertical height of $h_{falling}$, an efficiency of the conversion of kinetic energy η, and a deflection of the component due to a static force δ_{static}, the impact force can be calculated by the following equation [114]:

$$n = 1 + \sqrt{1 + \frac{2\, h_{falling}\, \eta}{\delta_{static}}} \tag{3.27}$$

Considering h=0, the impact force factor is $IF = 2$, in other words the situation specified is considered to be a normal force of 2g on the rear wheel. In this case specifically, the normal load is:

$N_r' = 2 * m_{total} * g = 2 * 245 * 9.81 = 4806.9N$

3.7 Loads in different situations

Table 3.10 sums up the loads applied to the rear wheel and the chain tension in every situation referred in section 3.6.

These loads will be crucial, allowing later verification of the critical situation and whether or not the design of the single sided swingarm can withstand these stresses.

Table 3.10: Loads on the motorcycle

Condition	N_r	S_r	T	F_t	ϕ
WD motorcycle	841.69	0	0	0	0
WD motorcycle + rider	1442.07	0	0	0	0
Braking	911.83	-1033.9	0	0	0
Straight line	1442.07	1586.3	4749.9	0	0
Curve	1442.07	1214.2	3642.6	1020.8	35.632
Lading on Rear Wheel	4806.9	0	0	0	0

3.8 Leyni Test

The Leyni test bench is used to evaluate the fatigue-resistance of the motorcycle's main components [2].

Stefano and Simone [115] developed a test that Ducati takes to determine if its swingarm structures are highly efficient, employing the Leyni test to evaluate the behavior of motorcycle components.

Cassani et al. [45] conducted a study implementing experimentally the Leyni test and utilizing finite element method in order to evaluate a single-sided Ducati Monster S4 R swingarm.

The Leyni test consists of a spinning drum at 20 km/h and 3.7 Hz that evaluates the durability of motorcycle components over 500,000 cycles [2, 46].

This test requires an initial static load of 1960N, which is substituted by a dummy inserted and compressed by a beam that pushes it down, and a maximum applied force of 5900N when the step contacts the wheel [2, 46, 116].

On the one hand, this test's primary benefits are its high adaptability, low cost, speed, and repeatability. On the other hand, this sort of test does not permit the application of horizontal or variable loads, due to the fact that the load is determined by the interaction of the suspension with the drum dynamics and making it impossible to obtain a fatigue curve [117].

This condition is not going to be tested on this thesis. However, it is vital to keep in mind that the components of this sort of motorcycle are subjected to severe fatigue stresses, and that there are experimental procedures designed to determine whether the swingarm can be used without issue in a motorcycle.

3.9 Boundary Conditions

The following boundary conditions were considered during the simulation of the loads on the swingarm.

- The swingarm is capable of vertical movement during bumps and surface irregularities. The movement is dictated by the load provided on the rear wheel which forces to move vertically causing the swingarm to move.
- The swingarm is permanently attached to the main frame, preventing any longitudinal movement, in other words, there is no movement in the direction the motorbike moves.
- The swingarm is linked to the structure of the frame through two swingarm spreads and to the suspension system via the shock absorber, which inhibits any potential lateral swingarm movement.
- The rigid connection to the frame also prevents all the possible movements of rotation around the longitudinal axis (roll motion) and about the vertical axis (yaw motion). During cornering where roll and yaw motion is verified creating a twisting and a bending moment on the swingarm [2].
- Due to the bearings in the spreads of the swingarm, it is possible that it rotates around the lateral axis (pitch motion) during bumps or road irregularities.

Chapter 4

Aluminium Double Sided Swingarm

This chapter aims to provide additional information on the double sided swingarm as well as the values of a swingarm properties of a motorcycle comparable to the one selected. This component was designed in a prior project by one of the students that graduated in Mechanical Engineering students at FEUP and it is represented in figure 4.1.

The results pretended on this chapter are the following:

- Calculate the safety factor utilized on this swingarm, which later will be compared to the safety factor used on the designed single sided swingarm.
- The mass of the swingarm, the lateral and torsional stiffness, so that it is possible to compare to the values obtained in the next chapter.
- Regarding the material, to determine if it is or not that the material selected is suitable for the double sided swingarm.
- The critical situation of the ones described in the previous chapter.
- The critical points of the swingarm and the ones that should take more concern during the design of the single sided swingarm.

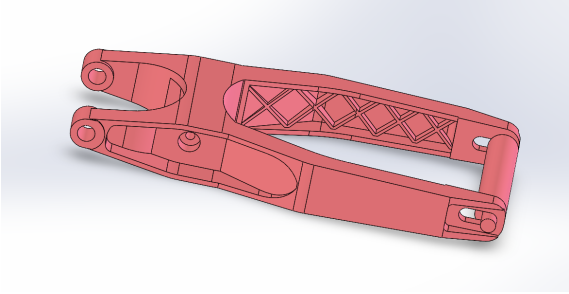


Figure 4.1: Double sided swingarm

This component will be assumed to be made of the same material as the single sided swingarm. Utilizing Abaqus, and assuming a mass density of 2750 kg/m^3, the component represented weights 4.33kg.

4.1 Stiffness Calculation

In this subsection, the lateral and torsional stiffness of a double sided swingarm will be evaluated. The values identified in the literature and reported in chapter 3.2 will be used to analyze and describe the handling and comfort of this swingarm.

The attainment of both torsional and lateral stiffness is calculating using *Cossalter's* approach for measuring stiffness, as shown in figure 4.2.

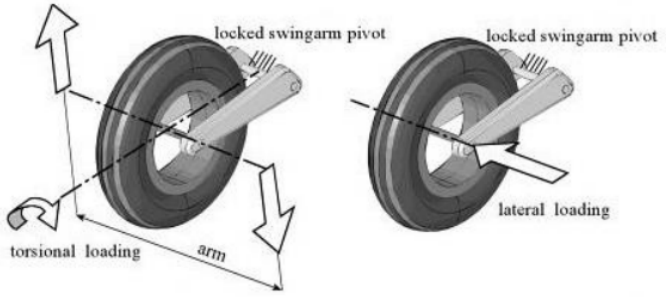


Figure 4.2: *Cossalter's* aproach for measurement of torsional and lateral stiffness Source: [11]

4.1.1 Torsional Stiffness

To determine the torsional stiffness of a double sided swingarm, the verified displacement angle between both sides of the swingarm when subjected to a certain torque must be measured [27].

The torque and the correspondent angular displacement can be adjusted to a graph that can be plotted as a line, and the slope will correspond to the swingarm's torsional rigidity.

$$K_{Torsional}(\frac{kN}{^\circ}) = \frac{Torsional\ Load(kNm)}{Total\ Angular\ Displacement(^\circ)} \tag{4.1}$$

As stated previously, the total angular displacement corresponds to the rotation suffered from the swingarm when submitted to a respective torque [27].

Finite element method

Finite element method was used to calculate the angular displacement of the swingarm when a torque was applied to it by applying two forces to the swingarm's ends of the spindle, as shown in figure 4.3.

The swingarm drawing was provided as a Solidworks file and using the STEP file, it was possible to import it into Abaqus, where the following simulations were performed. The mesh

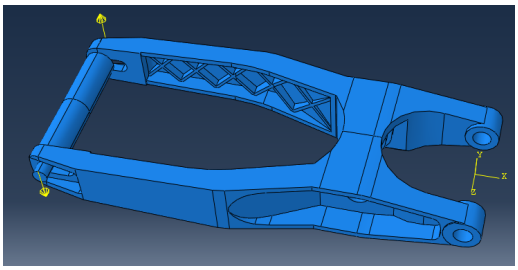


Figure 4.3: Torsional Test according to *Cossalter* Source: [27]

convergence is represented in appendix D.1. It was concluded that a global size of seeds of 3mm would give great results, which led to a mesh with 472386 Tetrahedral elements.

Four different tests were conducted, with forces applied on the spacer of 200 N, 500 N, 1000 N, and 5000 N and, due to the fact that spindle measures 0.244m, the respective torque is concluded to be 48.8 Nm, 122 Nm, 244 Nm, and 1220 Nm, respectively. Figure 4.4 shows the simulation of the application of the different torques on the spacer and the verified displacements are depicted in these scenarios. On the connection between the swingarm and chassis, boundary conditions were added to prevent any movement outside the rotation about the lateral axis.

As it is was previously said, it is possible to take the values of the figure 4.4, in order to plot a graph that relates the angular displacement of the swingarm and the torque that it is submitted in different occasions, shown in figure 4.5.

The values derived from the finite element method represent the translational displacement that both ends of the swingarm are subjected to. To determine the torsional angle, the angle formed by the spindle with the horizontal was calculated by using the function sine. The respective values are represented in table 4.1.

To sum up, the 4 situations described before, when put together on a graph are part of a line that describes the behaviour of this swingarm torsionally. It is possible to conclude that, the swingarm represented has a torsional stiffness of 469.4 Nm/deg.

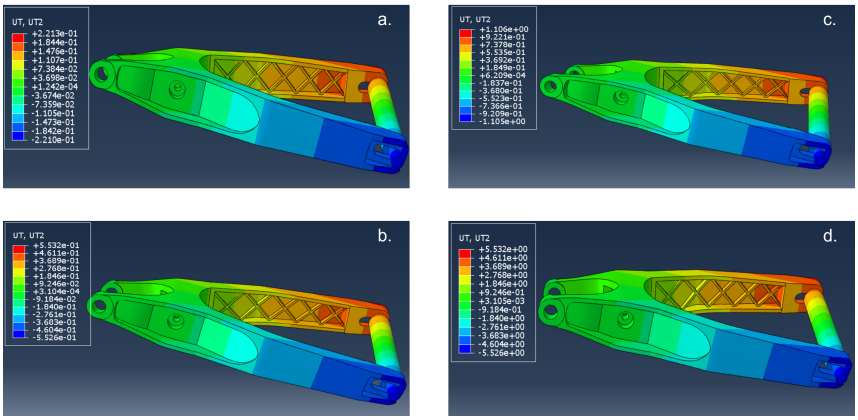


Figure 4.4: Simulation of torsional test with different torques a-48.8 Nm, b-122 Nm, c-244 Nm, d-1220 Nm

Table 4.1: Torque and calculation of angular displacement

Force	Moment	Displacement	Angle(rad)	Angle(°)
0	0	0	0	0
5000	1220	5.532	0.0453598	2.598926
1000	244	1.106	0.0090657	0.519426
500	122	0.5532	0.0045344	0.259804
200	48.8	0.2213	0.0018139	0.103931
Distance	0.244			

Finally, when comparing this swingarm to the values found in the literature, represented in table 4.2, it is possible to say that the swingarm the torsional stiffness is:

- much higher than the *Armentani et al.* [71] due to the fact that was evaluated with the use of spindle.
- higher than *Limebeer* [69] *and Sharp* [69, 70] suggested for high performance vehicles.
- really far from the values that *Cossalter* [11] suggested, so problems of handling can be verified and the motorcycle can feel a little bit uncomfortable.

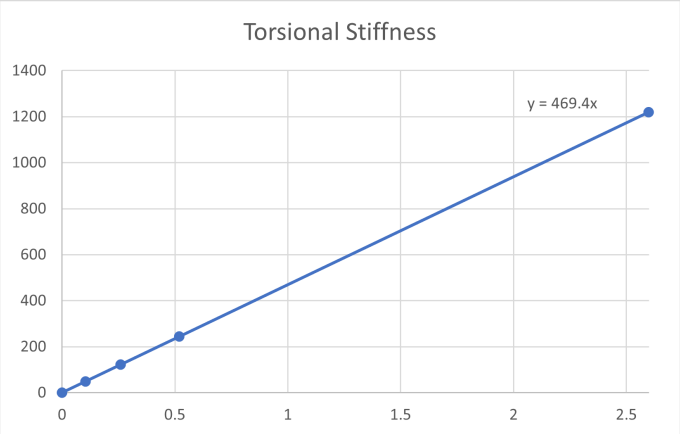


Figure 4.5: Graph representing how angular displacement and torque are related

Table 4.2: Comparison of torsional Stiffness

Swingarm Designation	Torsional Stiffness (Nm/deg)
Kawasaki ZX10R's swingarm, [71]	102.9
Suzuki GSX R1000's swingarm, [71]	140.8
Honda CBR1000R's swingarm, [71]	140.8
Limebeer [69] and *Sharp* [70][69]	209.4
Aluminium DSSA	469.4
S2008 Swingarm, [1]	670
SM 2008 Swingarm, [1]	890
BNG 2008 Swingarm, [1]	1330
Cossalter [11]	1000–2000

4.1.2 Lateral Stiffness

Lateral stiffness was also measured utilizing *Cossalter's* approach illustrated in figure 4.2. The boundary conditions, the type of mesh, and the number of elements on the simulations were the same as in the previous chapter, differing only on the loads applied to the swingarm.

Multiple scenarios with diverse lateral forces applied to the side of the spindle were tested and represented on a graph in order to approximate the stiffness by calculating the slope of the line that represent how the displacement of the swingarm changes with the variation of the lateral force applied.

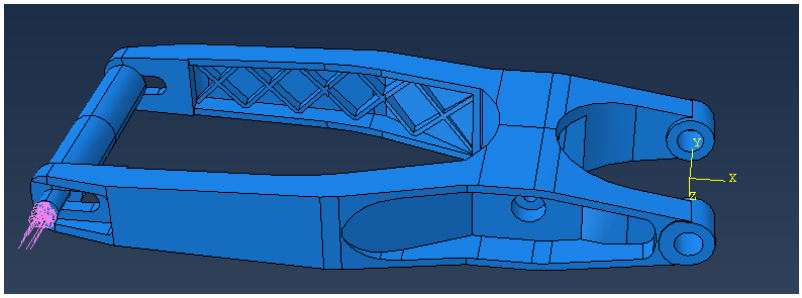


Figure 4.6: Lateral stiffness test according to *Cossalter* Source: [27]

$$K_{lateral}(\frac{kN}{mm}) = \frac{Lateral\ Load(kN)}{Total\ Displacement(mm)} \tag{4.2}$$

Finite element method

Once again, the displacements were calculated using finite element method software Abaqus.

Four different tests were conducted, with lateral forces applied on the spacer of 500N, 1000N, 2000N and 5000N, represented in figure 4.6. The respective simulations are represented in figure 4.7 and, as expected, as lateral loads are increased the displacement tend to be higher and maximum next to the attachment to the rear wheel.

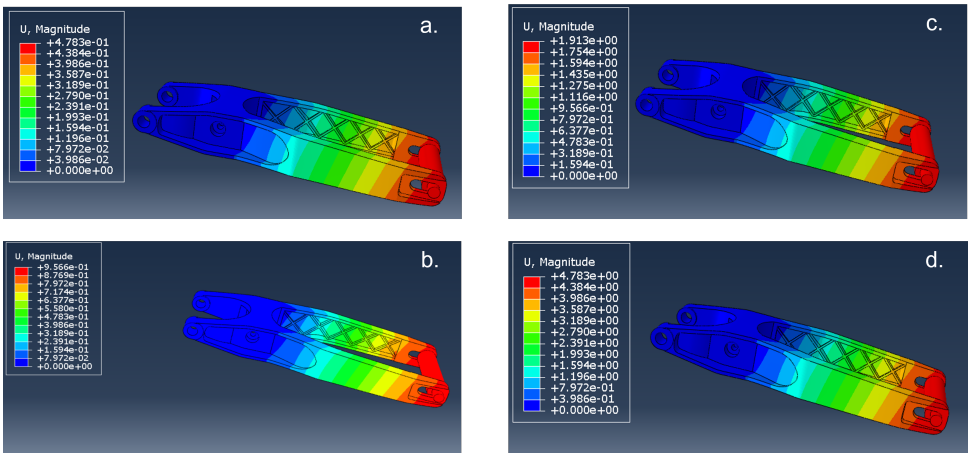


Figure 4.7: Simulation of lateral test with different loads a-500 N, b-1000 N, c-2000 N, d-5000 N

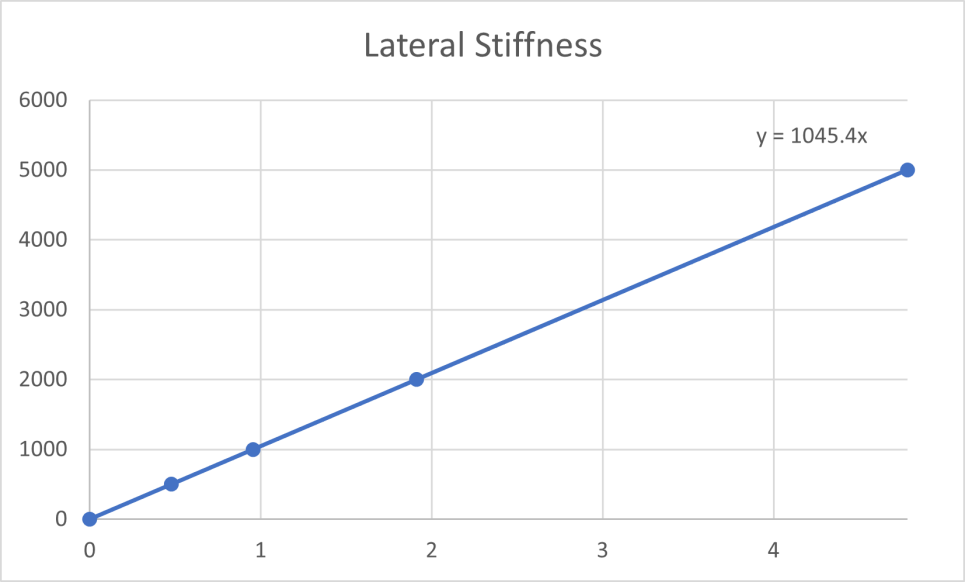


Figure 4.8: Graph representing how displacement and lateral load are related

As it is was previously said, it is possible to take the values of the figure 4.7, in order to plot a graph that relates the displacement of the swingarm and the lateral load that it is submitted in different occasions, shown in figure 4.8.

To sum up, the 4 situations described before, when put together on a graph are part of a line that describes the behaviour of this swingarm. It is possible to conclude that, the swingarm represented has a lateral stiffness of 1045.9 N/mm.

Table 4.3 sums up the values of the literature and compares to the result of the lateral stiffness calculated for this swingarm. The possible takeaways from this comparison are:

- Lateral stiffness is according to the *Cossalter* [11].
- Higher stiffness when comparing to *Armentani et al.* [71]
- From the values found in the literature it is possible to say that the lateral stiffness do not cause any handling problems, since its values are according to the literature
- It is possible to have a better balance between lateral and torsional stiffness

Table 4.3: Comparison of torsional and lateral stiffness of swingarms in the literature

Swingarm Designation	Lateral Stiffness (kN/m)
Kawasaki ZX10R's swingarm, [71]	603
Suzuki GSX R1000's swingarm, [71]	804
Honda CBR1000R's swingarm, [71]	965
Aluminium DSSA	1045.4
Cossalter [11]	800–1600

4.2 Loads applied on the swingarm

In chapter 3.6, the loading conditions to which the swingarm is subjected throughout its lifetime were detailed in depth. An estimation of the loads imparted to the rear wheel with a certain degree of accuracy was also discussed.

To test the swingarm, it is necessary to determine the effect of these previous loads in the swingarm. The type of swingarm, whether it is a single or double sided swingarm, really impacts the loading scenario. In case of a double sided swingarm, the determined loads can be applied to the spindle.

Some other assumptions were made in order to make it possible to calculate the loads applied to the swingarm:

- This motorcycle's rear wheel has dimensions of 140/80-18, which correspond to a diameter of 457.2mm (18") and a width of 140mm.
- The diameter of chain sprocket is three times smaller than motorcycle's rear wheel
- Pitch moment null in the rigid connection to the frame, in other words, the pitch moment produced by the normal load on the swingarm is absorbed by the rear suspension. This is going to be crucial to calculate suspension force.
- The horizontal distance between the attachment to the chassis and the suspension axle mount is 132mm and distance between the attachment to the chassis and the connection to the rear wheel axle is 520mm.
- Lateral distance between the chain and the symmetric axis of the swingarm is neglected.
- Center of gravity height is considered 779mm

Using these assumptions and the equations defined in chapter 3.6, an Octave script, represented in Appendix B.2, was developed in order to calculate loads applied on the swingarm. The input variables of the script are represented in table 3.10.

Table 4.4 represents the loads applied to the center of the spindle, which is going to be used to estimate the stresses during the respective critical situations.

Table 4.4: Double sided Swingarm loads

	Fx (N)	Fy (N)	Fz(N)	Fk (N)	Mx (N.mm)	Mx (N.mm)	Mx (N.mm)
WD Motorcycle	0	841.7	0	-3379.5	0	0	0
WD Motorcycle + rider	0	1442.1	0	-5790.1	0	0	0
Braking	-1033.9	911.8	0	-5450.0	0	0	-236140
Straight Line	6336.2	1442.1	0	-5790.1	0	0	0
Cornering	4856.8	1766.8	10.4	-7093.9	-204970	85000	0
Rear Wheelie	0	4806.9	0	-19300.1	0	0	0

4.3 Load Simulation

4.3.1 Weight distribution of the motorcycle

In this case, only vertical loads are applied to the motorcycle and it is anticipated that this loading scenario is the safest for a motorbike. It occurs when the motorbike is simply supporting its own weight.

After simulating the swingarm using FEM, the results obtained are represented in figures 4.9 and 4.10.

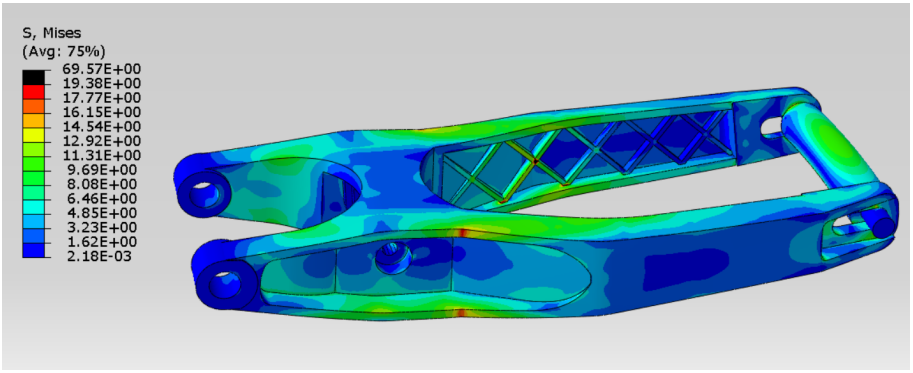


Figure 4.9: Simulation results of the influence of the motorcycle's weight distribution on the swingarm

As expected, the swingarm is under really low stresses on this loading condition, as almost the whole swingarm is under 20 MPa.

There is an increasing stress on the swingarm next to the suspension mount axle, due to the greater vertical force on the rear suspension comparing to the normal load produced by the rear wheel.

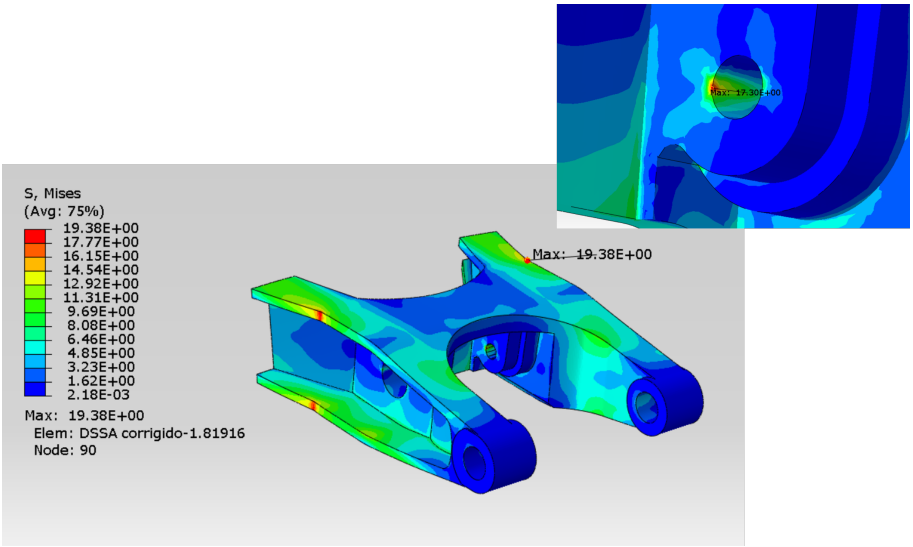


Figure 4.10: Effect of the weight distribution of the motorbike on the rear suspension mount axle

4.3.2 Weight distribution of the motorcycle and rider

This scenario is quite similar to the last since the confirmed loads are at the same location and heading in the same direction. However, they are somewhat larger due to the weight of the rider, which suggests that the stress distribution with increased stresses is expected anticipated.

The findings obtained after modeling the swingarm using FEM are shown in figures 4.11 and 4.12.

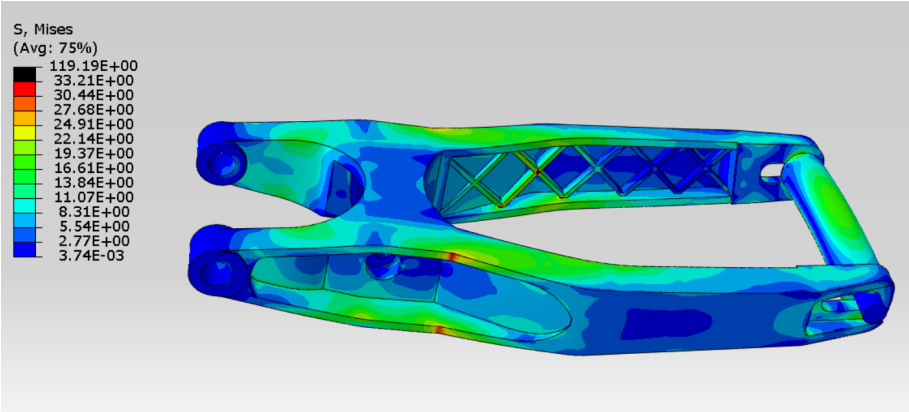


Figure 4.11: Simulation results of the influence of the weight distribution of the motorbike and rider on the swingarm

Once again, the swingarm is subjected to very low stresses under this loading situation, as almost the whole swingarm is under 40 MPa and there is an increase in stress on the swingarm near to the suspension mount axle.

The presence of the rider almost doubled the total stress applied to the swingarm without altering its distribution.

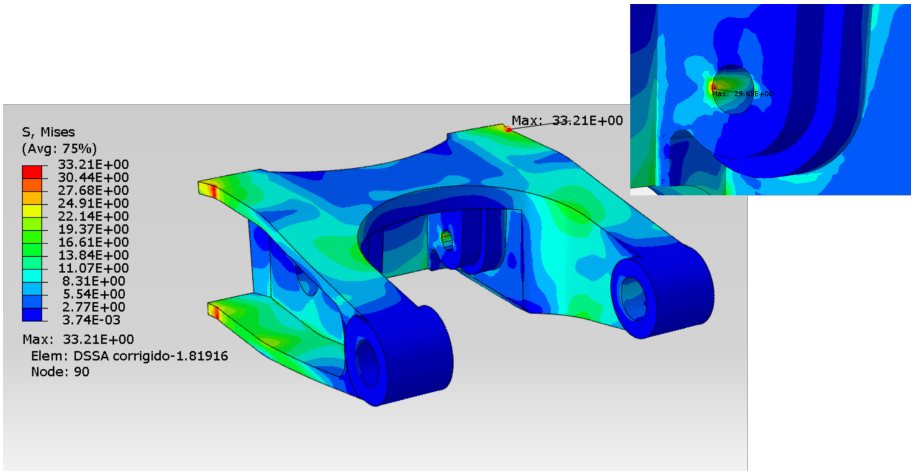


Figure 4.12: Effect of the weight distribution of the motorbike and rider on the rear suspension mount axle

4.3.3 Braking

This case is somewhat different than the previous ones because of the introduction of a friction force between the tire and the road, which is responsible for a longitudinal load on the swingarm and a pitch moment applied on the rear wheel axle.

Furthermore, despite the fact that the normal load is 36% smaller than the prior condition owing to weight transfer (described in chapter 3.6.2), the suspension force difference is only 6% due to the pitch moment. Because of that, it is expected that the region next to the suspension mount axle is still under the maximum stresses.

The results of the simulation using FEM are represented in figures 4.13 and 4.14.

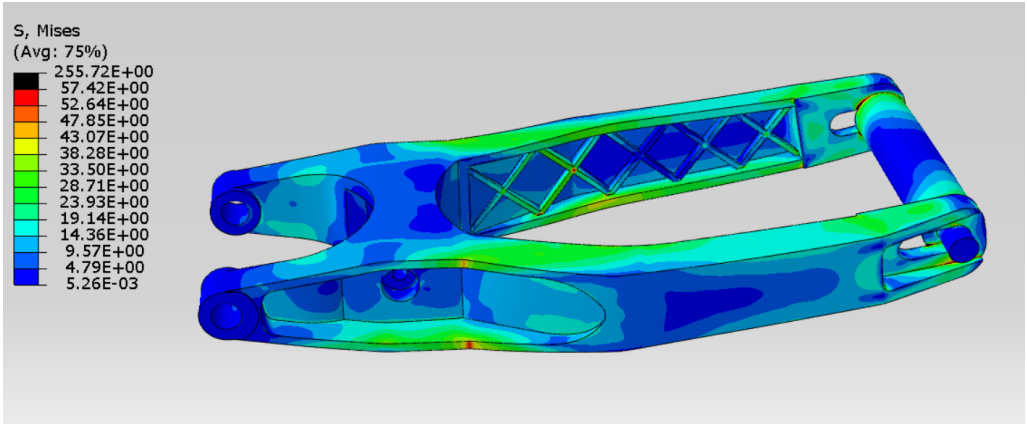


Figure 4.13: Simulation results of the influence of braking on the swingarm

Although, the stress distribution has altered significantly compared to previous instances, as a result of the additional loads to which the swingarm is subjected, the magnitude has not changed much. Nevertheless, it is important to underline that in this situation the elements in the spindle are submitted to stresses similar to as the suspension mount.

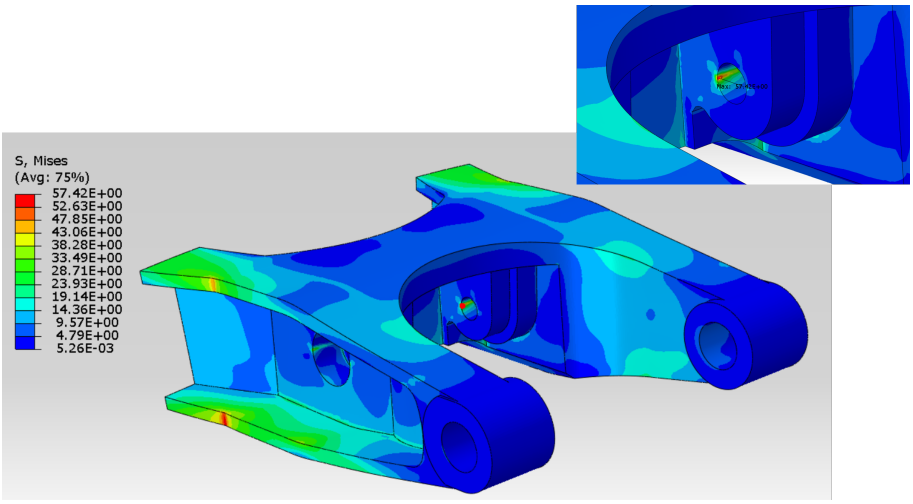


Figure 4.14: Effect of braking on the rear suspension mount axle

4.3.4 Straight line

As stated previously, in this type of swingarm, the lateral distance between the chain and the symmetric axis of the swingarm is assumed to be neglected. Therefore, the yaw moment induced by the chain tension is regarded as zero.

Additionally, in this condition, the maximum chain tension, as well as the maximum traction between the motorcycle and the road, is established. Consequently, the maximum longitudinal force to which the swingarm can be subjected is applied to the swingarm.

Figures 4.15 and 4.16 represents the results of the simulation using FEM.

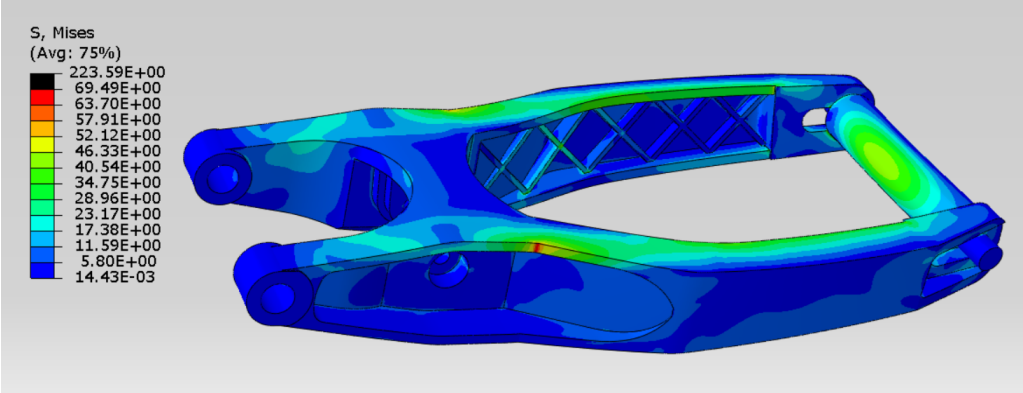


Figure 4.15: Simulation results of the influence of maximum tension scenario on the swingarm

The stress distribution has changed considerably in comparison to previous cases. Besides that, because of the fact that the longitudinal force has an important role on this simulation, the rear suspension mount does not contain the maximum stress, which is located on the top face due to the asymmetry of this swingarm.

Although, the swingarm is under higher stresses in this case when compared to previous situations, it is considered to be under relatively low stresses, as almost the whole swingarm is under 70MPa.

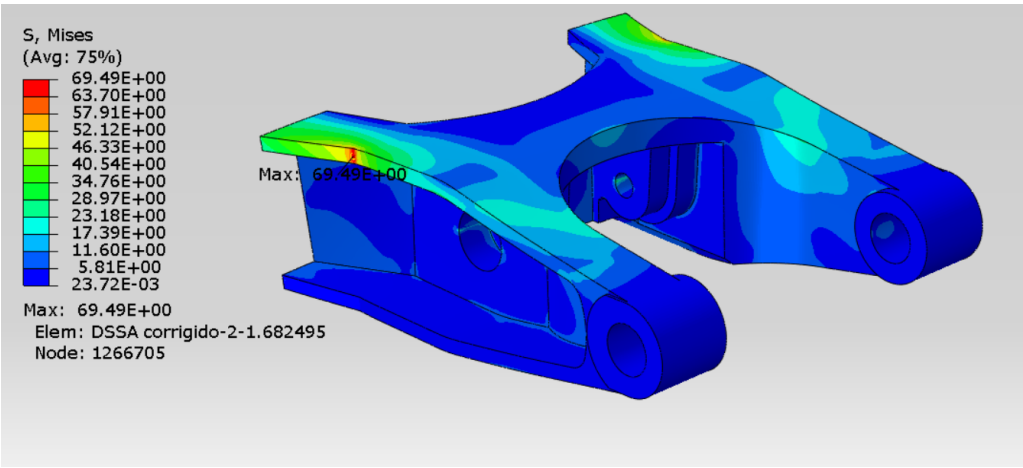


Figure 4.16: Effect of maximum tension scenario on the rear suspension mount axle

4.3.5 Cornering

Once again, as explained in the previous situation, the yaw moment caused by chain tension is considered to be zero. However, during a turn, a leaning motorcycle tends to shift the contact point from the middle plane of the tire to the tire's periphery. Because of that, there is a yaw bending produced by the friction force acting at a distance from the wheel's middle plane. To facilitate the calculations, the contact point is assumed the worst case scenario, which considers the furthest possible point, half of the thickness, which maximizes the yaw moment (M_y).

Furthermore, a twisting moment (M_x) is applied resulting from the misalignment of force R with regard to the hub's center, as it is possible to see from figure 3.12,

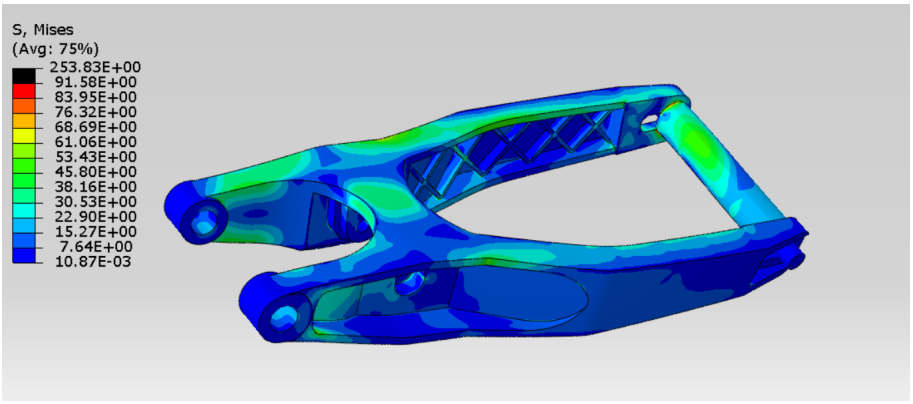


Figure 4.17: Simulation results of the influence of cornering on the swingarm

The simulation results obtained are represented in figures 4.17 and 4.18. The addition of the twisting and yaw bending moment, altered the stress distribution of the swingarm significantly as well as the location of critical point. It is important to note that the swingarm is starting to be submitted under relevant stresses (90MPa) and it is important that the material selection can provide stability to this type of loads.

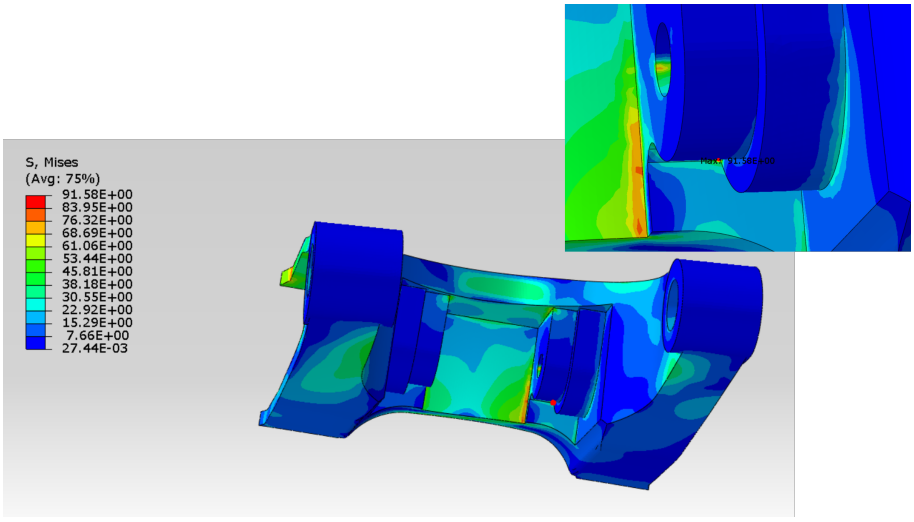


Figure 4.18: Effect of cornering on the rear suspension mount axle

4.3.6 Landing on the Rear wheel

Motorcycles typically do not land with both wheels at the same moment after a jump. Therefore, to maximize the normal load, in this situation, it is assumed that the motorcycle only landed on the rear wheel, maximizing its loading condition.

Although the same type of loadings (normal load and suspension load) is applied in this case as well as in the first two cases, it is important to note that in this situation the normal load and, consequently, the suspension force are several times higher than in those previous cases. As a result of that, it is anticipated that the stress distribution does not change much while having much higher stresses across the swingarm.

The findings obtained after modeling the swingarm using FEM are shown in figures 4.19 and 4.20.

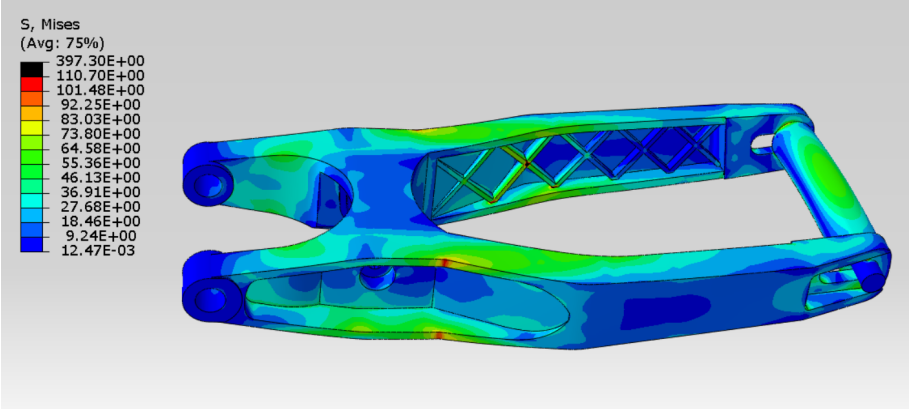


Figure 4.19: Simulation results of the influence of landing on the rear wheel on the swingarm

In this situation, the swingarm is submitted up to 110 MPa on the rear suspension mount axle. It is evident that the material selection and an optimize structure design of the swingarm become critical factors in order to withstand these kind of loading conditions.

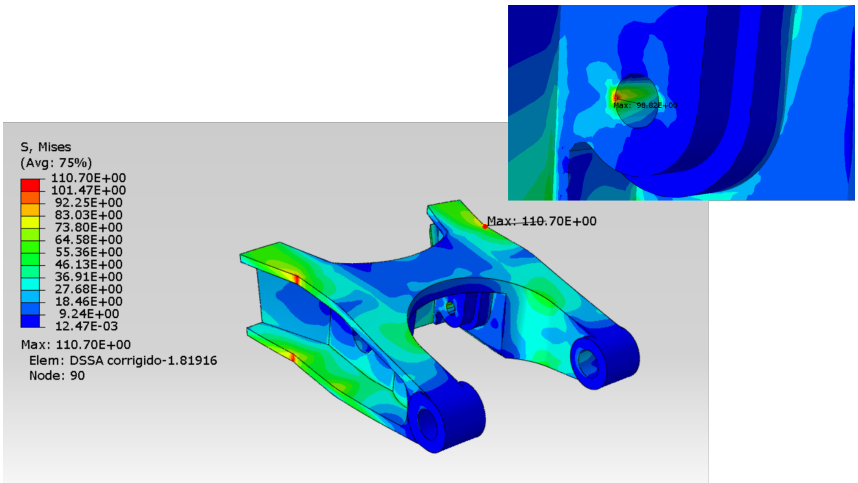


Figure 4.20: Effect of landing on the rear wheel on the rear suspension mount axle

4.3.7 Stress concentration

In every situation, the simulation obtained revealed a stress concentration on the ribs, as illustrated by figure 4.21.

This is because of a slight error in the initial design, which kept the bottom and top faces of the ribs ever touching the rest of the swingarm. So, in order not to alter the lateral and torsional stiffness, as well as to account for the effect of the ribs in the various conditions tested, an extrude was done.

Furthermore, it is also important to note that the sharp edges verified in this location on the analysed model are not created when the manufacturing process is casting. Since this is the proposed manufacturing method and fillets can be produced to reduce tensions even further, the highest stresses measured on the swingarm's ribs can be disregarded.

However, when designing a swingarm it is important to take this stress concentration into account and, during experimental tests, to have a better look into it, and verify if it can be a problem to the swingarm in general and to the safety of the rider.

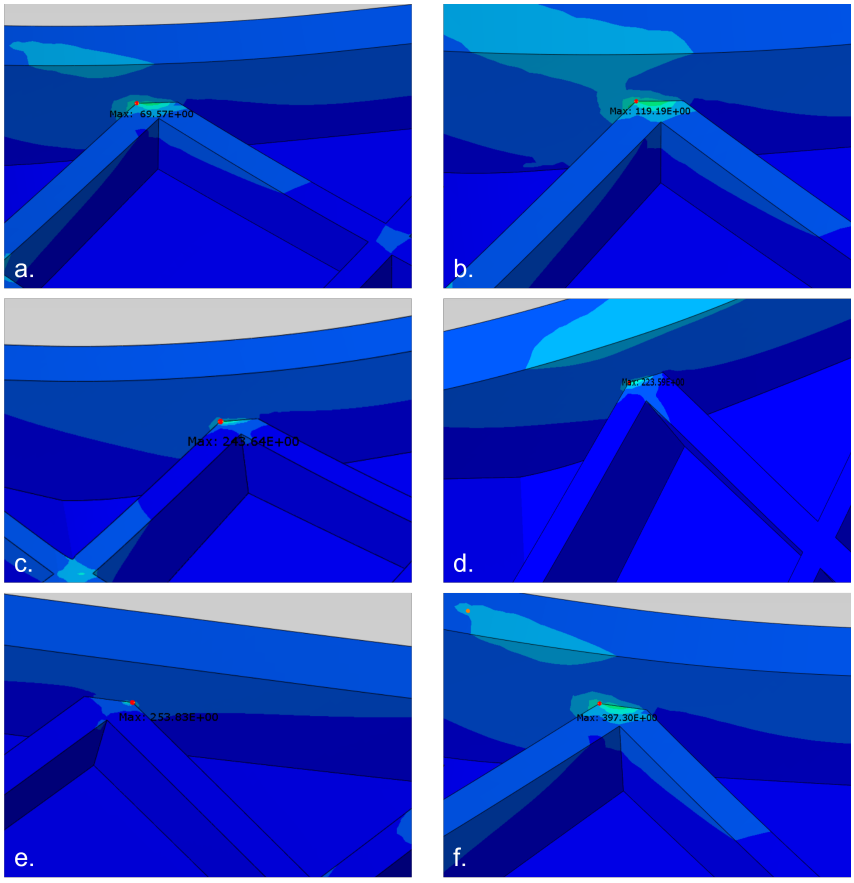


Figure 4.21: Stress Concentration on each situation: a- WD Motorcycle; b- WD Motorcycle+rider; c- Braking; d- Straight Line; e- Cornering; f- Rear Wheelie

4.3.8 Safety factor of each situation

Considering the yield tensile strength of Aluminium Alufont-52 alloy (280 MPa), it is possible to calculate the safety factor of the swingarm during every condition.

Table 4.5: Safety factor for each simulation

Condition	Maximum stress	Safety factor
WD Motorcycle	19.38	14.45
WD Motorcycle+rider	33.21	8.43
Braking	57.42	5.90
Straight Line	69.49	4.03
Cornering	91.58	3.06
Landing on the rear Wheel	110.70	2.53

The highest safety factor during every condition is 2.53, as detailed in table 4.5. Furthermore, as calculated by *Pugsley Method*, the minimum safety factor required for a swingarm must be at least 2.08. Because of that, it is possible to conclude that the minimum safety factor is respected and that the swingarm does not yield.

Furthermore, it is also possible to say that the critical condition is landing on the rear wheel with a normal load of 2g, which is going to be important for the next chapter.

4.3.9 Conclusions

To sum up, the following conclusions were possible to take away from this chapter:

- the connection to the frame is never under a lot of stress so there is no necessity to change it in the single sided swingarm.
- the critical condition is landing on the rear wheel.
- suspension mount is the most critical part of the swingarm, so it must be taken extra precautions during the design.
- the spindle is also submitted to somewhat high stresses, in braking and wheelie for example.
- in the double sided swingarm, the safety factor of the critical situation is 2.53, while the required safety factor is 2.08, which suggests that either:
  - stiffness requirements dictated the design choice.
  - there is a limitation on the cost of the manufacturing process that prevents the swingarm to have a more suitable design.
  - the material selected had a smaller tensile yield strength.

Chapter 5

Single Sided Swingarm

5.1 Standard Design

As previously stated, this thesis aims to design a swingarm capable of replacing the one on AJP's motorcycle. Because of that, some requirements must be previously specified before proposing a suitable design that can withstand the loads applied to the motorcycle as well as have the required stiffness.

Some characteristics of the single-sided swingarm are uncommon or not found on double sided swingarms. As a result, it is essential to detail and explain the significance of these modifications.

Attachment to the rear wheel

The attachment of the single-sided swingarm to the rear wheel axle has a larger diameter and a bigger width than that of the typical double-sided swingarm, in order to accommodate two bearings responsible for supporting the rear wheel shaft while allowing the rotation of the swingarm as well as increasing the contact area.



Figure 5.1: Rear wheel mount on a single sided swingarm. Source: [118]

The larger diameter of the connection represented in Figure 5.1 is a result of the requirement for an excentric rear wheel hub in order to loosen or tighten the chain in accordance with the required chain tension.

Location of the chain

Due to the increasing loads, in a single sided swingarm, the components of the motorcycle can have a different disposition when compared to traditional swingarms.

One of these examples is that the chain sprocket on single-sided swingarms is typically further from the center of the wheel than the swingarm, in order to reduce the yaw moment applied to the swingarm, figure 5.2 clarifies the difference on the position of this components.

On the one hand, on a single sided swingarm, the traction force is equally distributed by both sides of the connection to the rear axle, hence the yaw moment is reduced by minimizing the lateral distance between the rear wheel mid plane and the chain sprocket, which explains why this distance was disregard on the double sided swingarm.

On the other hand, the explanation for the different component's order in a single sided swingarm is that, during cases of high traction between the rear tire and the road, the yaw moment generated by the traction force and the yaw moment produced by the chain tension are opposite, thereby minimizing the total moment to which the swingarm is submitted. However, the swingarm has to be designed taking the chain position into account, which can be different from one motorcycle to another. As a result, in this type of motorcycle the distance between the rear wheel mid plane and the chain sprocket cannot be ignored



Figure 5.2: Chain sprocket location on both types of swingarms (Left- Double Sided Swingarm; Right- Single sided swingarm). Source: [119]

Special Rims

The rear wheel on a motorcycle with a single sided swingarm contains a rim that is typically open on the side that the swingarm is attached to the rear wheel axle. This occurs in order to give enough space so that the swingarm connects the nearest possible to the mid plane of the rear wheel, which translates in a minimization of the twisting moment that the swingarm is submitted.

Figure 5.3 is the portrayal of a motorcycle's rear wheel rim with a single-sided swingarm. As it is possible to see, one side of the component is opened to accommodate the connection between the swingarm and rear wheel axle.



Figure 5.3: Ducati Panigale V4's rear motorcycle rim . Source: [120]

Swingarm Shape

On top of that, there is another consequence to the motorcycle design due to the close distance from the attachment to the rear axle of the swingarm and the center of the wheel.

In particular, the curvature of the swingarm is modified such that the swingarm and tire do not come into touch with one another. Due to this, the design of a single-sided swingarm is curved, and the maximum distance between the motorcycle's mid-plane and the swingarm is maximized adjacent to the tire's radius to prevent possible contact.

Figure 5.4 depicts this circumstance on an actual motorcycle. As can be seen, the swingarm of this motorcycle connected to the rear axle nearly at the center of the rear wheel in order to reduce the loads applied to the swingarm. Therefore, the design must be modified such that this is achievable.



Figure 5.4: Rear wheel and Single sided swingarm. Source: [118]

5.2 Requirements

In order to redesign a swingarm to fit a specific motorcycle, some requirements have to be pre-established so that the previous swingarm can be replaced without further issues:

- the horizontal distance between the attachment to the chassis and the suspension axle mount have to be approximately the same (132 mm)
- the distance between the attachment to the chassis and the connection to the rear wheel axle must be similar (520 mm)
- the connection cavity of the swingarm with the rear wheel shaft requires a diameter of 100 mm and a length of 70 mm in order to be able to fit the two bearing that is required to support the swingarm, while allowing rotation.
- to prevent possible contact, the swingarm must be 20 mm away from the rear tire at a distance from the rear axle equal to the tire's radius. In other words, the geometry of the swingarm must be defined so that the maximum distance from the motorcycle's mid-plane is 90 mm and occurs at a distance of 228.6 mm from the rear wheel hub.
- the distance the motorcycle's mid plane and the chain sprocket is considered to be 150 mm.
- the distance between the motorcycle's mid plane and the center of connection cavity of the swingarm with the rear wheel axle is 70 mm.

5.3 Stiffness Calculation

The aim of this chapter is to describe how the lateral and torsional stiffness of a single sided swingarm was evaluated. The *Cossalter's* [11] approach was once again utilized in order to calculate both lateral and torsional stiffness.

However, in single-sided swingarms, there is only one connection between the swingarm and the motorcycle's rear wheel axle. Because of this, measuring both of these attributes can be somewhat challenging.

The designed single sided swingarms are going to be tested using finite element method in order to measure its stiffness. The standard values of torsional and lateral stiffness that the aim of this design pretend to achieve are the ones which *Cossalter* [11] suggested:

- Lateral Stiffness: 800-1600N/mm
- Torsional Stiffness: 1000-2000Nm/°

5.3.1 Lateral Stiffness

Lateral stiffness was measured without the spindle. In double-sided swingarms, the absence of it results in a decrease in lateral stiffness because both ends are not connected. However, this is not the case here because there is only a connection to the rear wheel axle.

The calculation of the rigidity follows the same logic as in chapter 4.1.2. A 1000N force is applied on the free end of the swingarm, as illustrated in figure 5.5, and the displacements are measured in order to be possible to calculate the lateral stiffness using equation 5.1.

$$K_{lateral}(\frac{kN}{mm}) = \frac{Lateral\ Load(kN)}{Total\ Displacement(mm)} \tag{5.1}$$

Figure 5.5 represents the simulation done to calculate the lateral stiffness of the swingarm.

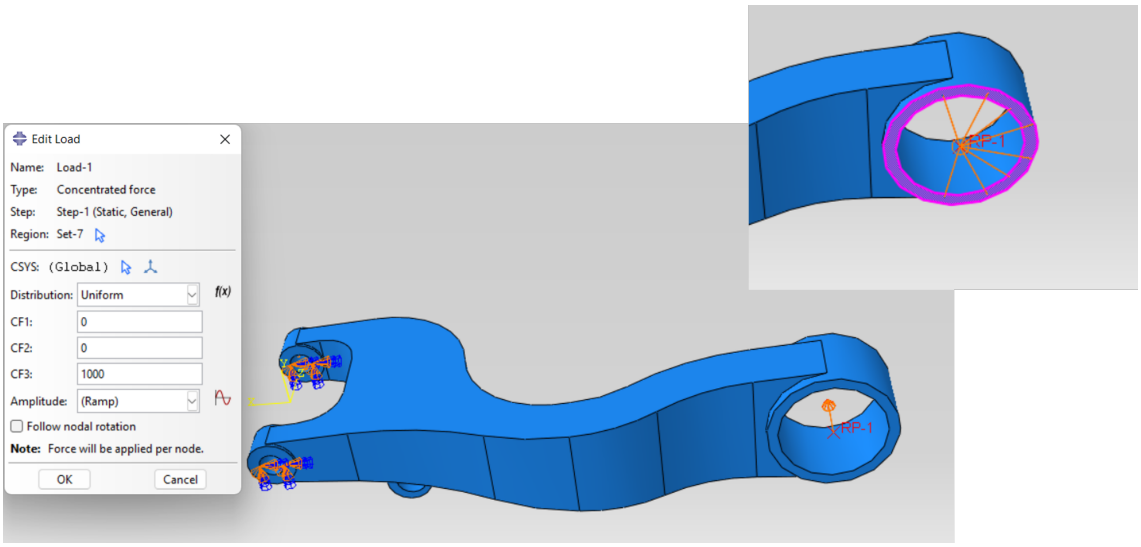


Figure 5.5: Lateral stiffness test of SSSA

5.3.2 Torsional Stiffness

On the other hand, to measure the torsional stiffness, the same method which was employed by *Sarti* [33] was utilized.

In this case, it is crucial to take into account the distance between where the vertical loads are applied and where the connection to the swingarm is made, so that it is possible to calculate where exactly is the axis of rotation responsible for the twisting moments.

As described in chapter 5.2, the horizontal distance between the connection of the swingarm to the rear axle and the center connection of the rear wheel to the rear shaft is 140mm.

As a result, in order to create the model, a circular beam was connected to the swingarm, so that a torsional moment could be applied with 140mm horizontal offset, as represented by figure 5.6. The properties of the beam are the following:

- Material: Alufont-52 (E=71 GPa, $\upsilon = 0.33$)

- Diameter: 100mm
- Length: 180mm
- Type of connection to the Swingarm: Tie

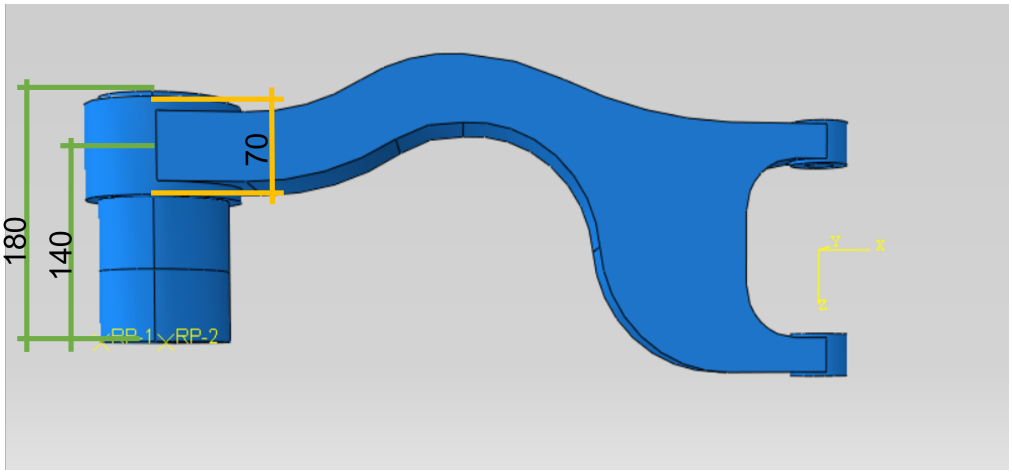


Figure 5.6: Torsional stiffness test measurements

As can be seen by figure 5.7, at the free end of the beam, not only was applied a 100Nm twisting moment, but also a mass and inertia were applied on Reference Point-2 in order to replace the rear wheel. The properties were extracted from *Sarti's thesis* [33].

- $Mass = 10kg$
- $I_x = 0.16\ kg.m^2$
- $I_y = 0.16\ kg.m^2$
- $I_z = 0.31\ kg.m^2$

Since it was not possible to directly extract the swingarm's angle values, the torsional angle must be determined. Consequently, the maximum vertical displacement (Max. VD) and lowest vertical displacement (Min. VD) of the swingarm on the plane represented in figure 5.7 are extracted using FEM. Afterwards, the angle can be calculated using sine function and using the following equation:

$$Angular\ Displacement = arcsin\ (\frac{Max.VD - Min.VD}{70}) \tag{5.2}$$

Finally, the torsional stiffness can be calculated by applying equation 5.3.

$$K_{Torsional}(\frac{kNm}{\circ}) = \frac{Torsional\ Load(kNm)}{Total\ Angular\ Displacement(^\circ)} \tag{5.3}$$

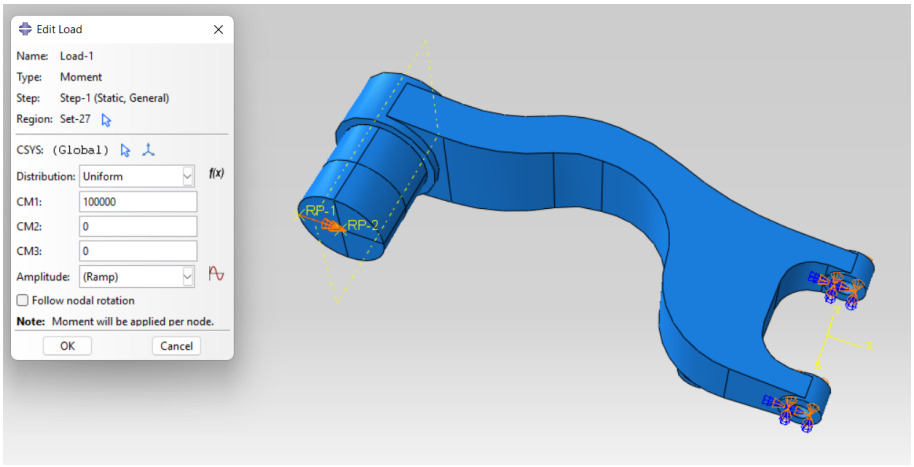


Figure 5.7: Lateral stiffness test of SSSA

5.4 Initial Design

The initial design of the swingarm was based on the single sided swingarm of the Ducati 916. Two different representations were drawn. Later, both of them are going to be exposed to optimization in order to reduce the mass as much as possible while maintaining as much lateral and torsional stiffness as feasible. The main difference between the two initial designs is the position of the suspension mount axle.

On the one hand, one of them contains the suspension mount inside the swingarm, similarly to what happens to the double sided swingarm tested on the previous chapter. On the other hand, the other one has a suspension mount axle on the standard place in single sided swingarms, which is on the top or bottom faces depending on the type of rear suspension scheme utilized. The suspension mount structure is constant in both cases and it is the same in the double sided swingarm.

- *Part 1* contains a suspension mount on the same place as the AJP's swingarm (Figure 5.8)

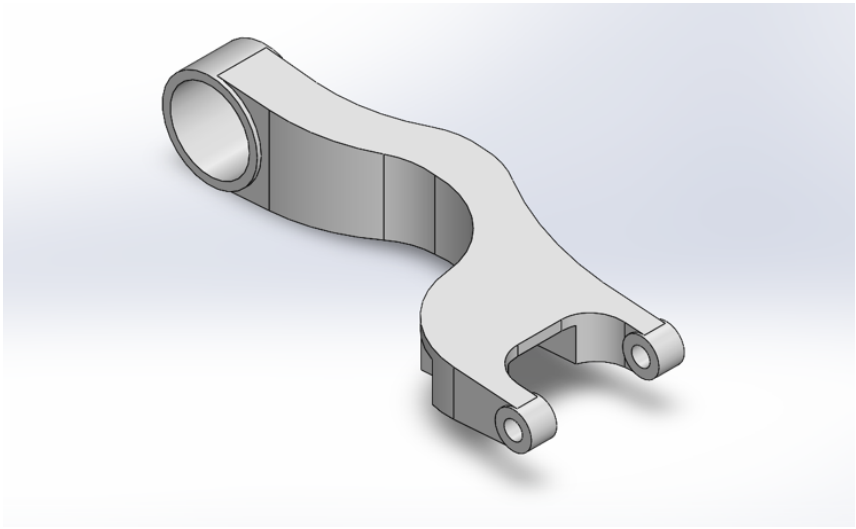




Figure 5.8: Part1

- *Part 2* contains a suspension mount on the bottom face of the swingarm (Figure 5.9), due to the fact that the suspension scheme employed on the AJP uses a connection rod.

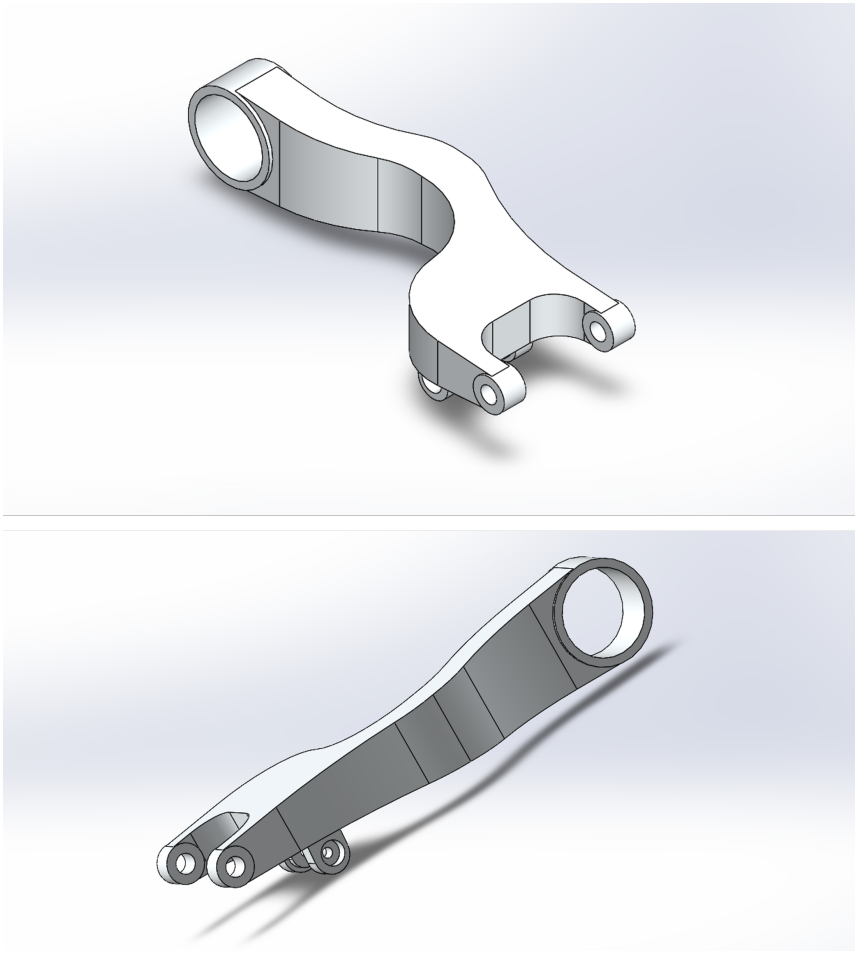


Figure 5.9: Part2

Subsequently, it was possible to measure the mass and the torsional and lateral stiffness of this designs in order to compare it to the previous one.

Both single sided swingarms design proposals were drawn in Solidworks file and using the STEP file, it was possible to import it into Abaqus, where simulations were performed. The mesh convergence of *Part2* is represented in appendix D.2. It was concluded that a global size of seeds of 3mm would give great results, which led to a mesh with 676707 Tetrahedral elements. To further refine the mesh nearby to the suspension mount, some more elements were added there increasing the number of Tetrahedral elements to 812287, as represented in figure D.3. The same size of seeds is assumed for *Part1*.

It was possible to conclude that the swingarm would have a better torsional and lateral stiffness when compared to the double sided swingarm. However, the design would be unrealistic due to its high mass.

5.4.1 Part1

Mass

Considering the aluminium alloy Alufont-52 with a density of 2750 kg/m^3, this design weights 7.88kg.

Lateral Stiffness

The lateral stiffness tested was tested by applying a load of 1000N on the free end of the single sided swingarm, as represented in figure 5.5. The finite element method simulation of this test is represented on figure 5.10.

The tests resulted in a maximum lateral displacement of 0.438mm, which results in a lateral stiffness of:

$K_{lateral} = \frac{1000}{0.438} = 2283.11$

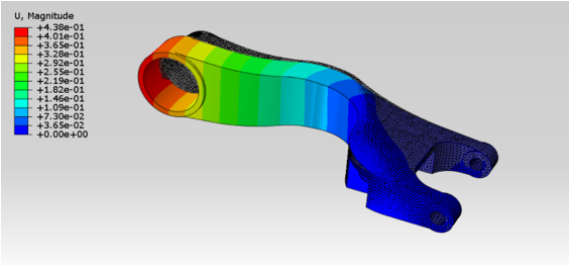


Figure 5.10: Lateral Stiffness test Part1

Torsional Stiffness

On the other hand, the torsional stiffness was tested by applying a torque of 100Nm as represented in figure 5.7 and the results of the torsional test are represented in figure 5.11

As explained in chapter 5.3.2 and using equation 5.2, the angular displacement could be calculated:

$$Angular\ displacement = arcsin\ (\frac{0.0305-(-0.0113)}{70}) = 0.0342^{\circ}$$

$$K_{torsional} = \frac{100}{0.00342} = 2922.80$$

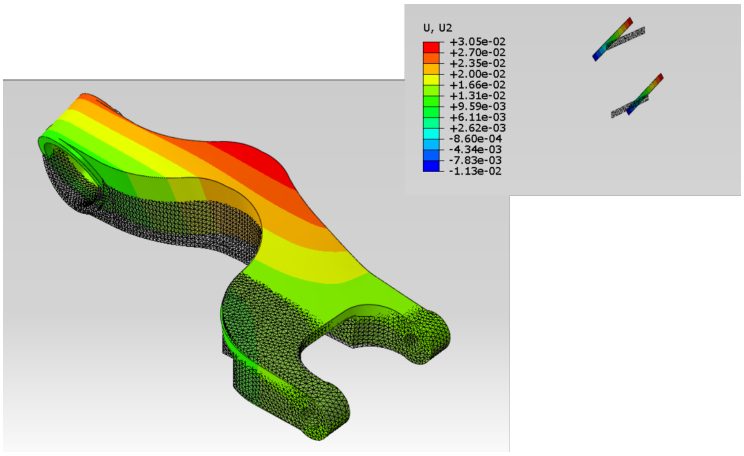


Figure 5.11: Lateral Stiffness test Part1

5.4.2 Part2

Using the same logic, the mass, the torsional stiffness, and the lateral stiffness was measured using the finite element method for *Part2*. The results of the respective test simulations represented in figure 5.12.

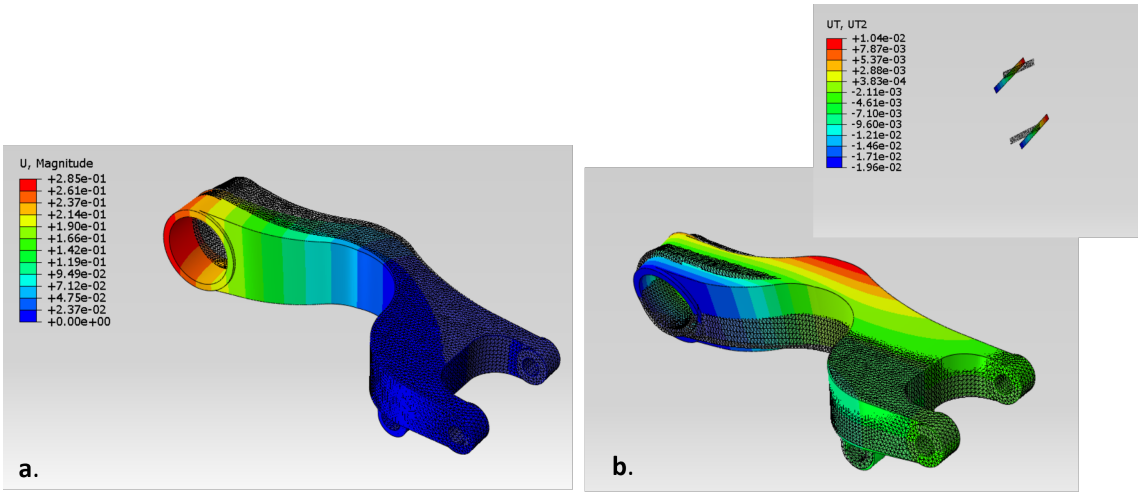


Figure 5.12: Torsional and Lateral Stiffness test Part2

- **Mass**

  Considering the the aluminium alloy Alufont-52 with a density of 2750 kg/m^3, this design weights 9.51kg.

- **Torsional Stiffness**

  The torsional test represented in figure 5.12 shows a maximum displacement of 0.0104mm and a minimum of -0.0196mm.

  $Angular\ displacement = arcsin\ (\frac{0.0104mm-(-0.0196)}{70}) = 0.0246^{\circ}$

  $K_{torsional} = \frac{100}{0.00246} = 4047.43N/^{\circ}$

- **Lateral Stiffness**

  The tests revealed a maximum lateral displacement of 0.285mm, resulting in a lateral stiffness of:

  $K_{lateral} = \frac{1000}{0.285} = 3511.24N/mm$

5.5 Second Design

To deal with the previous problem and to substantially reduce swingarm's mass, the manufacturers design a hollow structure. By initially assuming a thickness of 10mm in between the single sided swingarm. It was also recognized that next to the suspension mount there is the necessity of more material due to high stresses, which are expected as concluded in the previous chapter.

As it is assumed the manufacturing process is casting and the material was selected taking that into account, the structure must be modified in order to allow for the removal of the sand core, which has to be sustained by chaplets. In order to give space to remove the core, a hole must be located on the connection of the swingarm to the rear wheel axle. The subsequent designs lack this characteristic. Nonetheless, it is essential to keep this in mind.

5.5.1 Part1

Due to the fact that the suspension mount structure is inside the swingarm in *Part 1*, the hollow would be really difficult to design next to the suspension mount. Because of that, it was decided that the hollow structure would just be designed as represented in figure 5.13

The lateral and torsional stiffness were measured using the same method as before. For the lateral stiffness, the lateral displacement is 0.526mm. On the other hand, for torsional stiffness, the maximum and minimum displacement is respectively 0.0348mm and -0.0146mm. The properties of this design are represented in table 5.1 as well as the reduction of these properties compared to the first design.

Table 5.1: Properties of the second design of *Part1*

Property	Unity	Value	Reduction
Mass	kg	6.07	22.97%
Torsional Stiffness	$Nm/^{\circ}$	2473.15	15.38%
Lateral Stiffness	N/mm	1901.14	16.73%

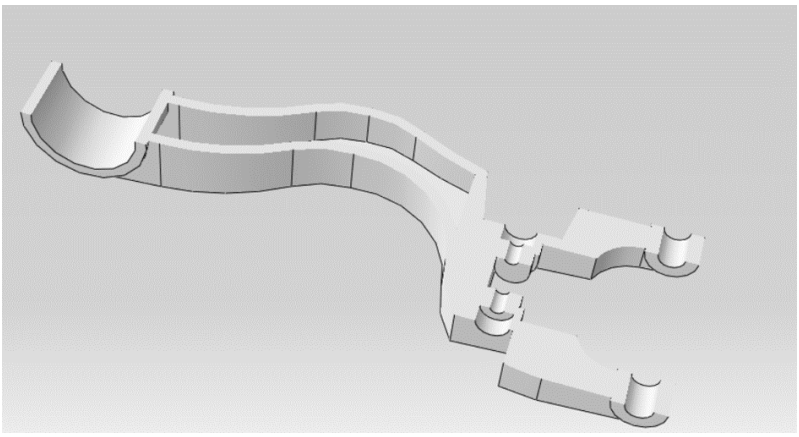


Figure 5.13: Hollow Structure Part1

5.5.2 Part2

However, in *Part 2* the structure could be designed with a hollow all over the structure, as represented in figure 5.14. Therefore, it is expected that the mass would decrease much more here and the influence of the thickness would be much notorious.

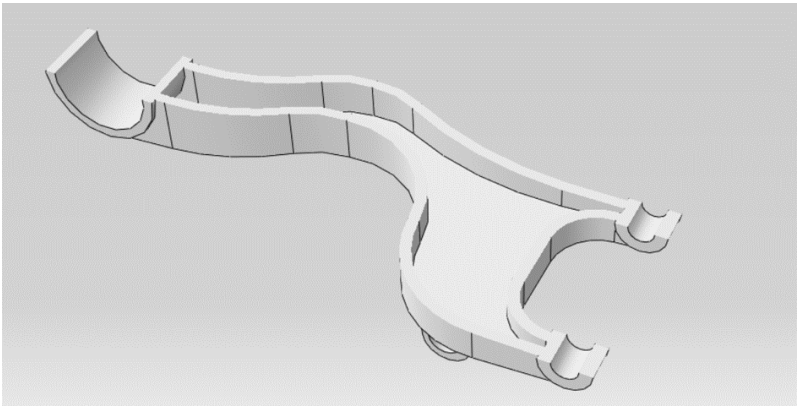


Figure 5.14: Hollow Structure Part2

The lateral displacement for lateral rigidity is 0.48 mm. In contrast, the maximum and minimum displacements for torsional stiffness are 0.00539 mm and -0.0435 mm, respectively. The properties of this design are listed in table 5.2, along with their reduction in comparison to the original design. As it is possible to conclude the mass reduction is much more significantly when compared to *Part1*.

Table 5.2: Properties of the second design of *Part2*

Property	Unity	Value	Reduction
Mass	kg	5.31	44.16%
Torsional Stiffness	$Nm/^{\circ}$	2498.94	38.63%
Lateral Stiffness	N/mm	2083.33	40.67%

5.6 Loads calculation

In depth information was provided in chapter 3.6, regarding the loading conditions to which the swingarm is submitted. A relatively precise assessment of the loads given to the rear wheel was also explored.

In order to test the swingarm, it is required to identify how these previous loads affected the swingarm. The type of swingarm, whether single or double sided, has a significant effect on the loading scenario. As explained before, while the double sided swingarm are just exposed to twisting moments during cornering, the single sided swingarm is always under this type of moments, due to the asymmetry.

Because of that, it is expected that in every situation the swingarm is expected to have twisting moments due to the normal force applied to the swingarm.

To maximize cornering loads on the motorcycle, it is assumed that the motorcycle is turning right so that the maximum torque arm is verified on the swingarm which is located on the other side. In this situation, the moment arm of the normal load, applied to the further end of the motorcycle tire, is considered to be the sum of half of the width of the tire with the distance u, which is lateral distance between the mid plane of the wheel and attachment to the swingarm.

Moreover, as explained before the distance the motorcycle's mid plane and the chain sprocket cannot be neglected in this case and it is considered to be 150mm. This is going to increase the yaw moments produced by the swingarm and during high tension scenarios this moment can be extremely high. The respective moment arm's distance is the difference between the lateral distance inclosed by the mid plane of the wheel and the chain sprocket, e and the lateral distance that separates the mid plane of the wheel and attachment to the swingarm u, which means that the distance between the chain force and the center of the connection of the swingarm is: $d = e - u$

All the other assumptions made in the last chapter to calculate the loads on the double sided swingarm are maintained.

Once again, an Octave program was developed, which is represented in Appendix B.3. The equations defined in chapter 3.6 are going to enable the creation of the script and to obtain suitable results.

Table 5.3 represents the respective loads inserting the input variables of the script represented in table 3.10.

Table 5.3: Single sided Swingarm loads

	Fx (N)	Fy (N)	Fz(N)	Fk (N)	Mx (N.mm)	My (N.mm)	Mz (N.mm)
WD Motorcycle	0	841.7	0	-3379.5	-58918	0	0
WD Motorcycle + rider	0	1442.1	0	-5790.1	-100940	0	0
Braking	-1033.9	911.8	0	-5450.0	-63828	-72373	-236350
Straight Line	6336.2	1442.1	0	-5790.1	-100940	-268950	0
Cornering	4856.8	1766.8	10.4	-7093.9	-249730	-121420	0
Rear Wheelie	0	4806.9	0	-19300.1	-336480	0	0

5.7 Iterations

In section 5.5, the second design of both *Part1* and *Part2* continue to have a really high mass when compared to the double sided swingarm. Because of that, it was decided that in order to achieve the lowest possible mass or, in the best scenario, the weight of the designed SSSA would have a similar weight as the DSSA, an iteration would be done.

In this iteration, the optimal modifications for each design would be calculated in order to determine which change would result in the greatest mass reduction while keeping the maximum feasible lateral and torsional stiffness.

It was determined that three distinct dimensions would be the most ideal to alter in both circumstances and would produce a diverse variety of results that would produce an optimal solution. These dimensions are represented in figure 5.15.

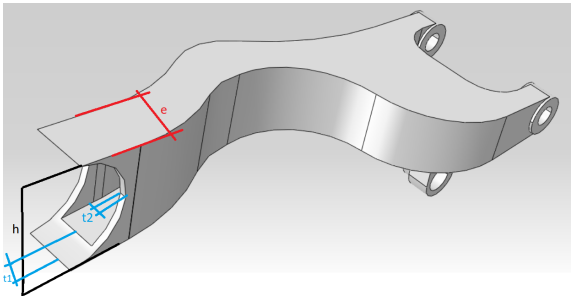


Figure 5.15: Illustration of possible modification

Firstly, the interior thickness of the swingarm can be varied. It is going to be assumed that the thickness on the top and bottom faces is t_1, while the thickness on the lateral faces is t_2, as it is demonstrated in figure 5.15. Three different thickness were selected in order to compare the results obtained by each (5mm, 7.5mm and 10mm). Due to the fact that t_1 does not necessarily have to be the same as t_2, 8 new different designs were created and tested in order to conclude which is the suitable alteration for each Part.

Secondly, the height, h (represented in figure 5.15), could also be changed. Although, as previously said the requirement of the attachment to the rear wheel axle must be constant, the connection of the hollow structure must not have to be tangent and different heights between the hollow structure and the connection to the rear axle structure were simulated. Two new different heights were tested corresponding to 110mm and 100mm, while the initial structure had 120mm.

Thirdly, the width, e of the structure was also under tests. It was simulated and concluded if decreasing the width would translate into good results on the structure or whether it would change substantially the structure torsional and lateral stiffness. The initial structure contained 60mm of width and tests of different widths until 45mm were carried out decreasing 5mm each time, which corresponds of the test of three different new designs.

5.7.1 Terminology

From now on, the terminology utilized, will consider different values of t_1, t_2, h, and e. For example, Part2-t10/5_h100_e50, corresponds to the design of *Part2*, which contains the suspension mount on the bottom face of the swingarm, with t_1=10mm, t_2=5mm, h=100mm, and e=50mm. In case one of these dimensions are not expressed, it is considered the standard values of $t_1 = 10mm$ and $t_2 = 10mm$, h=120mm and e=60mm.

5.7.2 Method of Iteration

This subchapter seeks to show how the goal of the best feasible solution with the highest possible torsional and lateral stiffness was attained.

Initially, a sensitivity analysis was performed, where a number of simulations were performed, each of which would modify one of the possible adjustments presented previously on the basic design presented in chapter 5.5, while leaving everything else unchanged. This was done in order to establish a hierarchy of the mass-reduction modifications that would have the least detrimental effect on the swingarm's stiffness.

After that, an iteration was done in order to achieve the previous mass of 4.33kg. The following process was utilized:

1. calculate the torsional and lateral stiffness of the design and choose the best alteration, based on these scenarios:

    - In case lateral is inside the standard interval while torsional stiffness is higher than the upper limit, it is going to be given more importance to the lateral stiffness and the selective parameter is going to be: $\Delta K_l/\Delta m$
    - In case torsional is inside the standard interval while lateral stiffness is bellow than the lower limit, it is going to be given more importance to the lateral stiffness and the selective parameter is going to be: $\Delta K_l/\Delta m$
    - In case torsional is inside the standard interval while lateral stiffness is higher than the upper limit, it is going to be given more importance to the torsional stiffness and the selective parameter is going to be: $\Delta K_t/\Delta m$
    - In case lateral is inside the standard interval while torsional stiffness is bellow than the lower limit, it is going to be given more importance to the torsional stiffness and the selective parameter is going to be: $\Delta K_t/\Delta m$
    - In case both lateral and torsional stiffness are superior or inferior or inside at the same time the standard intervals presented in 5.3. Both of them have the same importance and the deciding stiffness parameter is: $(2 * \Delta K_l + 1.6 * \Delta K_t)/\Delta m$. This will be explained more in detail in chapter 5.7.3

2. Design the next solution with the alteration selected before

3. Test whether this design surpasses the yield tensile strength on the critical condition (landing on the rear wheel with a normal force of 2g) with a safety factor of 2.08

4. In case the desired mass is not achieved and the critical condition does not cause the swingarm to yield continue with the iteration process. Whereas, in case the ideal weight is achieved or the safety factor is not respected, the last design which does not yield, would be considered the final design.

5. In the end, the best solution is addressed and the simulation of the other loading conditions are carried out in order to conclude if the critical condition assumed is the correct one.

5.7.3 Stiffness Parameter

As previously stated, according to *Cossalter* [11], the lateral stiffness standard range is 800-1600N/mm, while the torsional stiffness standard range is 1000-2000N/deg. In case K_l range is multiplied by 2, the lateral stiffness will have a standard value between 1600 and 3200N/mm and if K_t is multiplied by 1.6 it is also having an interval of 1600 to 3200 Nm/deg, as represented by figure 5.16

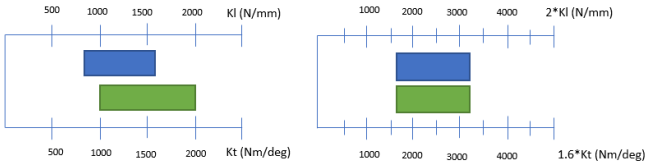


Figure 5.16: Representation of the standard range of torsional and lateral stiffness on left and on the right demonstrates that by multiplying the range interval of K_l by 2 and K_t by 1.6 both intervals become 1600-3200 in their respective units
Blue-lateral stiffness, Green-torsional stiffness

In order to give lateral and torsional stiffness equal relevance, the parameter $(2 * Kl + 1.6 * Kt)/3.6$ was employed to calculate a "weighted average" of torsional and lateral stiffness.

This will imply that, a torsional stiffness of 1750 Nm/deg, which is 87.5% of the upper limit of the standard range of values for torsional stiffness, have the same importance as the lateral stiffness of 1400 N/mm, which is 87.5% of the upper limit of the standard range of values for lateral stiffness (1750*1.6=1400*2=2800)

It is important to understand that this parameter is only for comparison purposes and must not be used anywhere else, as it is being used to sum properties with different units and have no mechanical meaning.

To explain it better, considering point A, B, and C represented in figure 5.17:

In case of a reduction of 200 N/mm of the lateral stiffness (Point A), which is 25% of the interval of the standard values of lateral stiffness, the variation of stiffness parameter is equal to 111.11.

In case of a reduction of 250 Nm/deg of the torsional stiffness (Point C), which is also 25% of the interval of the standard values of torsional Stiffness, the variation of stiffness parameter is also equal to 111.11.

In case of a reduction of 150 Nm/deg of the torsional stiffness and 80 N/mm of the lateral stiffness (Point B), which is 15% of the interval of the standard values of torsional stiffness and 10% of the interval of the standard values of lateral stiffness. The sum of the percentage of reduction of the stiffnesses results in 25% and the variation of stiffness parameter is also equal to 111.11.

Because of that, it is concluded that it being given the same importance to the torsional as the lateral stiffness.

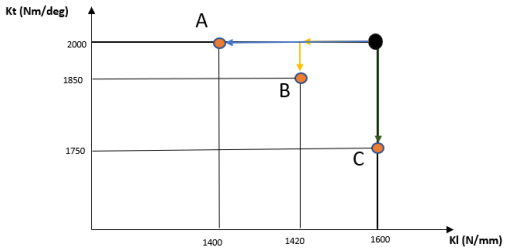


Figure 5.17: The variation of the stiffness parameter of three points with different properties. It shows that the stiffness of parameter defined can have the same value for different torsional and lateral properties

5.8 Part1

5.8.1 Hierarchy of changes

5.8.1.1 Thickness

As previously said, 8 new designs were tested in order to conclude how the stiffness and the mass are related and which is the most suitable for the problem in question.

Firstly, the values of mass and lateral stiffness for each alteration are represented in figure 5.18. It is also represented the value of the the slope of the line that relates lateral stiffness and mass.

This is crucial because the lower the slope, the higher the difference of mass for the same variation of lateral stiffness. As a result, the favorable results are the ones with the smallest slope.

With the previous figure, it is possible to conclude that the best possible alteration would be decreasing t_2 to 7.5mm. This would decrease the torsional stiffness by 4%, by only decreasing the mass by 6%. The ratio between the variation of the lateral stiffness and variation of mass is only 476 N/(kg.mm).

In addition to this, looking at the results of the decrease of only t_1, or t_2 or both the t_1 and t_2 a few interesting conclusions could be extracted. Firstly, as demonstrated in the hierarchy, it is possible to conclude that a higher t_1 leads to a smaller slope. As a result, it is possible to say that

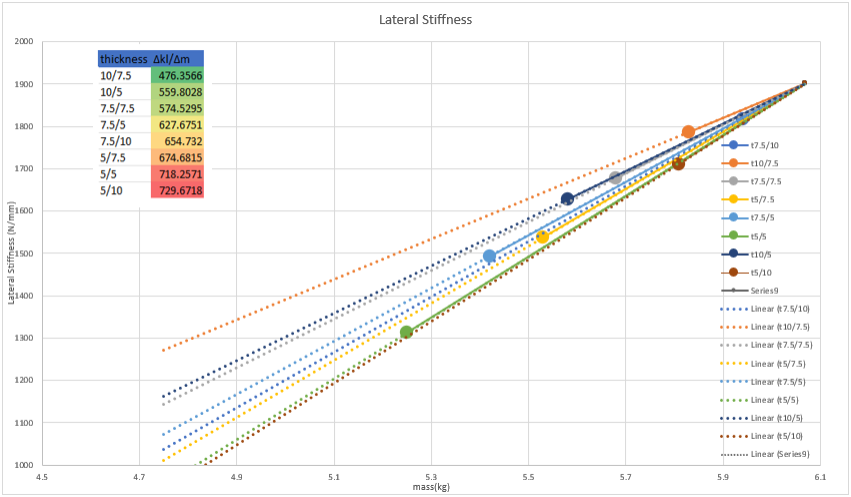


Figure 5.18: Lateral stiffness decrease by changing thickness on *Part1*

maintaining t_1 as high as possible will lead to better results in terms of higher lateral stiffness by reducing weight.

Finally, the reduction of the lateral stiffness is much bigger when comparing to the reduction of the weight as the thickness is lower. This can be seen by comparing the results from decreasing t_1 and t_2 to 5mm and when it is decreased to 7.5mm, the mass reduction is almost constant -6.4% from reducing from 10mm to 7.5mm, and -7.6% from reducing from 7.5mm to 5mm. However, the lateral stiffness is really influenced when comparing the -11.8% from reducing from 10mm to 7.5mm, and -16.3% from reducing from 7.5mm to 5mm.

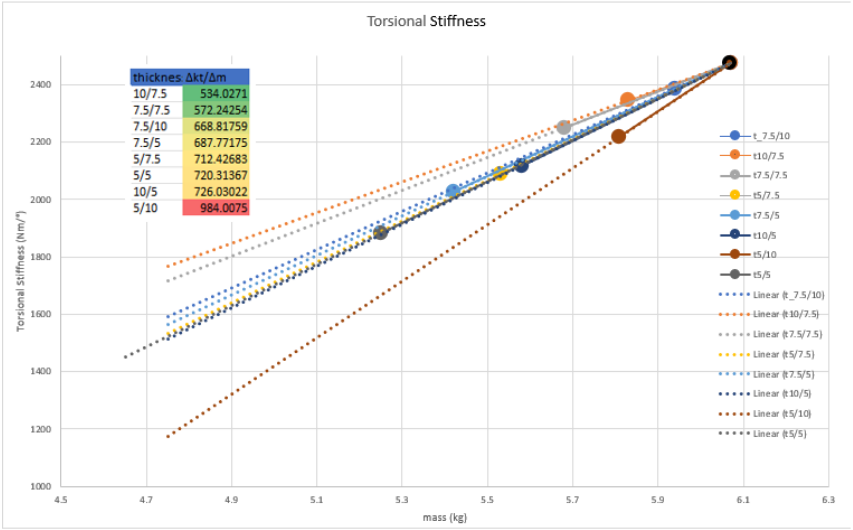


Figure 5.19: Torsional stiffness decrease by changing thickness on *Part1*

The values of the ratio between the variation of the torsional stiffness and variation of mass are presented in figure 5.19, which is going to be important to have a hierarchy in cases that this parameter is the deciding factor of each alteration to make on the design.

The torsional stiffness study has similar results when compared to the results obtained previously. Once again, the best solution is to simply decrease t_2 to 7.5mm. However, the mass difference of mass is not that impactful. Furthermore, it is also verified that as the thickness decreases, the torsional stiffness is really influenced more and more.

Moreover, in this case, the worst possible scenarios are when the difference between t_1 and t_2 is substantial. In these cases, either t_1=10mm and t_2=5mm or the opposite, the torsional stiffness has extremely decreased, which suggests that this type of solution should be avoided in cases that the torsional stiffness is important.

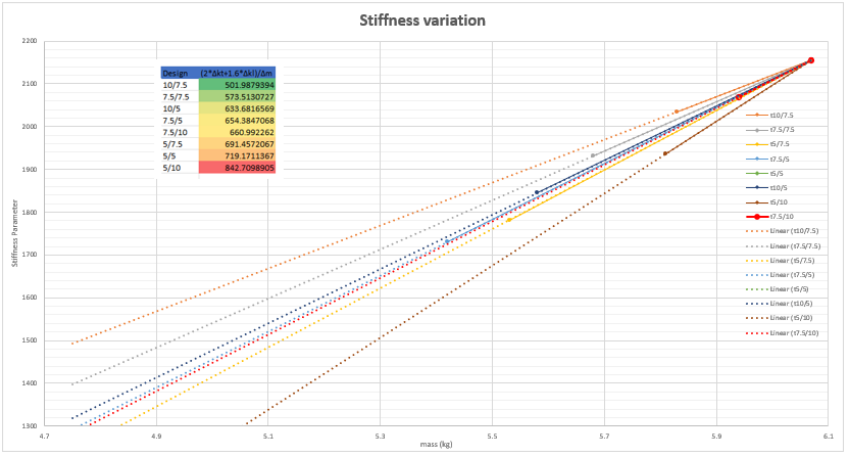


Figure 5.20: Stiffness parameter change with thickness on *Part1*

Finally, the values in cases where both the torsional and lateral stiffness are both higher than the upper limit, inside the range or smaller than the lower limit of the range of standard values of these type of stiffness are presented in figure 5.20. It was decided that to evaluate using the parameter $(2 * \Delta K_l + 1.6 * \Delta K_t)/\Delta m$ as explained before.

As expected the hierarchy in this case does not vary a lot from the previous ones. Once again having t_1=10mm and t_2=7.5mm is the best solution in terms of reducing the most mass possible without changing much the stiffness.

5.8.1.2 Height

In this case, only simulations with two different heights were carried out. It was tested how the swingarm would be affected by reducing the height, h, to 110mm and 100mm. The results are represented in figure 5.21.

As it possible to see from the obtained results, the way torsional stiffness relates with mass is not really affected by the height of the swingarm. However, the same does not apply for the lateral stiffness, where particularly as height increases the lateral stiffness reduction is much bigger when compared to the mass reduction. In this case, decreasing h to from 120mm to 110mm verifies a mass reduction which is 4.6% and reducing from 110mm to 100mm decreases 4.7% of the mass from reducing from 7.5mm to 5mm. However, the lateral stiffness reduction is really influenced

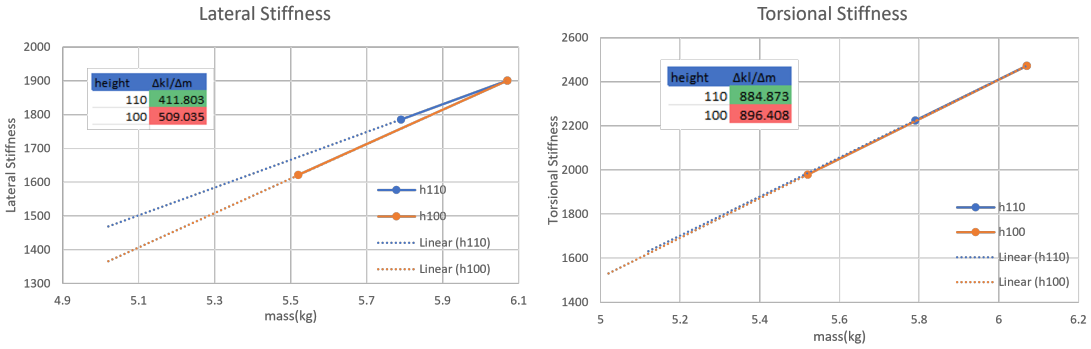


Figure 5.21: Torsional stiffness and Lateral change with height on *Part1*

when comparing the 6.1% from reducing from 120mm to 110mm, and 9.2% from reducing from 110mm to 100mm.

As anticipated, the value of the stiffness parameter, figure 5.22, would be largely affected by the ratio between lateral stiffness and weight, as the height of the swingarm has little effect on the relation torsional stiffness with mass.

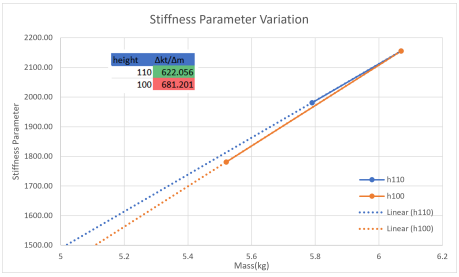


Figure 5.22: Stiffness Parameter variation with height on *Part1*

5.8.1.3 Width

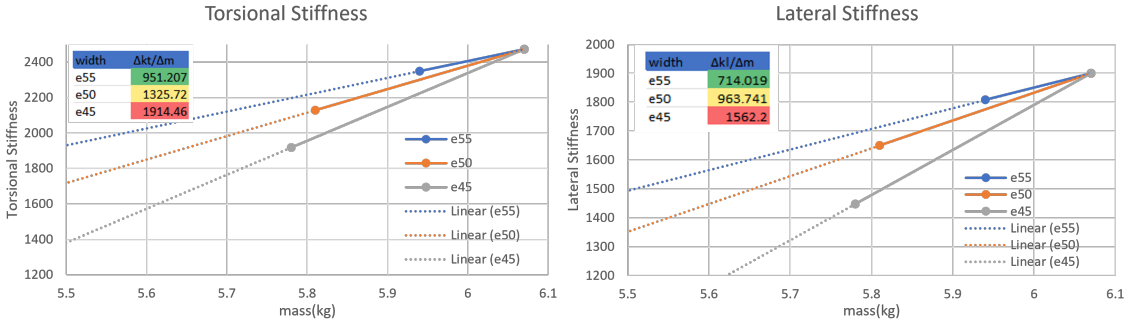


Figure 5.23: Torsional stiffness and Lateral change with width on *Part1*

Finally, the influence of the width on the mechanical properties of the swingarm as well as the weight is considered. The simulation results are represented in figure 5.23.

Taking into account the slope of each line, it is verified that as the thickness decreases, the torsional stiffness and the lateral stiffness are really influenced more and more. Because of that, the width has to be reduced in order to have a lighter swingarm and it must be the minimum possible so that the stiffness values are not as influenced.

The values of the ratio between the variation of the torsional stiffness and variation of mass and the variation of the lateral stiffness and variation of mass seems to be really similar. Because of that, it is expected that the stiffness parameter also is, which happens according to figure 5.24.

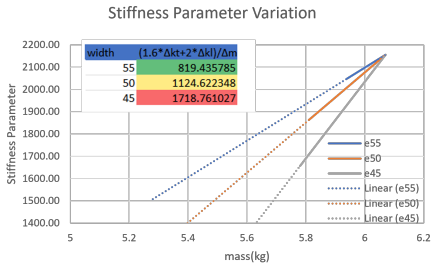


Figure 5.24: Stiffness Parameter variation with width on *Part1*

5.8.1.4 Final Hierarchy

Putting every data previously demonstrated together, a final hierarchy of the alterations on the different scenarios can be created and presented in table 5.4. It is important to remember that the lower the ratio between the variation of the stiffness and the variation of the mass is, the lighter the swingarm becomes without affecting too much its stiffness, which is what is preferred.

Table 5.4: Alteration Hierarchy *Part1*

Parte 1

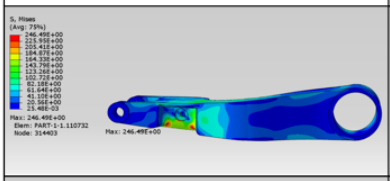
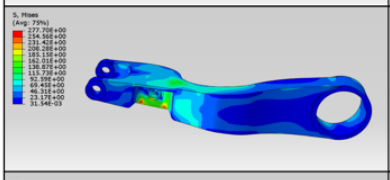
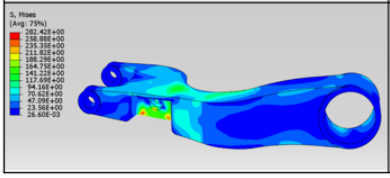
thickness	massa	Δkl/Δm	Δkt/Δm	(1.6*Δkt+2*Δkl)/Δm
10/10	6.07			
7.5/7.5	5.68	574.529	572.243	573.5130727
5/5	5.25	718.257	720.314	719.1711367
10/10	6.07			
10/7.5	5.83	476.357	534.027	501.9879394
10/5	5.58	559.803	726.03	633.6816569
7.5/5	5.42	627.675	687.772	654.3847068
7.5/10	5.94	654.732	668.818	660.992262
5/10	5.81	729.672	984.007	842.7098905
5/7.5	5.53	674.682	712.427	691.4572067

h	massa	Δkl/Δm	Δkt/Δm	(1.6*Δkt+2*Δkl)/Δm
120	6.07			
110	5.79	411.803	884.873	622.0562192
100	5.52	509.035	896.408	681.2005362

width	massa	Δkl/Δm	Δkt/Δm	(1.6*Δkt+2*Δkl)/Δm
60	6.07			
55	5.94	714.019	951.207	819.435785
50	5.81	963.741	1325.72	1124.622348
45	5.78	1562.2	1914.46	1718.761027

5.8.2 Iteration

Table 5.5: Iteration process of *Part1*

Iteration	Mass	Torsional Stiffness (Nm/°)	Lateral Stiffness	Max. Tension	Terminology
	6.07	1901.14	2473.14	246.5	*Part1-t10/10*
	5.83	1786.82	2344.98	277.70	*Part1-t10/7.5*
	5.68	1677.1	2249.96	282.42	*Part1-t7.5/7.5*

The iteration started with the design detailed in chapter 5.5 and taking into consideration the iteration process described in chapter 5.7.2. The iteration process is described on table 5.5. Finally, in the third iteration, the tensile yield strength is exceeded, which concludes the iteration process and the final design is achieved.

5.8.3 Final design of Part1

The *Part 1's* final design, represented in figure 5.25, has a mass of 5.68kg, which is significantly higher than the double sided swingarm that was studied previously, which had a mass of 4.33kg.

Nonetheless, this design features exceptionally high torsional and lateral stiffness, which will significantly enhance the rider's comfort and handling.

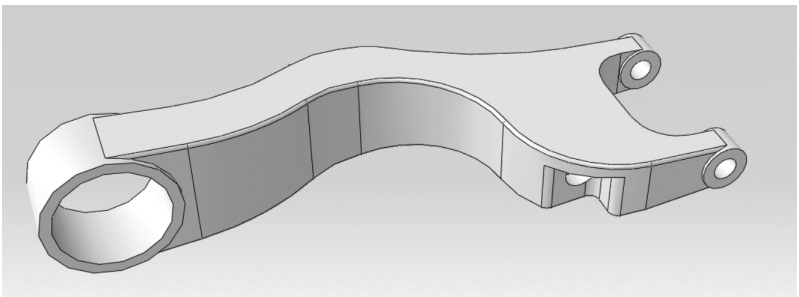


Figure 5.25: Final Design Part1 *Part1*

5.9 Part2

5.9.1 Hierarchy of changes

5.9.1.1 Thickness

Similarly, to the previous design, *Part2* also went through a iteration process in order to decrease its mass.

Firstly, the lateral stiffness was measured in order to be able to create a graph that represents the lateral stiffness with the mass. The alteration with favorable results are the ones with the smallest slope.

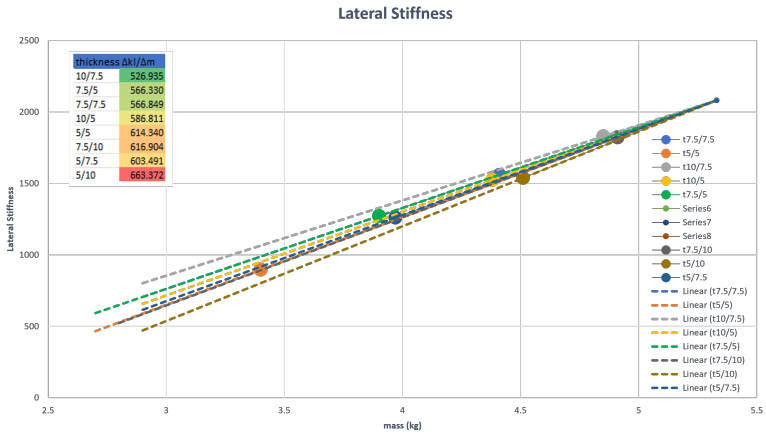


Figure 5.26: Lateral stiffness decrease by changing thickness on *Part2*

As demonstrated in figure 5.26, the most suitable transformation is when t_2 decreases to 7.5mm from the initial 10mm. However, the mass in this alteration is not really affected, which suggests that it might be possible that it should be complemented with another change.

Secondly, as demonstrated in the hierarchy, it is possible to conclude that a higher t_1 leads to higher slope than decreasing t_2. However, in cases where t_1 and t_2 are really different, the lateral stiffness decreases substantially.

Finally, as the thickness is lower and lower, while the mass has an approximately constant decrease, the lateral stiffness is substantially more influenced, which leads to higher values of ratio between the difference of lateral stiffness and the difference of mass.

In regard to torsional stiffness, there are three main conclusions that are possible to extract from the represented in figure 5.27.

In the first place, that the bigger the difference between t_1 and t_2, the higher the slope. This can be justified by the worst case scenarios being the maximum difference between t_1 and t_2, which suggests that it must be avoided to make in cases where the torsional stiffness is important. While this also happened in the lateral stiffness, it was not to the same extent to the point of being that linear.

In the second place, as seen in the lateral stiffness, as thickness is smaller and smaller, the torsional stiffness is also much more influenced when compared to the mass.

In the third place, when t_1 is bigger than t_2, for instance t_1 =10mm and t_2 =7.5mm, while the decreasing of torsional stiffness is almost the same, the mass reduction in the first case is higher when comparing to the opposite, t_2 =10mm and t_1 =7.5mm, which leads to better results in terms of what it is been looking for.

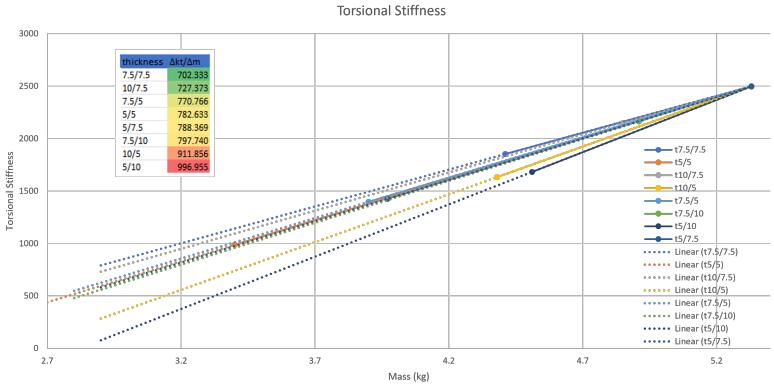


Figure 5.27: Torsional stiffness decrease by changing thickness on *Part2*

In relation to the stiffness parameter $(2\Delta K_l + 1.6\Delta K_t)/\Delta m$ as explained before, the deciding factor in cases where the torsional and lateral stiffness are equally important, because it would fit the best on the optimization of the swingarm.

It is anticipated the hierarchy in this case does not vary a lot from the previous ones, due to the fact that it takes both of the values into account, as it is illustrated by figure 5.28.

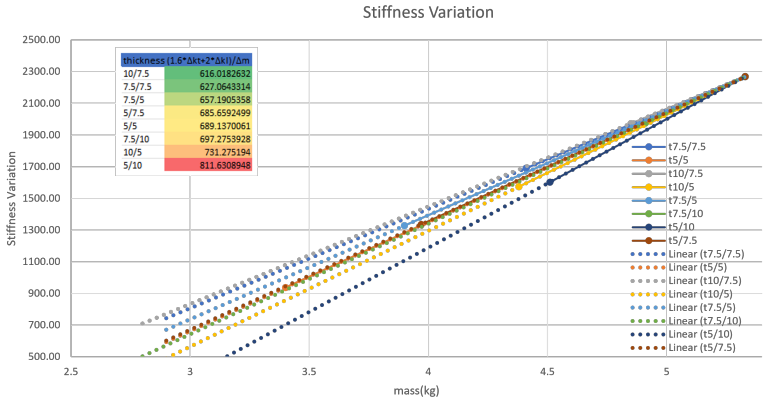


Figure 5.28: Stiffness parameter change with thickness on *Part2*

5.9.1.2 Height

Regarding alterations on the swingarm to *h*=100mm and *h*=110mm, figure 5.29 represents the results of the decrease of torsional and lateral stiffness in function of the decrease of mass.

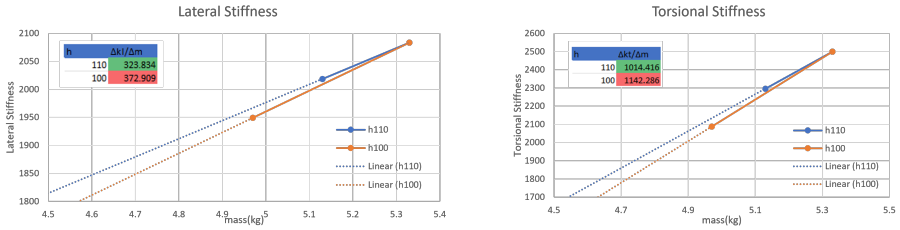


Figure 5.29: Torsional stiffness and Lateral change with height on *Part2*

In respect to the lateral stiffness the results are approximately the same as in *Part1*. As the difference of *h* increase, the lateral stiffness is severely more and more affected, which translates to higher difference of lateral stiffness when compared to the difference of mass.

On the other hand, while in *Part1* it was concluded that the ratio between the difference of torsional stiffness by the difference of mass was not affected by the height of the swingarm, the same does not apply here. Furthermore, it is also possible to say that the torsional stiffness is much more affected compared to the lateral stiffness by this alteration, as it possible to see from the value of the slope on figure 5.29.

Finally, due to the fact that, as the height increases, there is an escalation of the negative impact on the properties of the swingarm, such as the torsional and lateral stiffness. Because of that, the stiffness parameter, that evaluates how the decreasing of mass impacts the reduction of both these values, also follows the same pattern, as represented by the following figure 5.30.

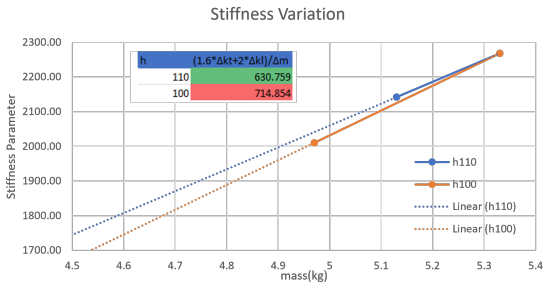


Figure 5.30: Stiffness Parameter variation with height on *Part2*

5.9.1.3 Width

Taking into account the slope of each line, it is demonstrated that when the thickness lowers, the torsional stiffness and lateral stiffness are in fact increasingly impacted. For lateral stiffness, higher values of the width cause the respective ratio to be almost constant, whereas for torsional stiffness smaller values of the width cause the respective ratio to be almost constant, as represented in figure 5.31. The variation of the stiffness parameter with the mass is also represented in figure 5.32.

Ultimately, the change of width is not really advantageous on this experiment. The values of the slope that relates the stiffness with the mass are much higher when compared to the previous

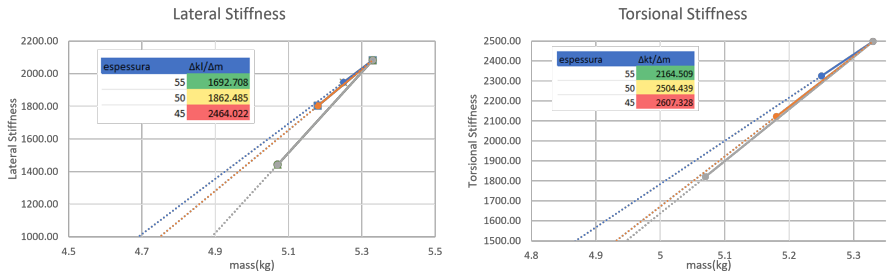


Figure 5.31: Torsional stiffness and Lateral change with width on *Part2*

alterations of height and thickness. Because of that, it is possible to conclude that the width should be as high as possible without jeopardizing the design of the motorcycle.

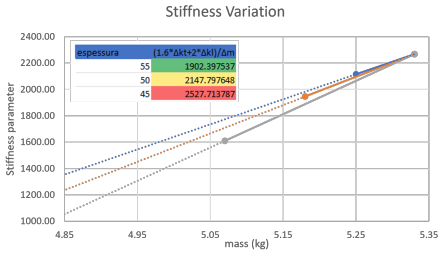


Figure 5.32: Stiffness Parameter variation with width on *Part2*

5.9.1.4 Final Hierarchy

By combining all previously presented information, a final ranking of the adjustments to the various scenarios can be established and presented in table 5.6. It is essential to note that as the ratio between the variation of stiffness and the change in mass decreases the alteration becomes more and more suitable.

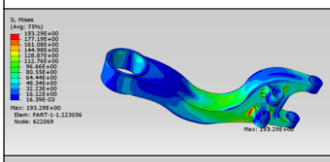
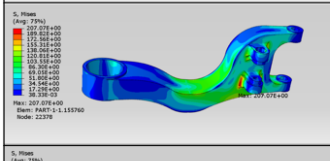
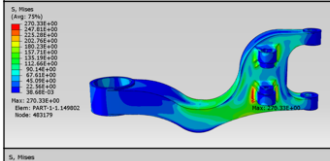
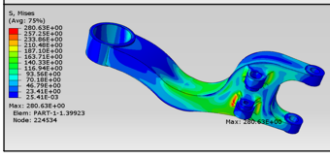
Table 5.6: Alteration Hierarchy *Part2*

Part2

thickness	massa	Δkl/Δm	Δkt/Δm	(1.6*Δkt+2*Δkl)/Δm
10/10	5.33			
7.5/7.5	4.41	566.849	702.333	627.0643314
5/5	3.4	614.340	782.633	689.1370061
10/10	5.33			
10/7.5	4.85	526.935	727.373	616.0182632
10/5	4.38	586.811	911.856	731.275194
7.5/5	3.9	566.330	770.766	657.1905358
7.5/10	4.91	616.904	797.740	697.2753928
5/10	4.51	663.372	996.955	811.6308948
5/7.5	3.97	603.491	788.369	685.6592499
h	massa	Δkl/Δm	Δkt/Δm	(1.6*Δkt+2*Δkl)/Δm
120	5.33			
110	5.13	323.834	1014.416	630.7592459
100	4.97	372.909	1142.286	714.8543268
width	massa	Δkl/Δm	Δkt/Δm	(1.6*Δkt+2*Δkl)/Δm
60	5.33			
55	5.25	1692.708	2164.509	1902.397537
50	5.18	1862.485	2504.439	2147.797648
45	5.07	2464.022	2607.328	2527.713787

5.9.2 Iteration

Table 5.7: Iteration process of *Part2*

Iteration	Mass	Torsional Stiffness (Nm/°)	Lateral Stiffness	Max. Tension	Terminology
	5.33	2083.3	2498.9	193.3	*Part2-t10/10*
	4.85	1830.4	2149.8	207.1	*Part2-t10/7.5*
	5.41	1561.8	1852.8	270.33	*Part2-t7.5/7.5*
	4.31	1531.2	1744.4	280.6	*Part2-t7.5/7.5_h110*

Following the iteration process described in chapter 5.7.2, a final design was obtained. The iteration process is described on table 5.7. In this case, both the mass of the double sided swingarm was achieved as well as the tensile yield strength was obtained during the simulation of the critical situation.

5.9.3 Final Design of Part2

The *Part 2's* final design, represented in figure 5.33, has a mass of 4.31kg, which is equivalent to the double sided swingarm that was studied previously, which had a mass of 4.33kg.

Furthermore, this design features exceptionally high torsional and lateral stiffness, being inside the standard values suggested by *Cossalter*, by only surpassing the tensile yield strength by 0.5MPa, which is going to be neglected.

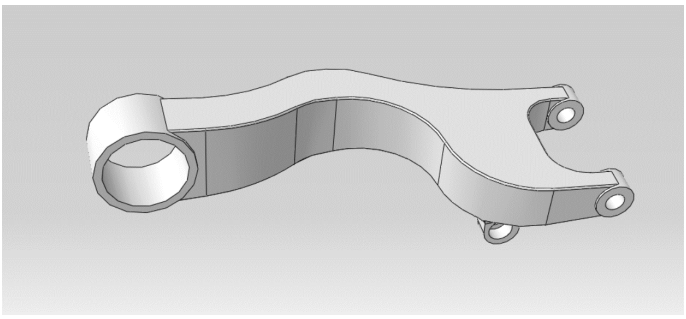
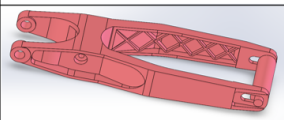
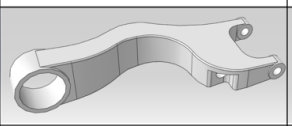
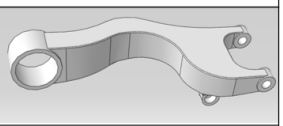


Figure 5.33: Final Design *Part2*

5.10 Comparison

Table 5.8: Comparison of the final designs with double sided swingarm

Swingarm	Double sided swingarm	*Part1-t7.5/7.5*	*Part2-t7.5/7.5_h110*
Design			
Mass(kg)	4.33	5.68	4.31
Kt (Nm/°)	469.4	1677.1	1744.4
Kl (N/mm)	1045.4	2249.96	1531.2
SF	2.53	2.08	2.08

After going through a sensitivity analysis, where it was verified how a certain variable change the properties of the swingarm, and an iteration process finally, two final designs were achieved. Taking into account the three designs described in this thesis represented in table 5.8, a few comparisons are possible to take away:

- in the double sided swingarm, the safety factor of the critical situation is 2.53, which suggests that either:
  - stiffness requirements dictated the design choice.
  - there is a limitation on the cost of the manufacturing process that prevents the swingarm to have a more suitable design.
  - the material selected had a smaller tensile yield strength.
- The higher stiffness comparing to the upper limit of the normal range of *Part1* it is justified by its massive weight.
- The torsional stiffness of the double sided swingarm is not within the normal values for swingarms, while on the designed single sided swingarms the torsional rigidity on the upper half of the standard range.
- The lateral stiffness of all swingarm are within the range of normal values.
- The single sided swingarm is under higher loads, hence the material selected had a really high tensile yield strength, which could affect the cost.
- Designing a suspension mount axle inside a single sided swingarm is really complex due to numerous places where stress concentration occurs and the designer must take extra precaution to avoid it. That is the reason why, usually, motorcycles manufacturers that produces single sided swingarms prefers to have the suspension mount on the top or bottom faces.

Comparing the two designs made on this research, it is possible to conclude that the final design of *Part2* would be the better option to a motorcycle, due to the fact that it is more than 1kg lighter and respects the stiffness requirements.

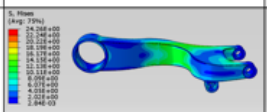
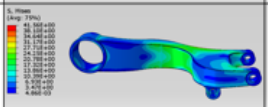
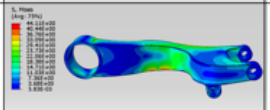
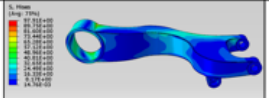
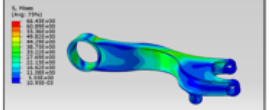
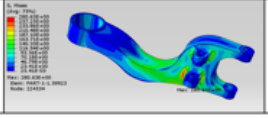
Comparing this design to the double sided swingarm, both these designs have the same weight. However, the single sided swingarm have a higher lateral and torsional stiffness, which suggests a better handling and comfort. Because of that, it is possible to conclude that it was obtained a great solution and the overall goal of the thesis was obtained. A detailed drawing is shown in appendix E.

5.11 Safety Factor confirmation

A safety factor of 2.08 is the smallest pretended safety factor as calculated by *Pugsley Method*. It was reached this value by testing the condition of landing on the rear wheel with a normal load of 2g, which was deemed as the critical condition. However, to make sure that the critical condition assumed during the iteration process was done correctly, all the other conditions described on chapter 3.6 were tested.

The safety factor of each individual condition, as well as the representation of corresponding simulation are represented in table 5.9. As it is possible to see, the critical condition was assumed correctly, and, therefore, it is possible to conclude that the designed swingarm will not suffer any type of yield.

Table 5.9: Safety factor during different conditions

Condition	Simulation	Safety Factor
Weight Distribution Motorcycle		11.54
Weight Distribution Motorcycle + rider		6.74
Braking		6.35
Straight Line		2.86
Cornering		4.21
Landing on the rear wheel		2.08

Chapter 6

Conclusion

The aim of this thesis was to replace a double sided swingarm of a motorcycle with a single sided swingarm. The motorcycle, in this dissertation, is submitted and tested during conditions that occurs during road driving. Firstly, in the chapter of the state of art, the geometry of the motorcycle was understood, the different swingarms were characterized, and finally swingarms of real motorcycles were examined. This chapter was important to have an overall understanding about the motorcycle.

In the following chapter, the different approaches to optimize a swingarm were described and comprehended. Taking different approaches into account was important in order to comprehend which are the crucial properties of the swingarm, so that the approach utilized on this dissertation could be explained.

After that, it was possible to demonstrate some situations that could cause critical loads to the swingarm. Using some information from the literature it was possible to calculate the loads on the motorcycle during these situations. Using an Octave Script, the loads on the each type of swingarm could be calculated.

Taking this into account, the double sided swingarm was tested using finite element method, with the aim of calculating the critical situation and points. It was concluded that the critical situation is landing on the rear wheel with a normal load of 2g, and the maximum stresses occurs next to the suspension mount. This was important so that the single sided swingarm was designed taking this into account. The lateral and torsional stiffness was also calculated in order to compare to the final design. However, it was demonstrated that the torsional stiffness are not in accordance with the normal range of standard values.

Similarly, after designing in *Solidworks*, the single sided swingarm was also tested. An hierarchy was created in order to rank the suitable alterations and it was proved that altering the width really affects the swingarm properties. Two final designs were drawn, however, it was concluded that having the suspension mount inside the single sided swingarm cause a high complexity of design and overall higher stresses, so that solution was disregarded.

Finally, the proposed design was compared with the double sided swingarm, and it was demonstrated that, while having the same mass, the designed single sided swingarm contained higher lat-

eral and torsional stiffness and the respective values are within the standard range for motorcycles. This proves that this concept would give the rider better handling and higher comfort. It was also shown that the critical situation in single sided swingarms is also landing on the rear wheel.

Overall, the goals of this thesis were achieved during this project with great results. The performance of the single sided swingarm designed, from the tests that were done, shows great results.

Future Works

There are other studies that could be made in order to complement this thesis:

In the first place, a double and single sided swingarm could be experimentally tested. The torsional and lateral stiffness as well as the mass could be measured in order to have another point of comparison to the designed swingarm. There could also be done some experimental rigs to validate the tests done using finite element method.

In the second place, a different material, such as carbon fiber could be utilized to design the material. The advantage of this study is that, the designer would be able to change the arrangement of fibers in order to alter the properties of the component and the structural stiffness of the material and could obtain a higher stiffness to weight ration compared to aluminium.

Thirdly, some experimental tests could be conducted on a real motorcycle to demonstrate that the defined condition is the critical condition for the motorcycle. This was intended to be completed during this thesis, but time ran out.

In the fourth place, a prototype of the single sided swingarm designed could be built in order to test whether the simulation results correspond to what happens experimentally. As stated before, the simulation, although it is a great tool to predict results, cannot be replaced by experimental results.

Furthermore, an algorithm could be developed in order to automate the sensitivity analysis, The results obtain could be compared to the final design obtained in this thesis, and conclude whether they are compatible.

Lastly, tests of the fatigue-resistance of the designed swingarm could be done. As stated previously, the *Leyni test bench* is used to evaluate the dynamic behaviour of the motorcycle's main components. Because of that, this fatigue test could be simulated using finite element method in order to evaluate the swingarm.

Bibliography

[1] Giacomo Risitano, Lorenzo Scappaticci, Carlo Grimaldi, and Francesco Mariani. Analysis of the structural behavior of racing motorcycle swingarms. *SAE 2012 World Congress & Exhibition*, 04 2012.

[2] Reno Kocheappen Chacko. *Design and Experimental Validation of a Carbon Fibre Swingarm Test Rig*. PhD thesis, University of the Witwatersrand, Faculty of Engineering and the Built . . . , 2013.

[3] Polychronis Spanoudakis, Evangelos Christenas, and Nikolaos C Tsourveloudis. Design and structural analysis of a front single-sided swingarm for an electric three-wheel motorcycle. *Applied Sciences*, 10(17):6063, 2020.

[4] B Smith and F Kienhöfer. A carbon fibre swingarm design case study. *JS Afr. Inst. Mech. Eng*, 31:1–11, 2015.

[5] S Swathikrishnan, P Singanapalli, and A S Prakash. Design and analysis of swingarm for performance electric motorcycle. *International Journal of Innovative Technology and Exploring Engineering (IJITEE)*, 8:3032–3039, 2019.

[6] Alessandro Airoldi, Simone Bertoli, Luca Lanzi, Marco Sirna, and Giuseppe Sala. Design of a motorcycle composite swing-arm by means of multi-objective optimisation. *Applied Composite Materials*, 19(3):599–618, 2012.

[7] INEGI. Sobre o inegi. http://www.inegi.pt/pt/sobre-o-inegi/o-inegi/. Accessed in 23.03.2022.

[8] David Moreno Giner. *Symbolic-Numeric Tools for the analysis of motorcycle dynamics. Development of a virtual rider for motorcycles based on model predictive control*. PhD thesis, Universidad Miguel Hernandez , Departamentos de la UMH:Ciencia de Materiales, Óptica y Tecnología Electrónica, 2016.

[9] WHO. Road traffic injuries. https://www.who.int/news-room/fact-sheets/detail/road-traffic-injuries. Accessed in 23.03.2022.

[10] Shuhei Nishitateno and Paul J. Burke. The motorcycle kuznets curve. *Journal of Transport Geography*, 36:116–123, 2014.

[11] Vittore Cossalter. *Motorcycle dynamics*. Lulu. com, 2006.

[12] Tony Foale. *Motorcycle handling and chassis design: the art and science*. Tony Foale, 2006.

[13] Magdi S Mahmoud. *Advanced control design with application to electromechanical systems*. Butterworth-Heinemann, 2018. Chapter 6.

[14] Joel Rodrigues Couto. Análise acoplada com dinâmica de multicorpo e com elementos finitos. Master's thesis, Faculdade de Engenharia da Universidade do Porto, 2016.

[15] Amit Shahar, Virginie Dagonneau, Séphane Caro, Isabelle Israël, and Régis Lobjois. Towards identifying the roll motion parameters of a motorcycle simulator. *Applied ergonomics*, 45(3):734–740, 2014.

[16] Motorcycle Safety Foundation. *Motorcycle Operating Manual*, 2020.

[17] Roberto Lot. A motorcycle tire model for dynamic simulations: Theoretical and experimental aspects. *Meccanica*, 39:207–220, 06 2004.

[18] Continental. The science of traction. https://www.conti-bike.co.uk/science-of-traction/. Accessed in 04.04.2022.

[19] Avelino de Jesus da Silva Costa Ferreira. *Projeto de conceção, desenvolvimento e avaliação experimental de componentes para suspensão de motociclos*. PhD thesis, ISEP, 2016.

[20] Pierluigi Zampieri. Motorcycle dynamics i. Bologna University - School of Engineering and Architecture.

[21] Marcus de Freitas Leal, José Antônio Ferreira Borges, and Sergio Butkewitsch. Optimal robust design of motorcycle suspension systems. Technical report, SAE Technical Paper, 2000.

[22] K Venkata Mangaraju, V Yogaraja, M Karthik, Bapanna K Dora, R Babu, and R Venkatesan. Kinematic and dynamic analysis of monoshock rear suspension. Technical report, SAE Technical Paper, 2004.

[23] K Venkata Mangaraju, D Govardan, Chandan Chavan, R Babu, and R Venkatesan. Optimization of damping characteristics for two wheelers. Technical report, SAE Technical Paper, 2008.

[24] Kevin Cameron. The evolution of rear suspensions. https://www.cycleworld.com/story/bikes/evolution-rear-suspension/, 2020. Accessed in 24.04.2022.

[25] JACOB BRYANT, ALLYSA GRANT, and ZACHARY WALSH. Motorcycle rear suspension.

[26] Dorling Kindersley. *The Motorbike Book*. Dorling Kindersley, 2012.

[27] João Diogo da Cal Ramos. Front and rear swing arm design of an electric racing motorcycle. Master's thesis, Instituto Superior Técnico, Universidade de Lisboa, 2016.

[28] Jet Sanchez. Single-sided vs double-sided swingarm: What's the difference? https://www.motodeal.com.ph/articles/motorcycle-features/single-sided-vs-double-sided-swingarm-whats-difference, 2021. Accessed in 27.04.2022.

[29] I Falloon. *The BMW Story: Production and Racing Motorcycles from 1923 to the Present Day*. Veloce Publishing, 2019.

[30] Miguel Ângelo Nogueira da Costa Oliveira et al. Validação estrutural de um novo conceito de chassis de motociclo. Master's thesis, Faculdade de Engenharia da Universidade do Porto, 2009.

[31] BMW. Single-sided swing-arm. https://www.bmw-motorrad.co.za/en/engineering/detail/suspension/single-sided-swingarm.html. Accessed in 26.04.2022.

[32] Amândio de Aveiro. Bmw gs e gs series. https://bmwmotoclube.com/bmwforum/viewtopic.php?t=4942. Accessed in 18.05.2022.

[33] Giacomo Sarti. Progettazione di un forcellone motociclistico innovativo per motociclette da competizione. Master's thesis, Universita degli Studi di Padova, 2013.

[34] Rob Wagner. Difference between softail & hardtail motorcycles. https://itstillruns.com/difference-between-softail-hardtail-motorcycles-12185214.html. Accessed in 18.05.2022.

[35] Alibaba. Motorcycle single sided swingarm swinging arm conversion kits for sport bike. https://www.alibaba.com/product-detail/Motorcycle-Single-Sided-Swingarm-Swinging-Arm_1600208447703.html. Accessed in 25.04.2022.

[36] Jonathon Klein. What exactly is a motorcycle swingarm? https://www.thedrive.com/motorcycles/41059/what-is-a-swingarm. Accessed in 26.04.2022.

[37] Daniel San Román López. Diseño y fabricación de un basculante para motocicleta de competición, 2018. Universidad Pontificia Comillas.

[38] Kevin Duke. Exploring lightweight materials on motorcycles. https://www.motorcycle.com/features/exploring-lightweight-materials-motorcycles.html, 2014. Accessed in 25.04.2022.

[39] Michele Chiarello. Progettazione di un forcellone motociclistico innovativo in alluminio e fibra di carbonio per la categoria moto2. Master's thesis, Universita degli Studi di Padova, 2018.

[40] Pratik Patole. Why rectangular box type swingarm is better than tubular swingarm. https://www.bikesmedia.in/reviews/why-rectangular-box-type-swingarm-is-better-than-tubular-swingarm.html. Accessed in 26.04.2022.

[41] Rolling Thunder Frames. Single sided swing arm – tubular. https://rollingthunderframes.com/product/single-sided-swing-arm-tubular/. Accessed in 26.04.2022.

[42] MCS. Bimota db5 mile. https://www.motorcyclespecs.co.za/model/bimota/bimota_db5%2007.htm. Accessed in 26.04.2022.

[43] Yamaha. Swingarm. https://global.yamaha-motor.com/business/cf/example/casting/ex009/. Accessed in 26.04.2022.

[44] Accossato Racing. Accossato racing swing arm tig welding. https://www.youtube.com/watch?v=TcXZHDMGB0c. Accessed in 26.04.2022.

[45] Stefano Cassani and Alessio Mancuso. Shape optimization of a high performance motorbike single sided swingarm. Technical report, SAE Technical Paper, 2005.

[46] Bevan Ian Smith. *Development of a carbon fibre swingarm*. PhD thesis, University of the Witwatersrand, Faculty of Engineering and the Built . . . , 2014.

[47] Lorenzo Peroni. Valutazione della rigidezza progressiva di una sospensione posteriore motociclistica. Master's thesis, SCUOLA DI INGEGNERIA E ARCHITETTURA, 2014.

[48] Yamaha. A day to remember. https://global.yamaha-motor.com/stories/offroadmania/ch3/. Accessed in 24.04.2022.

[49] Maxi Scoot. Swingarm aluminium cantilever for wheels 10" / 12" pit bike / dirt bike. https://www.maxiscoot.com/en/. Accessed in 26.04.2022.

[50] Bike Review. Classic collectable: Honda vfr750r rc30, 1987-1990. https://bikereview.com.au/classic-collectable-honda-vfr750r-rc30/. Accessed in 26.04.2022.

[51] Alan Cathcart. Elf racing - elf motorcycle chassis designs - retrospective. https://www.motorcyclistonline.com/elf-racing-elf-motorcycle-chassis-designs-retrospective/. Accessed in 26.04.2022.

[52] Rennie Scaysbrook. The legendary honda rc30. https://www.v1moto.com/blog/the-legendary-honda-rc30–33909. Accessed in 26.04.2022.

[53] Paulo Araújo. A honda rc30 tem 30 anos. https://www.andardemoto.pt/desporto/38727-a-honda-rc30-tem-30-anos/. Accessed in 26.04.2022.

[54] Bike Review. Retro - 80s to 2000sbike reviewsclassic classic collectable: Honda vfr750r rc30, 1987-1990. https://bikereview.com.au/classic-collectable-honda-vfr750r-rc30/. Accessed in 25.04.2022.

[55] Honda rc30 schwinge swing arm. https://www.youtube.com/watch?v=tCbSVdLeOgQ. Accessed in 26.04.2022.

[56] Amatumoto. Honda rvf750 rc45 1998. https://gpmotorbikes.com/product/rvf750-rc45-hrc/. Accessed in 25.04.2022.

[57] Peter Jackson. How the iconic ducati 916 changed the superbike game forever. https://robbreport.com/motors/motorcycles/ducati-916-superbike-2838459/. Accessed in 26.04.2022.

[58] Kevin Ash. Massimo tamburini. https://web.archive.org/web/20130906155759/http://www.ashonbikes.com/content/massimo-tamburini. Accessed in 26.04.2022.

[59] Dane Walker. Ducati 916 sp3 corse swingarm. https://fi.pinterest.com/pin/165648092534377409/. Accessed in 25.04.2022.

[60] Margarida Peres. The new bmw r 1200 gs. https://www.press.bmwgroup.com/portugal/article/detail/T0132406PT/the-new-bmw-r-1200-gs?language=ptl. Accessed in 26.04.2022.

[61] Jon Urry. Bmw r1200gs (2013 – 2018) | buyers guide. https://shop.motousher.com/collections/ducati-hypermotard-950-sp-2019/products/ducati-hypermotard-950-sp-c-bow-soft-bag-carrier. Accessed in 25.04.2022.

[62] Press Release. Bmw wins innovation award for carbon fiber swingarm. https://blog.motorcycle.com/2018/04/03/manufacturers/bmw/bmw-wins-innovation-award-hp4-races-carbon-fiber-swingarm/. Accessed in 27.04.2022.

[63] Auto Esporte. Bmw lança moto de corridas hp4 race. https://autoesporte.globo.com/carros/noticia/2017/11/bmw-lanca-moto-de-corridas-hp4-race-por-r-490-mil.ghtml. Accessed in 27.04.2022.

[64] Peter McLaren. Definitely maybe: Carbon fibre swingarms in motogp. https://www.crash.net/motogp/feature/892455/1/definitely-maybe-carbon-fibre-swingarms-motogp, 2018. Accessed in 27.04.2022.

[65] Bucci Composites. Ducati 1299 superleggera. https://www.bucci-composites.com/en/it/ducati-1299-superleggera-swingarm-carbon-fiber-compositesl. Accessed in 27.04.2022.

[66] Don Canet. 2017 ducati 1299 superleggera superbike. https://www.cycleworld.com/2017-ducati-1299-superleggera-superbike-motorcycle-review, 2017. Accessed in 27.04.2022.

[67] Syed Hassaan Abdullah1 Mohd Ahmed Wajahath and Abdul Rahman. Design of racing motorcycle swingarm with shape optimisation. *International Journal for Scientific Research & Development*, 2018.

[68] Nigel O'Dea. Motorcycle swingarm redesigned in carbon composite. *Reinforced Plastics*, 55(6):38–41, 2011.

[69] D Limebeer and R Sharp. Bicycles, motorcycles and models (single-track vehicle modelling and control). *IEEE Control Syst. Magazine*, pages 34—-61, 2006.

[70] RS Sharp. The influence of frame flexibility on the lateral stability of motorcycles. *Journal of Mechanical Engineering Science*, 16(2):117–120, 1974.

[71] E Armentani, S Fusco, and M Pirozzi. Numerical evaluation and experimental tests for a road bike swingarm. In *Science and Motor Vehicles JUMV International Automotive Conference with Exhibition, Beograd, Serbia*, 2007.

[72] Kelvin Lake, Richard Thomas, and Owen Williams. The influence of compliant chassis components on motorcycle dynamics: an historical overview and the potential future impact of carbon fibre. *Vehicle system dynamics*, 50(7):1043–1052, 2012.

[73] Vijay Manikrao Athawale, Rajanikar Kumar, and Shankar Chakraborty. Decision making for material selection using the uta method. *The International Journal of Advanced Manufacturing Technology*, 57(1):11–22, 2011.

[74] Prof. S Božič, Prof. E Gombač, and Prof. A Harmel. Redesign of motorcycle rear suspension with cad technology. *School Center Postojna*, 2009.

[75] Dent Goalie. The pros and cons of carbon fiber material vs aluminum cars. https://dentgoalie.com/manufacturing-comparison/. Accessed in 07.04.2022.

[76] Richard Bach. Aluminium in transport. https://www.aluminiumleader.com/application /transport/, 2010. Accessed in 07.04.2022.

[77] Carlos Filipe do Lago Vieira. Structural evaluation of a motorcycle frame. Master's thesis, Faculdade de Engenharia da Universidade do Porto, 2014.

[78] Jürgen Hirsch. Recent development in aluminium for automotive applications. *Transactions of Nonferrous Metals Society of China*, 24(7):1995–2002, 2014.

[79] Rushikesh Atmaram Sonawane and Rasiklal M Dhariwal. Design and optimization of high-performance motorcycle swingarm. *INTERNATIONAL JOURNAL*, 6(5), 2021.

[80] Darrel R Tenney, John G Davis Jr, R Byron Pipes, and Norman Johnston. Nasa composite materials development: lessons learned and future challenges. In *NATO RTO AVT-164 Workshop on Support of Composite Systems*, 2009.

[81] Mark Bruderick, Douglas Denton, M Shinedling, and M Kiesel. Carbon fiber composite body structures for the 2003 dodge viper. *Daimler Chrysler Cooperation and Michael Kiesel, Quantum Composites Inc*, 2002.

[82] JM Corum. Basic properties of reference crossply carbon-fiber composite. Technical report, Oak Ridge National Lab.(ORNL), Oak Ridge, TN (United States), 2001.

[83] MotoGP. Swingarms: Tech talk with simon crafar. https://www.youtube.com/watch?v=9MO5LMi5sY0, 2021. Accessed in 08.04.2022.

[84] Nima Khademian and Yaser Peimaei. Lightweight materials (lwm) in transportation especially application of aluminum in light weight automobiles (lwa). *International Conference on Interdisciplinary Studies in Technology*, 02 2020.

[85] RHEINFELDEN. Technical information. https://rheinfelden-alloys.eu/wp-content/uploads/2015/11/TDB_Alufont-52_AlCu4Ti_EN_V2.pdf, 2015. Accessed in 25.06.2022.

[86] RHEINFELDEN. Primary aluminium casting alloys. https://www.foundry-planet.com/fileadmin/redakteur/Material/08-03-10-Leporello_engl.pdf. Accessed in 25.06.2022.

[87] makeitfrom. En ac-21100 (aicu4ti) cast aluminum. https://www.makeitfrom.com/material-properties/EN-AC-21100-AlCu4Ti-Cast-Aluminum. Accessed in 25.06.2022.

[88] Steven R Schmid, Bernard J Hamrock, and Bo O Jacobson. *Fundamentals of machine elements*. CRC Press, 2013.

[89] Alfred Pugsley. *The safety of structures*. Edward Arnold, 1966.

[90] AJP. About us. https://ajpmotos.com/pt-pt/pages/about-us. Accessed in 14.04.2022.

[91] AJP. Pr7 2021. https://ajpmotos.com/pt-pt/products/pr7-2021. Accessed in 18.04.2022.

[92] MCS. Ajp pr7 adventure. https://www.motorcyclespecs.co.za/model/AJP/AJP_PR7.htm. Accessed in 16.04.2022.

[93] MCS. Ajp pr7 660 adventure. https://www.motorcyclespecs.co.za/model/AJP/AJP%20PR7%20660%20Adventure%2015.htm. Accessed in 16.04.2022.

[94] Ultimate Specs. Ajp pr7 adventure 650. https://www.ultimatespecs.com/motorcycles-specs/ajp/ajp-pr7-adventure-650-2020. Accessed in 16.04.2022.

[95] M. Haskins. What is dry weight? https://www.wikimotors.org/what-is-dry-weight.htm. Accessed in 18.04.2022.

[96] John Bradley. *The Racing Motorcycle: A Technical Guide for Constructors: Volume 2, Chassis Materials and Construction Techniques*. Broadland leisure publications, 2003.

[97] Apurva Chakraborty. Performance gains of load sensing brake force distribution in motorcycles. Technical report, SAE Technical Paper, 2019.

[98] Giulio Panzani, Simone Formentin, and Sergio M Savaresi. Active motorcycle braking via direct data-driven load transfer scheduling. *IFAC Proceedings Volumes*, 45(16):1257–1262, 2012.

[99] Alberto. Why the front brake is bigger than the rear brake? - motorbike tutorials. https://www.youtube.com/watch?v=nSjILPS5_8U. Accessed in 20.04.2022.

[100] Pedro Huertas-Leyva, Marilee Nugent, Giovanni Savino, Marco Pierini, Niccolò Baldanzini, and Simon Rosalie. Emergency braking performance of motorcycle riders: skill identification in a real-life perception-action task designed for training purposes. *Transportation research part F: traffic psychology and behaviour*, 63:93–107, 2019.

[101] V Cossalter. *Cinematica e Dinamica della Motocicletta*. Edizioni Progetto, 2001.

[102] Nerijus Kudarauskas. Analysis of emergency braking of a vehicle. *Transport*, 22(3):154–159, 2007.

[103] John El Khoury and Antoine G Hobeika. Assessing the risk in the design of passing sight distances. *Journal of transportation engineering*, 133(6):370–377, 2007.

[104] AH Ariffin, A Hamzah, MS Solah, NF Paiman, Z Mohd Jawi, and MH Md Isa. Comparative analysis of motorcycle braking performance in emergency situation. *Journal of the Society of Automotive Engineers Malaysia*, 1(2), 2017.

[105] Hans Pacejka. *Tire and vehicle dynamics*. Elsevier, 2005.

[106] Kazuyuki Kabe and Naoshi Miyashita. A study of the cornering power by use of the analytical tyre model. *Vehicle System Dynamics*, 43(sup1):113–122, 2005.

[107] Egbert Bakker, Hans B Pacejka, and Lars Lidner. A new tire model with an application in vehicle dynamics studies. *SAE transactions*, pages 101–113, 1989.

[108] Rhett Allain. Just how far can a motorcycle lean in a turn? https://www.wired.com/2015/09/just-far-can-motorcycle-lean-turn/, 2015. Accessed in 12.05.2022.

[109] MotoGP. Motogp™ lean angle experience. https://www.youtube.com/watch?v=J73XRD GPcpE, 2013. Accessed in 12.05.2022.

[110] David Aguilera Turégano. Diseño de un basculante trasero para motocicleta, 2011. Universitat Politècnica de Catalunya.

[111] Walter Bergman. Theoretical prediction of the effect of traction on cornering force. *SAE Transactions*, 69:614–640, 1961.

[112] Bret Schaller. *Experimental validation of finite element analysis software applied to the design of a motorcycle swingarm*. PhD thesis, Embry-Riddle Aeronautical University, 1996.

[113] KTM. Anti-wheelie. https://www.ktm.com/pt-br/tech-guide/anti-wheelie.html. Accessed in 10.07.2022.

[114] Prof J. E. Akin. Impact load factors for static analysis. Rice University.

[115] V Stefano and P Simone. Structural optimization of the rear swingarm of ducati hypermotard. *1st European HyperWorks Technology Conference*, 2007.

[116] Silvia Gaiani. Industrialization of an aluminium alloy single swingarm for ducati monster s4 r. *Development Trends of Motorcycles II*, pages 288–303, 2005.

[117] SD Piazza. Ducati chassis design: Simulation and experiment testing.

[118] KMP. Single-sided + 250 speed triple otec rim. https://www.kmp.fr/gb/the-shop/12418-single-sided-250-speed-triple-otec-rim.html, 2021. Accessed in 24.06.2022.

[119] Martin Asuncion. How to adjust your motorcycle chain - step-by-step guide. https://www.motodeal.com.ph/articles/motorcycle-features/how-adjust-your-motorcycle-chain-step-step-guide, 2021. Accessed in 24.06.2022.

[120] Motowheels. Bst 7 spoke wheels: Ducati panigale 1199-1299-v4-v2, sf v4. https://motowheels.com/i-23900013-bst-7-spoke-wheels-ducati-panigale-1199-1299-v4-v2-sf-v4.html. Accessed in 24.06.2022.

Appendix A

AJP PR7

AJP PR7 2021 [91]

	PR7
ENGINE	Single cylinder, 4 stroke, 4 valves - DOHC, liquid cooled
BORE X STROKE	100 x 76.4 mm
DISPLACEMENT	600 cc
FEEDING	Athena fuel injection system Ø45 mm
STARTER	Electric
CLUTCH	Oil bath, multi-disc
TRANSMISSION	6 speed
FRAME	Composite - aluminum / steel
SEAT HEIGHT	920 mm
WHEELBASE	1540 mm
GROUND CLEARANCE	310 mm
FUEL TANK	17 L
FRONT TYRE	90/90 - 21''
REAR TYRE	140/80 - 18''
FRONT SUSPENSION	ZF Sachs Ø48 mm close-circuit – 300 mm stroke – fully adjustable
REAR SUSPENSION	ZF Sachs prog. system with reser. - 280 mm stroke - fully adjustable
FRONT BRAKES	2 piston BREMBO caliper - Disc Ø300 mm
REAR BRAKES	Single piston BREMBO caliper - Disc Ø240 mm

AJP PR7 Adventure 2016 [92]

Make Model	AJP PR7 Adventure
Year	2016
Engine	Single cylinder, SWM, DOHC
Capacity	600.3 cc / 36.6 cu in
Bore x Stroke	100 x 76.4 mm
Cooling System	Liquid cooled
Lubrication	Wet sump
Compression Ratio	12.4:1
Exhaust	Two into one
Induction	Electronic fuel injection, 45mm throttle body
Ignition	Electronic
Starting	Electric
Clutch	Oil bath, multi disc

Transmission	6-Speed
Final Drive	Chain
Frame	AJP's hybrid steel and aluminum frame
Front Suspension	48 mm USD fork
Front Wheel Travel	299.7 mm / 11.8 in
Rear Suspension	AJP progressive linkage system, fully adjustable Sachs piggyback shock
Rear Wheel Travel	279.4 mm / 11.0 in
Front Brakes	Single 300 mm disc, 2 piston caliper
Rear Brakes	Single 240 mm disc, single piston caliper
Front Tyre	90/90-21
Rear Tyre	140/80-18
Wheelbase	1539 mm / 60.6"
Ground Clearance	320 mm / 12.6"
Seat Height	919 mm / 36.2"
Wet Weight	165 kg / 364 lbs
Fuel Capacity	17 L / 4.5 US gal

AJP PR7 Adventure 660 [93]



.

Make Model.	AJP PR7 660 Adventure
Year	2016
Engine	Single cylinder, 4-stroke
Capacity	659.7 cc / 40.3 cub in
Cooling System	Liquid cooled
Oil Capacity	Stored in twin spar
Exhaust	2-into-1

Induction	Electronic fuel injection, 44 mm Mikuni throttle body
Starting	Electric
Max Power	35.8 kW / 48 hp @ 6000 rpm
Max Torque	58 Nm / 5.9 kgf-m / 42.8 ft lbs @ 5500 rpm
Final Drive	Chain
Frame	Lightweight twin spar, aluminium and steel
Rake	26.5°
Front Suspension	48 mm Marzocci inverted fork
Front Wheel Travel	300 / 11.8 in
Rear Suspension	Cast aluminium swingarm with progressive linkage, Ohlins shock
Rear Wheel Travel	280 mm / 11.0 in
Front Brakes	300 mm Disc, 2-piston caliper
Rear Brakes	240 mm Disc
Wheels	Steel, wire spokes
Front Tyre	90/90-21
Rear Tyre	140/80-18
Wheelbase	1532 mm / 60.3 in
Ground Clearance	300 mm / 11.8 in
Dry Weight (Est)	155 kg / 342 lbs
Fuel Capacity	17 L / 4.5 US gal

AJP PR7 Adventure 650 [94]

Brand	**AJP**
Model	**AJP PR7 Adventure 650**
Start year	**2020**
Year	**2020**
Category	**Enduro / offroad**
Factory Warranty (Years / miles)	**-**

AJP PR7 Adventure 650 Dimensions, Aerodynamics and weight

Frame type	**Aluminum/steel**
Seat details	**-**
Wheelbase	**1,540 mm (60.6 inches)**
Length	**-**
Width	**-**
Height	**-**
Seat Height	**920 mm (36.2 inches) If adjustable, lowest setting.**
Alternate Seat Height	**-**
Ground Clearance	**310 mm (12.2 inches)**
Trail size	**-**
Wheels details	**-**
Front Tyres - Rims dimensions	**90/90-21**
Rear Brakes Dimensions - Disc Dimensions	**240 mm (9.4 inches)**
Curb Weight (including fluids)	**-**
Dry Weight	**155.0 kg (341.7 pounds)**
Front Percentage of Weight	**-**
Rear Percentage of Weight	**-**
Weight-Power Output Ratio :	**0.3097 HP/kg**
Fuel Tank Capacity	**17.00 litres (4.49 gallons)**
Reserve Fuel Capacity	**-**
Carrying Details and Capacity	**-**
Front Suspension	**ZF Sachs Ø48mm fully adjustable**
Front Suspension Travel	**300 mm (11.8 inches)**
Rear Suspension	**ZF Sachs progressive system with reservatory fully adjustable**
Rear Suspension Travel	**300 mm (11.8 inches)**

Rear Tyres - Rims dimensions	**140/80-18**
Front brakes	**Single disc. 2-piston calipers**
Rear brakes	**Single disc. Single-piston caliper**
Front Brakes Dimensions - Disc Dimensions	**300 mm (11.8 inches)**
Rear Brakes Dimensions - Disc Dimensions	**240 mm (9.4 inches)**
Curb Weight (including fluids)	**-**
Dry Weight	**155.0 kg (341.7 pounds)**
Front Percentage of Weight	**-**
Rear Percentage of Weight	**-**
Weight-Power Output Ratio :	**0.3097 HP/kg**
Fuel Tank Capacity	**17.00 litres (4.49 gallons)**
Reserve Fuel Capacity	**-**
Carrying Details and Capacity	**-**
Front Suspension	**ZF Sachs Ø48mm fully adjustable**
Front Suspension Travel	**300 mm (11.8 inches)**
Rear Suspension	**ZF Sachs progressive system with reservatory fully adjustable**
Rear Suspension Travel	**300 mm (11.8 inches)**

AJP PR7 Adventure 650 Engine and Transmission Technical Data

Engine type - Number of cylinders	**Single cylinder, four-stroke**
Engine details	**Minarelli engine**
Fuel system	**Injection. Delphi**
Engine size - Displacement - Engine capacity	**600.00 ccm (36.61 cubic inches)**
Bore x Stroke	**100.0 x 76.4 mm (3.9 x 3.0 inches)**
Compression Ratio	**-**
Number of valves per cylinder	**4**
Camshaft Valvetrain Configuration	**Double Overhead Cams/Twin Cam (DOHC)**
Maximum power - Output - Horsepower	**48.00 HP (35.0 kW)) @ 6000 RPM**

Maximum torque	**58.00 Nm (5.9 kgf-m or 42.8 ft.lbs) @ 5500 RPM**
Engine Maximum RPM	-
Cooling system	**Liquid**
Lubrication system	-
Engine oil capacity	-
Exhaust system	-
Gearbox	**6-speed**
Transmission type, final drive ratio	**Chain**
Clutch type	-
Driveline	-

AJP PR7 Adventure 650 Performance

Top Speed	-
Acceleration 0 to 100 km/h (0 to 62 mph)	-
Acceleration 0 to 400m (1/4 mile)	-
Recuperation 60 to 140 km/h in highest gear	-
Fuel Consumption - MPG - Economy - Efficiency	-
CO2 emissions	-
Emissions	-

AJP PR7 Adventure 650 Electrical Systems, Ignition and Equipment

Ignition Type	-
Electrical Details	-
Starter Type	**Electric & kick**
Instruments	-
Lights	-

Appendix B

Codes

B.1 Script code to calculate loads during cornering

```
%Propriedades da curva
V=150;
C=250;

%Força normal e coeficiente de tração
Pdeforca    = 60 %;
y=1.1;
h= 0.779;
e=0
g=9.81;

%Dimensoes da roda
Rs = 0.2 ;
rt =0.2/3 ;
t=0.007;


m=245;
vms =V/3.6;
Nr=m*9.81*Pdeforca/100
Fcent = m*vms^2/C;

%Confirmação do Roll Angle Roll angle
firad   =  atan (vms^2/(C*g))+asin(t*sin(vms^2/(C*g))/(h-t));
fi=firad *180/ pi %°


%Cálculo das forças na roda
Ft=Pdeforca/100*Fcent
yy=Ft/Nr
yx=(y^2-yy^2)^(1/2)
S=(y^2*Nr^2-Ft^2)^0.5
s2=yx*Nr
T=S*Rs/rt
R=(S^2+Ft^2)^0.5

%Cálculo das forças na swingarm
Fx=S+T
Fy=Nr*cos(firad)+ Ft*sin(firad)
Fz=-Nr*cos(firad)+ Ft*sin(firad)
Mx= Fy*t
My=T*e+S*t
Mz= T*rt-S*Rs


```

Figure B.1: Script code to calculate loads during cornering

B.2 Script code to calculate loads on a double sided swingarm

```
%Dimensões da roda
Rs=0.4572/2;
rt=Rs/3
e=0.15
t=0.07;
h= 0.779;


%Valores do cálculo
Nr= input('Nr value: ')
S= input('S value: ')
T= input('T value: ')
Ft= input('Ft value: ')
fi= input('fi value: ') %°


%Cálculo das forças na swingarm
firad=fi*pi/180%rad
R=((Nr*cos(firad)+ Ft*sin(firad))^2+(Nr*sin(firad)- Ft*cos(firad))^2)^0.5
beta=acos((Nr*cos(firad)+ Ft*sin(firad))/R)
Fx=S+T
Fy=(Nr*cos(firad)+ Ft*sin(firad))
Fz=Nr*sin(firad)- Ft*cos(firad)

if firad==0
Mx=0
My=0
else
Mx= -(Nr*cos(firad)+ Ft*sin(firad))*(t)-(Nr*sin(firad)- Ft*cos(firad))*Rs
My=S*t
endif

Mz= T*rt-S*Rs
Fk=(-Mz*1000-Fy*(398+132))/132
```

Figure B.2: Script code to calculate loads on a double sided swingarm

B.3 Script code to calculate loads on a single sided swingarm

```
%Dimensões da roda
Rs=0.4572/2;
rt=Rs/3
e=0.15
t=0.07;
h= 0.779;
u=0.07;

%Valores do cálculo
Nr= input('Nr value: ')
S= input('S value: ')
T= input('T value: ')
Ft= input('Ft value: ')
fi= input('fi value: ') %°


%Cálculo das forças na swingarm
firad=fi*pi/180%rad
R=((Nr*cos(firad)+ Ft*sin(firad))^2+(Nr*sin(firad)- Ft*cos(firad))^2)^0.5
beta=acos((Nr*cos(firad)+ Ft*sin(firad))/R)
Fx=S+T
Fy=(Nr*cos(firad)+ Ft*sin(firad))
Fz=Nr*sin(firad)- Ft*cos(firad)

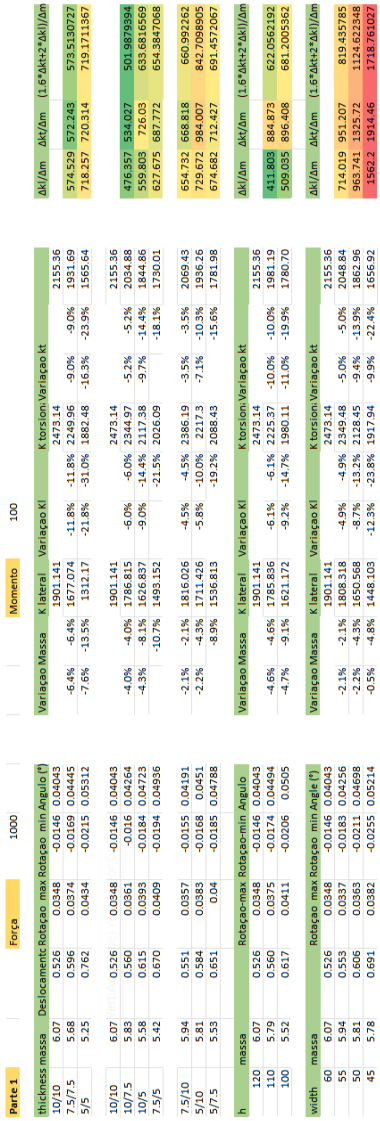
if firad==0
Mx=-Nr*u
My=-T*(e-u)+S*u
else
Mx= -(Nr*cos(firad)+ Ft*sin(firad))*(u+t)-(Nr*sin(firad)- Ft*cos(firad))*Rs
My=-T*(e-u)+S*(u+t)
endif

Mz= T*rt-S*Rs
Fk=(-Mz*1000-Fy*(398+132))/132
```

Figure B.3: Script code to calculate loads on a single sided swingarm

Appendix C

Anexo em volume separado



| Parte 1 | | Força | 1000 | | |

| Parte 1 | | | Força | 1000 | | | Momento | 100 | | |

Appendix D

Mesh

D.1 Double Sided Swingarm

Mesh Convergence

In order to test the mesh convergence, a load of 1000N was applied on spacer of the double sided swingarm. After that, a stress in a certain point was taken. Finally, a graph and table where the number of elements in function of Max. Stress is represented, which shows the convergence of the respective stress. As it is possible to conclude, using a global size of seeds corresponding to 3mm, does not contain an error, which means that the mesh is not a cause of error on the simulation of the double sided swingarm. The mesh convergence study is represented in figure D.1 and table D.1.

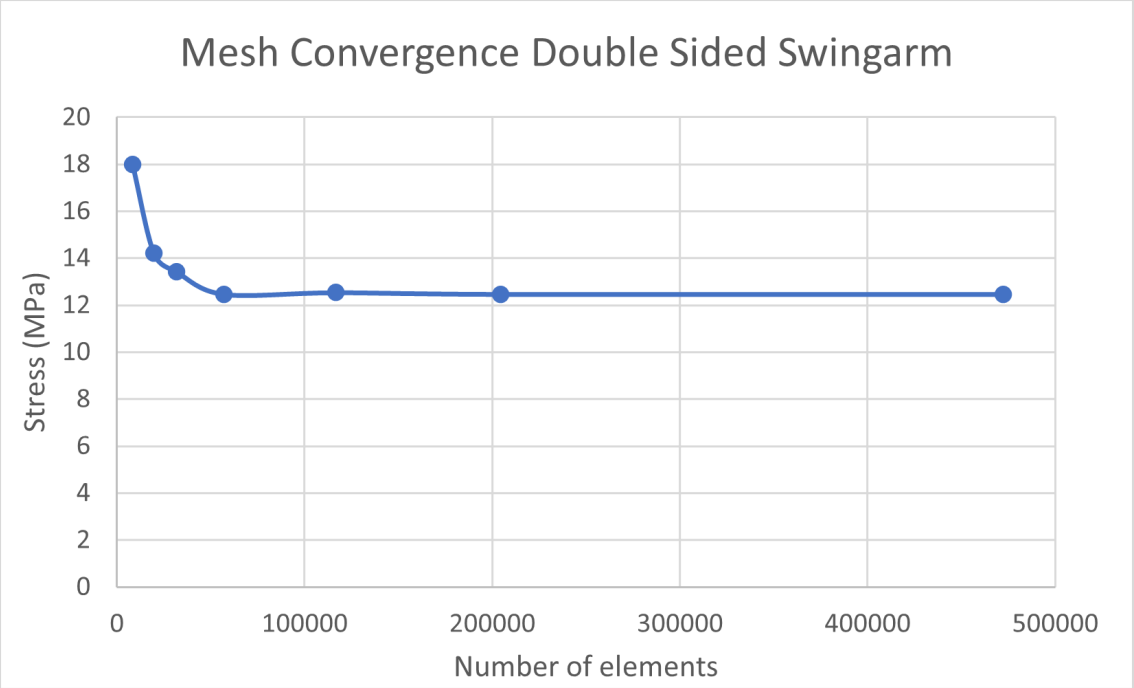


Figure D.1: Mesh Convergence double sided swingarm

Table D.1: Mesh Convergence values in double sided swingarm

Global size of seeds	Number of elements	Stress	Variation
20	8191	17.98	-
10	19572	14.21	21%
8	31937	13.41	5.6%
6.5	58858	12.47	7%
5	116651	12.54	0.6%
4	204610	12.47	0.6%
3	472386	12.47	0.0%

D.2 Single Sided Swingarm

Mesh Convergence

Similarly, the same test was done one the single sided swingarm, in this case to *Part2* and assumed the same results for *Part1*. In order to know the best global size of seeds in order to have the most efficient mesh. This study is particularly important, due to the fact that during the defining of the hierarchy a lot of simulations were done and having great results as fast as possible is really important.

It was applied a force of 1000N on the free end on the swingarm and, once again, stress in a certain point was taken. As it can be seen from the graph, using a global size of seeds corresponding to 3mm does not cause any errors on the simulation.

The mesh convergence study is illustrated in figure D.2 and table D.2.

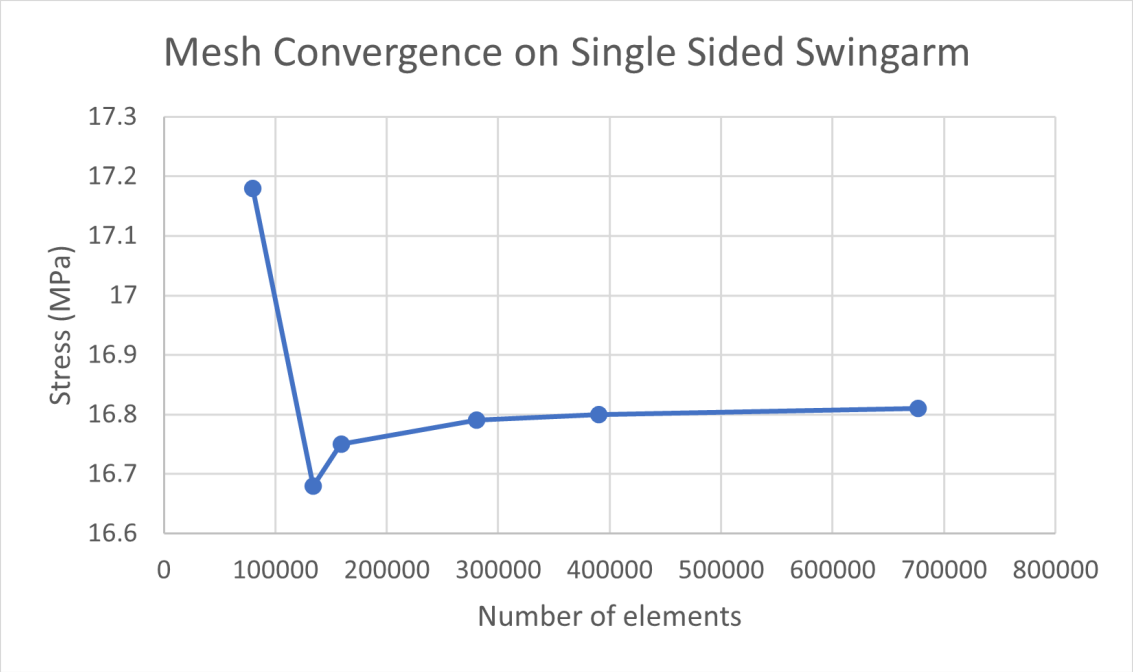


Figure D.2: Mesh Convergence of *Part2* single sided swingarm

Table D.2: Mesh Convergence values in *Part2*

Global size of seeds	Number of elements	Stress	Variation
20	79422	17.18	-
10	133843	16.68	2.9%
8	158894	16.71	0.4%
5	280570	16.79	0.2%
4	389932	16.8	0.1%
3	676707	16.81	0.1%

Refined Mesh

On places where it was verified stress concentration, in addition to adding a fillet in order to reduce the stress, a refined mesh was applied there. That is because, these places where the stress is the maximum in the entire swingarm are the areas that are the yield can occur and it is necessary to have the study with the most detail possible. Because of that, a local seed was applied there with a global size of 1mm, as shown in figure D.3.

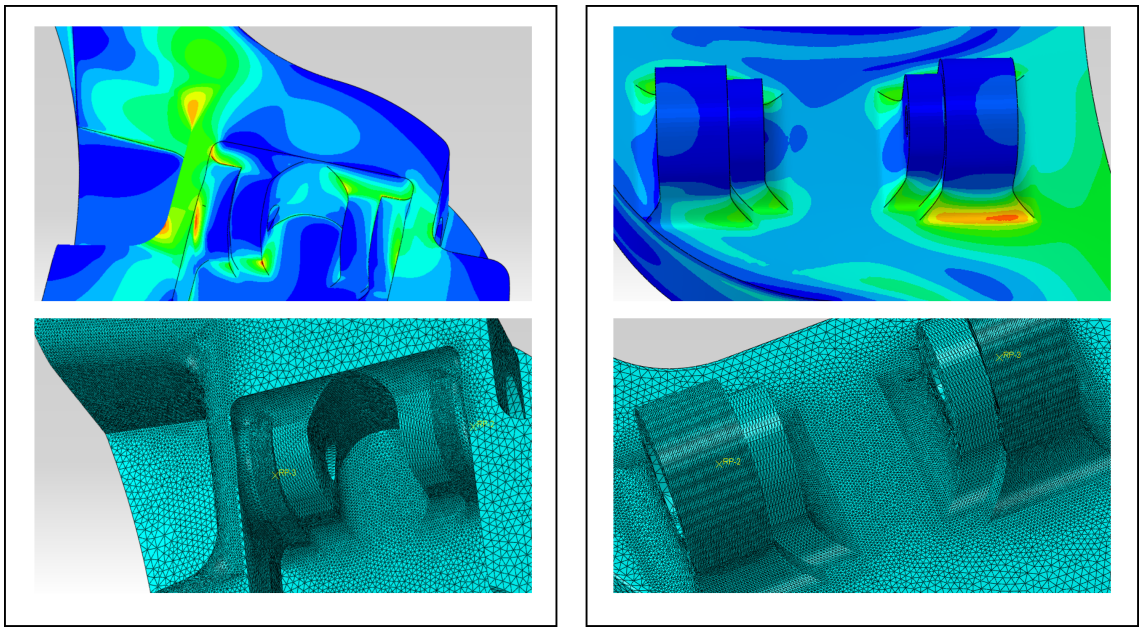
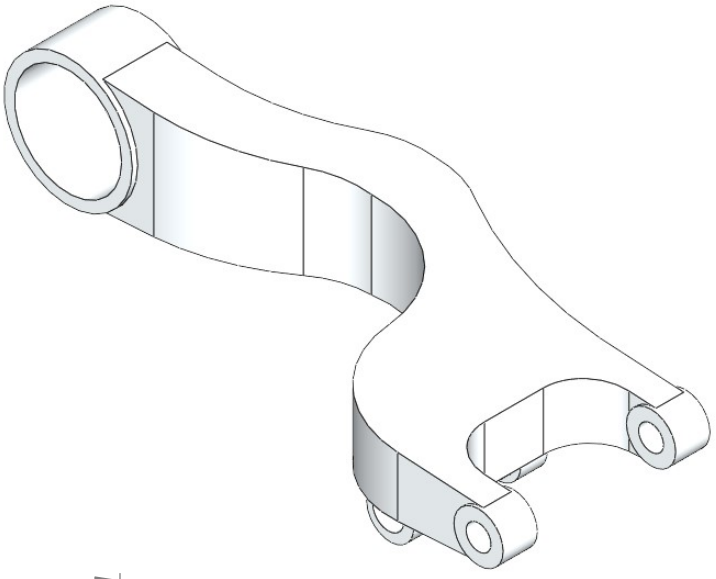
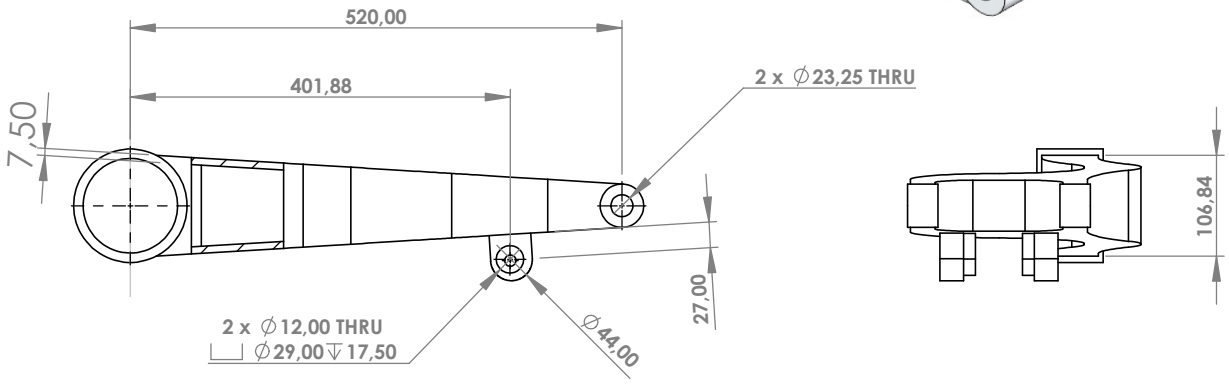


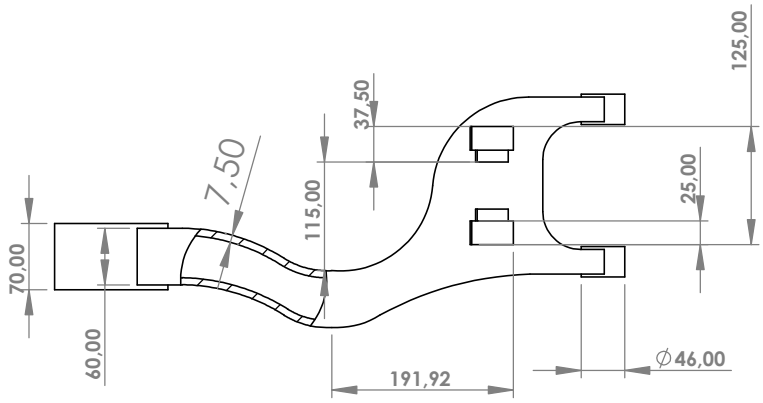
Figure D.3: Refined mesh on fillets with high concentration of stresses: Left- *Part1*; Right- *Part2*

Appendix E

Final Design







UNLESS OTHERWISE SPECIFIED: DIMENSIONS ARE IN MILLIMETERS SURFACE FINISH: TOLERANCES: LINEAR: ANGULAR:	FINISH:		DEBURR AND BREAK SHARP EDGES	DO NOT SCALE DRAWING	REVISION	
	04/07/2022					

	NAME	SIGNATURE	DATE
DRAWN			
CHK'D			
APPV'D			
MFG			
Q.A			

TITLE:

Single Sided Swingarm

MATERIAL:

DWG NO.

FINAL DRAWING

A4

WEIGHT:

SCALE:1:6

SHEET 1 OF 1

SOLIDWORKS Educational Product. For Instructional Use Only.